Order Number 1341363

Investigation of surface faulting, Brazoria County, Texas using aerial photography, field data, well log data, seismic profiles and fault modeling

Boccanera, Justine Ann, M.S.

University of Houston, 1989

U·M·I
300 N. Zeeb Rd.
Ann Arbor, MI 48106

INVESTIGATION OF SURFACE FAULTING, BRAZORIA COUNTY, TEXAS USING AERIAL PHOTOGRAPHY, FIELD DATA, WELL LOG DATA, SEISMIC PROFILES AND FAULT MODELING

A Thesis

Presented to

The Faculty of the Department of Geosciences

University of Houston - University Park

In Partial Fulfillment

of the Requirements for the Degree

Master of Science in Geology

By

Justine Ann Boccanera

May 1989

INVESTIGATION OF SURFACE FAULTING,
BRAZORIA COUNTY, TEXAS
USING AERIAL PHOTOGRAPHY, FIELD DATA, WELL LOG DATA,
SEISMIC PROFILES AND FAULT MODELING

Justine Ann Boccanera

Approved:

Chariman of the Committee
Dr. Carl E. Norman
Department of Geosciences

Committee Members:

Dr. William R. Dupre
Department of Geosciences

Dr. DeWitt C. Van Siclen
Department of Geosciences

Dr. Michael W. O'Neill
Department of Civil Engineering

Dean, College of Natural Sciences and Mathematics

ACKNOWLEDGEMENTS

Numerous individuals, businesses, and state agencies donated time, data, and use of their facilities to make this project possible. It is a credit to those involved that I was never refused a resonable request.

Mr. John Campbell and his staff at the Soil Conservation Service office in Angleton allowed access to the eight generations of black and white aerial photographs that served as the foundation of this study. False-color infrared aerial photographs were obtained from the Department of Civil Engineering at the University of Houston. The Gulf Coast Geological Library and the Geological Data Library graciously donated their data, use of equipment and facilities.

My thanks to Mr. Mark Porter and his business associate for getting me started on seismic interpretation in Brazoria County. Thank you to Ms. Gay Lewis and Mr. Paul Lewis of Lewis Seismic Exchange; they directed me to the geophysical companies that donated nearly 400 miles of seismic data for the study. My thanks to Mr. Jay Kallina and Mr. Steven Kallina of JDK Inc., who courteously allowed use of their facilities and access to seismic data which proved very important to the study. The seismic profiles that appear in the thesis are courtesy of Mr. Ron Nichol and Mr. Joe Knight

of Spectrum-Seis-Quest, Inc. Although they wish to remain anonymous, I extend thanks to an additional geophysical company for use of two extensive, and very valuable, seismic profiles.

Thank you to Mr. Wade Parsons, District Foreman, at the Amoco Production Company's Hastings Oil Field facility, and Ms. Margaret Baker, Process Supervisor, at Dow Chemical Corporation's Crude Oil Processing Plant for permission to do field investigations on their property.

Sincerest thanks to my advisor, Dr. Carl E. Norman, for his help and guidance throughout the project. The original manuscript was greatly improved by his critical reviews. I appreciate the time invested both in the classroom and in the field. Thanks to my committee members from the Department of Geosciences, Dr. William R. Dupre and Dr. De Witt C. Van Siclen, and from the Department of Civil Engineering, Dr. Michael W. O'Neill, for their suggestions and constructive criticisms.

Greatest thanks to my family, including my husband Dan, for years of patience, help, and encouragement (they always said I could do it). Very special thanks to Mr. David Melnyk. I will forever be in debt for the countless hours he spent assisting me in the field. He is a gifted individual whose high spirits, clever imagination and intellectual perspicacity made this project both bearable and a great success. Special thanks to my friend Ms. Iva Roddey for her time, enthusiasm, and expertise. Thanks to Conquest Exploration Company for use of supplies and facilities and for giving me my first job in the oil industry. Thank you to the geologists and geophysicists I have worked with at Conquest Exploration and the Amerada-Hess Corporation, including Mr. Don Woolverton and Mr. Bill Vasterling (Conquest Exploration Co.), and Mr. Bill Wilfong (Amerada-Hess Corp.). Frequent discussions of Gulf Coast geology and the technical aspects of geophysical data acquisition, processing, and interpretation have proved invaluable. Their friendship and encouragement are also greatly appreciated. Finally, thank you to the rest of my friends at the University of Houston (those still here and those who have moved on), and my friends at home; they never lost faith and have been a constant source of moral support.

INVESTIGATION OF SURFACE FAULTING,
BRAZORIA COUNTY, TEXAS
USING AERIAL PHOTOGRAPHY, FIELD DATA, WELL LOG DATA,
SEISMIC PROFILES AND FAULT MODELING

An Abstract of a Thesis

Presented to

the Faculty of the Department of Geology

University of Houston - University Park

In Partial Fulfillment
of the Requirements for the Degree
Master of Science

By

Justine Ann Boccanera

May 1989

ABSTRACT

Brazoria County is located along the northwestern Gulf of Mexico coastal plain. Just to the north of Brazoria County, in Harris County, nearly 300 active surface faults have been identified to date. In contrast, only 25 active surface faults were known to exist in Brazoria County prior to this study even though it covers a larger area, and is located in the same geologic province, as Harris County.

A rigorous investigation of surface faulting in Brazoria County was undertaken to: increase knowledge of surface faulting in the Gulf coastal region; serve as a land-use planning guide for future development in Brazoria County, and more specifically to: locate and map surface faults throughout Brazoria County; determine the distribution of faulting and how it compares to that documented in Harris County; determine if surface faulting in Brazoria County is related to known structural trends; examine the subsurface geometry and movement history of selected faults; and, test two models, the Gibb's construction and a compaction model, to predict listric fault shape.

This study was conducted using aerial photograph reconnaissance, exhaustive field investigations, interpretation of well log and seismic data, and application

of predictive models. In the course of the investigation 105 lineaments that may represent previously unknown active surface faults were identified. The pattern of surface fault occurrence in Brazoria County is found to be very similar to that in Harris County. Surface fault patterns are determined to be related to regional growth fault trends and local salt dome density. Surface faults in Brazoria County are confirmed to be the surface expression of much larger faults present in the subsurface. In the Arcola Oil Field, interrelated movement histories of major faults and the development of related structures are traced back to the Early Oligocene. Of the tested predictive models, the Gibb's construction fails to describe listric fault shape while the compaction model is found to be an excellent predictive tool.

TABLE OF CONTENTS

LIST OF FIGURES

LIST OF PLATES

(Plates are folded into the rear pocket of this thesis)

FOR MY FAMILY

INTRODUCTION

This work is primarily an aerial photographic and field investigation of surface faults in Brazoria County, Texas. However, some representative surface faults were also studied in the subsurface to determine their three dimensional geometry and movement history.

Brazoria County is located along the northwestern Gulf of Mexico coastal plain (Figure 1). Faulting is a widespread phenomenon in this region. The Vicksburg and Frio Fault trends are bands of regional faults that ring the Gulf margin (Figure 2). Locally, salt structures influence patterns of faulting. Because of the oil producing potential of growth fault and salt structures, concentrated attention is usually focused on delineation of these features in the subsurface. Documentation of surface fault expression in the Texas Gulf Coastal counties is rare; however, one exception is Harris County where the surface faulting has gained a good deal of attention. In dollar amounts, the damage to man-made structures by fault activity in Harris County has been substantial, motivating efforts to delineate the surface faults so as to avoid potential destruction of property. To date, nearly 300 active surface faults have been mapped in the Houston metropolitan area (Figure 3). The fault problem in Harris County is such that

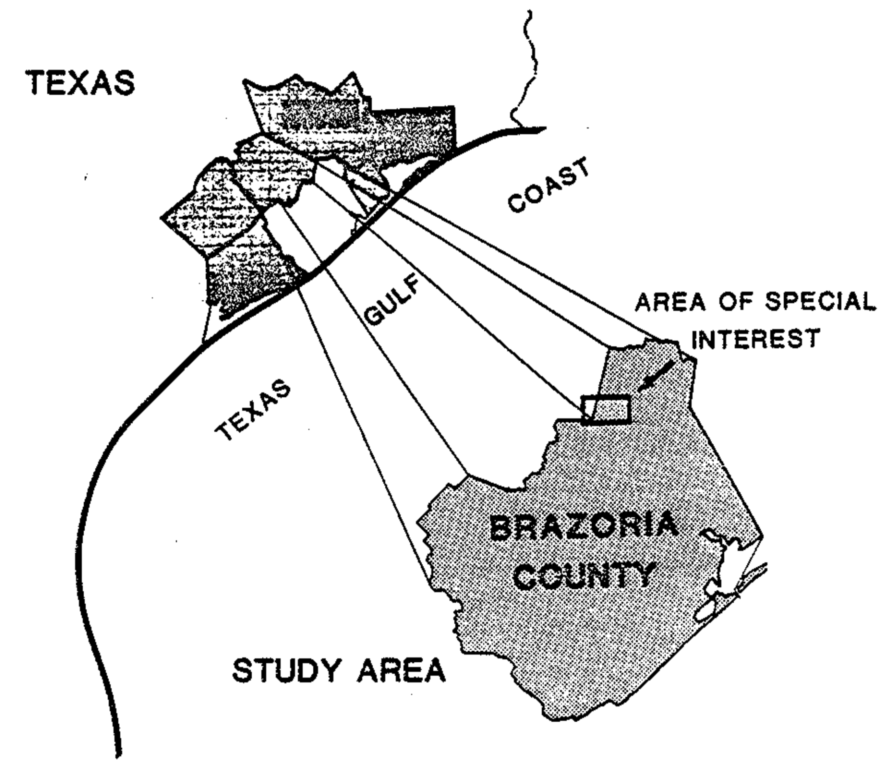

FIGURE 1: Study area, Brazoria County, Texas, in the Upper Texas Gulf Coastal zone. The area of special interest is the Arcola Oil Field, discussed in Chapter 4.

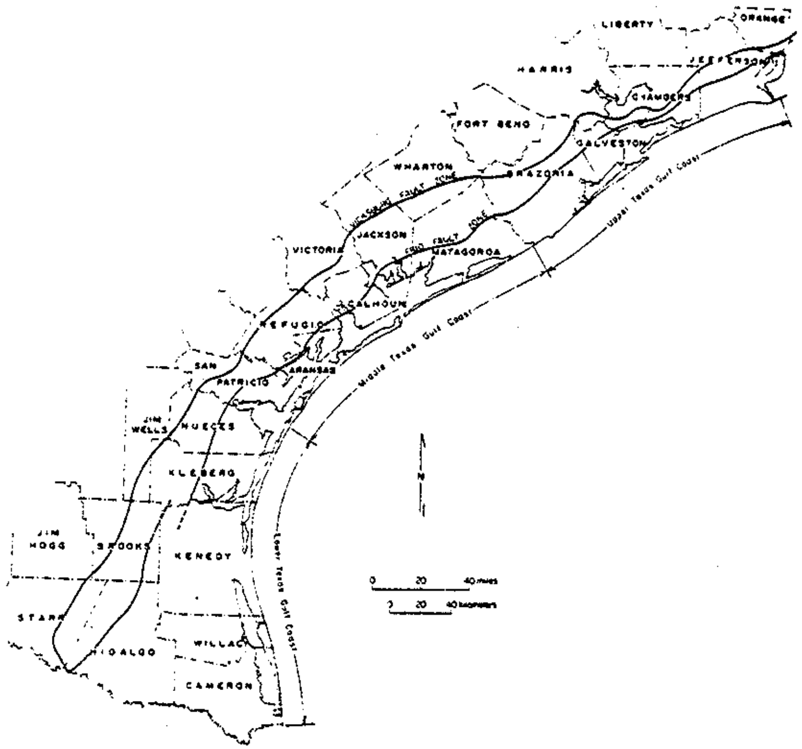

FIGURE 2: Vicksburg and Frio fault trends. (From Loucks, 1978).

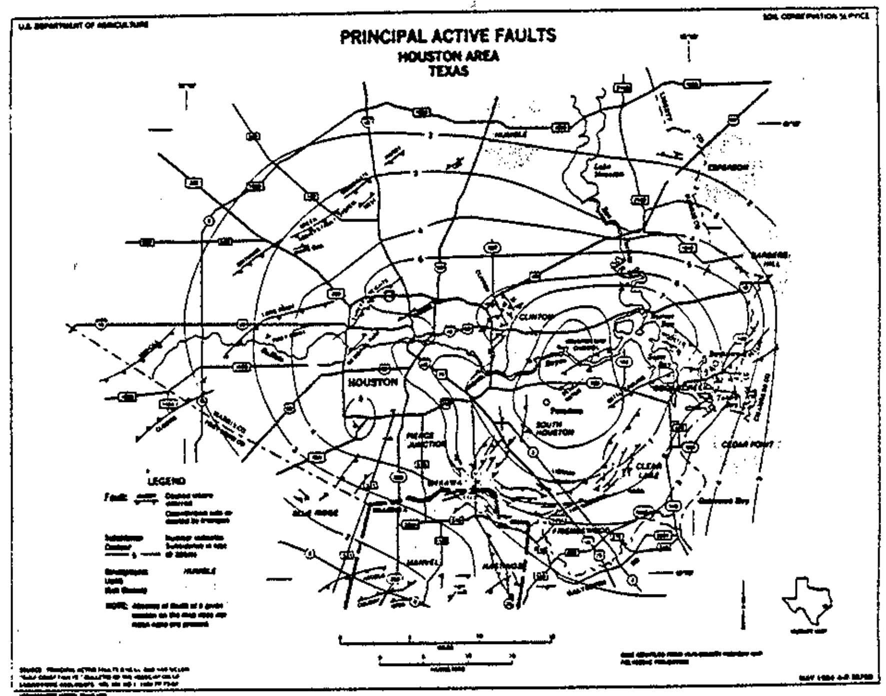

FIGURE 3: Active surface faults, Houston metropolitan area. Contours indicate amount of surface subsidence in feet. (From O'Neill and Van Siclen, 1984).

site investigations aimed at identifying possible surface faults are routinely done and often required before large construction projects are permitted. Of special concern is the permitting of facilities that present potential hazards to the environment, such as waste disposal sites.

Areally larger, and located in the same geologic province as Harris County, Brazoria County was known to contain only about 25 surface faults prior to this study. The large number of surface faults identified to the north in Harris County suggested that more such features were likely in Brazoria County. Thus, a county-wide investigation of surface faulting would provide a valuable land-use planning guide for future developments. To emphasize the need for such a study, the 1980 U. S. Census documents the rural character of Brazoria County as quickly changing, with northern portions posting a 50 to 60 percent population increase during the decade of the 1970's. The associated expansion of residential, commercial, and industrial facilities will necessitate further detailed site-specific studies.

It is the purpose of this study to identify surface faults in Brazoria County by use of aerial photographs, field investigations, reflection seismic profiles and geophysical logs. Until the current study, published information on the surface expression of faults here has

been limited to a small portion of the county included in studies done by Verbeek and Clanton (1978 & 1981), Elsbury and others (1980), and O'Neill and Van Siclen (1984). In this study I have identified and mapped active surface faults throughout the county, measured their offsets at the surface and in the subsurface (where data allows), examined some subsurface geometry and movement histories (in the Arcola test area), examined the patterns of surface fault occurrence in the county, and related these patterns to known regional trends and localized patterns (as around salt structures). In addition, the relationships between the down-to-coast Arcola fault and its antithetic partners are examined and models for predicting listric fault character are tested.

This investigation is considered to be a "first look" at the surface faulting in Brazoria County. It is hoped that the present study will serve as a solid foundation on which to approach other questions about the surface faulting in this region.

Previous Work

Faulting In The Northwestern Gulf Of Mexico Coastal Region

Studies of surface faulting in the coastal counties of Texas have been concentrated in Harris County, particularly in and around the city of Houston. These studies extend back more than 60 years, yet additional faults are still being identified. Because no county-wide investigation of surface faults had been done in Brazoria County, the present study is the first of its kind in this area.

In the northern Gulf of Mexico region subsurface fault patterns are divided into two broad characteristic styles: 1) Closely spaced faults forming complex patterns in association with salt and shale uplifts; and 2) Long, gently curving regional faults, which are generally longer than those related to salt/shale uplifts and trend subparallel to the coastline and generally to each other. The term " regional" means that these faults strike more or less parallel to the general trend of the shoreline of the Gulf of Mexico.

Studies of the subsurface character of Cenozoic and Tertiary age fault systems of the Gulf region abound. Good discussions may be found in Ocamb (1961), Hardin (1961),

Carver (1968), Cloos (1968), Bishop (1973), Bruce (1973), Crans et al. (1980), Christensen (1983), Jackson and Galloway (1984), Lowell (1984) and Ellis and McClay (1988). The general characteristics of listric fault systems are summarized in Bally (1981), Bally et al. (1981) and Shelton (1984).

Salt domes often control the patterns of faulting in the Gulf Coast. Discussions of salt domes may be found in Murray (1968), Lehner (1969), Humphris (1978), Stude (1978), Halbouty (1979), Martin (1980) Seni and Jackson (1983), Jackson and Talbot (1986), and Lerche (1987). Bishop (1977) presents a good discussion of shale diapirs. Studies that address all of these topics may be found in Quarles (1953), Bruce (1973), Dailly (1976), Withjack and Scheiner (1982) and Ewing (1983).

Both regional and salt dome related faults in the Gulf Coast are nearly always growth faults, particularly those that extend up to the present land surface. These are also called contemporaneous, or more precisely, syndepositional faults. This means the fault was active during sedimentation, resulting in a thickened (expanded) stratigraphic section on the downthrown block which progressively increases the vertical separation of stratigraphic markers across the fault with depth (Figure 4). If a fault extends to the land surface, continued

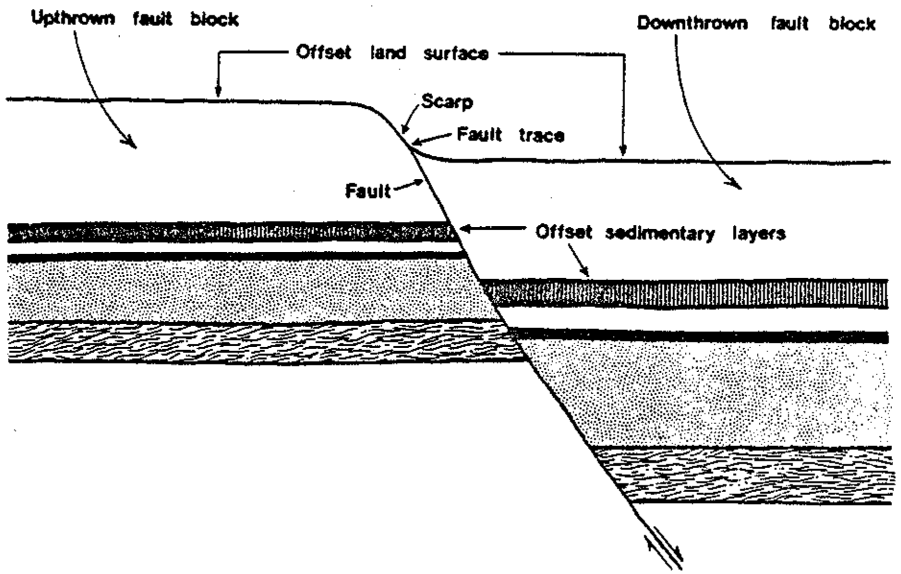

FIGURE 4: Vertical section through a growth fault. Note thickening of sedimentary layers on the downthrown side. This indicates active movement along the fault while sediments were being deposited. (From Verbeek, Ratzlaff and Clanton, 1979).

vertical movement will create a scarp, or vertical offset, of the land surface. Graben structures commonly develop within the regional fault systems with the "master" normal fault typically being a down-to-coast fault of considerable throw associated with one or more up-to-coast antithetic features of lesser displacement.

The Gulf Coast faults are almost invariably normal faults which reflect the extensional regime characteristic of this region. They are generally listric in nature, characterized by a decreasing dip angle with depth. Listric faults generally exhibit very steep dips near the surface, commonly 60-75 degrees from the horizontal, and gradually flatten with depth until they become roughly parallel to the bedding surfaces (Figure 5a). The fault surface is, therefore, a curved surface, concave upward. The concept of listric normal faults was apparently introduced by Edward Suess in the early 1900's in his descriptions of coal mine faults in northern France (Bally et al., 1981).

Movement associated with listric normal faults can be resolved into a downward component, and a horizontal component. The effect of movement on the flatter, deeper portion of the fault is to pull the two fault blocks apart creating a "potential void" (Van Siclen, 1978). This "potential" is not usually realized, however, because gravity simultaneously rotates the downthrown block so that

A.)

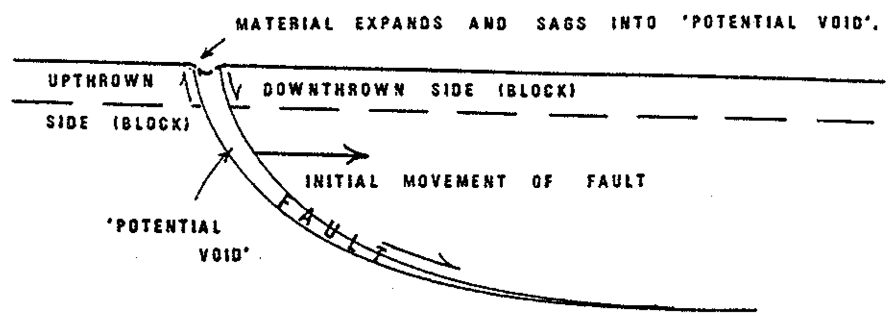

B.)

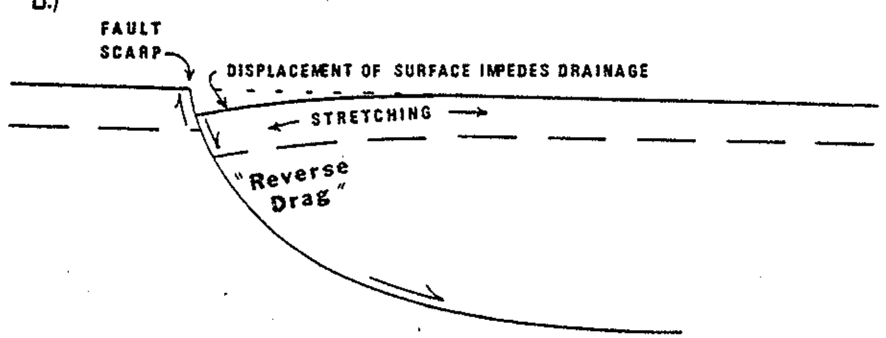

FIGURE 5: a.) Listric fault shape, steep near the surface, gradually flattening out with depth until movement is parallel to the bedding plane. Horizontal component of movement creates a "potential void" space.
b.) Development of reverse drag with movement along the listric fault. (From Van Siclen, 1981; modified from Bruce, 1973).

its strata dip back toward the fault plane, a condition referred to as reverse drag. This phenomenon thus creates an economically-important class of hydrocarbon-trapping structures (Figure 5b).

Surface Fault Studies

Only in the last 20 years or so, has the surface expression of Gulf Coast faults gained popular attention. Population increases and expanding urbanization has made identification of these faults of some importance. Surface faulting was first reported in the Texas Gulf Coast in the mid 1920's, beginning with articles by Minor (1925) and Pratt and Johnson (1926). These papers documented the development of 3 surface fault scarps in eastern Harris County at the Goose Creek Oil Field. Although it was later proved that the associated faults had been active in the Late Cenozoic, it is believed that high rates of oil production over the previous 10 years had reactivated or accelerated movement on them.

Another early identification of surface faults was by Barton (1930 & 1936). He first recognized what are today named the Hockley, Brittmoore and Breen faults in Harris County, and the Hitchcock fault in Galveston County (Norman, 1987). Barton recognized these features on the basis of prominent offsets at the surface and called them "flexure scarps". He said they marked deep-seated faults that have, "been buried to some extent by later alluvial deposits" (Barton, 1930, p. 1303). It does not appear that he viewed these features as currently active.

In 1962 Weaver and Sheets published a field guide to active surface faults and areas of subsidence in Houston and surrounding communities. The road log consistently points out the close proximity of active surface faults to areas of subsurface fluid production. Van Siclen (in Turner, Collie and Braden, 1966), mapped the Piney Point and over 40 additional surface faults in Harris County and in 1967 presented a more comprehensive article on active surface faulting in the Houston metropolitan area. He emphasized that, "Wherever well control is adequate, the surface faults are found to extend into larger faults at depth. However, the reverse is not true; many deep faults have no known surface expression." This is still the case. Van Siclen's paper included two diagrams, one prepared by McClelland Engineers, that showed the close correlation of water-level decline with subsidence between Katy and downtown Houston, and with the vertical displacement on the Long Point fault, for three intervals between 1906 and 1964. Based on these correlations, the production of subsurface fluids and the resultant reductions in formation fluid pressures was cited

as the major cause of increased historic fault activity. Examining the possible effects of oil and gas production on subsidence, Holzer and Bluntzer (1984) conclude that hydrocarbon production exhibits very little additional influence on overall subsidence of the Houston-Galveston area, which they also largely attribute to ground water withdrawal.

In the 1970's a number of articles were published on surface faulting in the Houston metropolitan area and in the Harris-Galveston County subsidence district. In 1971 Sheets attempted to draw attention to the economic aspects of the Houston fault problem, noting natural geologic causes and downplaying man's role in their activity. Taking exception to Van Siclen's (1967) intrepretation of the cause of fault movement, Castle and Youd (1972) stated that reductions in fluid pressure would increase the stability of the sedimentary section within the subsided area, and so not contribute toward surface failure. They dismissed the decline of piezometric levels as a direct cause of surface faulting. Instead they supported Lee and Shen's (1969) proposal that differential surface subsidence and the associated differential compaction at depth due to fluid withdrawal, is the primary cause of fault reactivation. Castle and Youd proposed that the historically active surface faults are located in positions of extensional strain on the perimeter of subsided areas.

Reid (1973) presented his findings on creep studies performed on three Houston faults. He found an average increase in vertical separation of 1.20 cm/year for the Long Point, Piney Point and Eureka Heights faults. He also pointed out an association between accelerated piezometric pressure declines and increased rates of movement along the faults. He attributed much of the recent vertical separation to consolidation of depressured aquifers.

In the early 1970's the Bureau of Economic Geology, University of Texas at Austin, conducted a very broad study of surface lineaments throughout the Texas coastal zone (Fisher et al., 1972). Hundreds of lineaments of regional extent were identified and mapped at a 1:125,000 scale on the Physical Properties Map of a series of seven volumes of a Geologic Atlas of the Texas Coastal Zone. The features mapped in this study are very straight to gently curved, show little relationship to salt domes and are very long, many extending for more than 60 miles. Generally they bear only vague resemblance to surface and subsurface faults actually mapped in this region (Figure 6). It is my opinion, based on my research in Brazoria County, and the research of others in this region, that the lineament map is not an accurate or reliable source of information on the

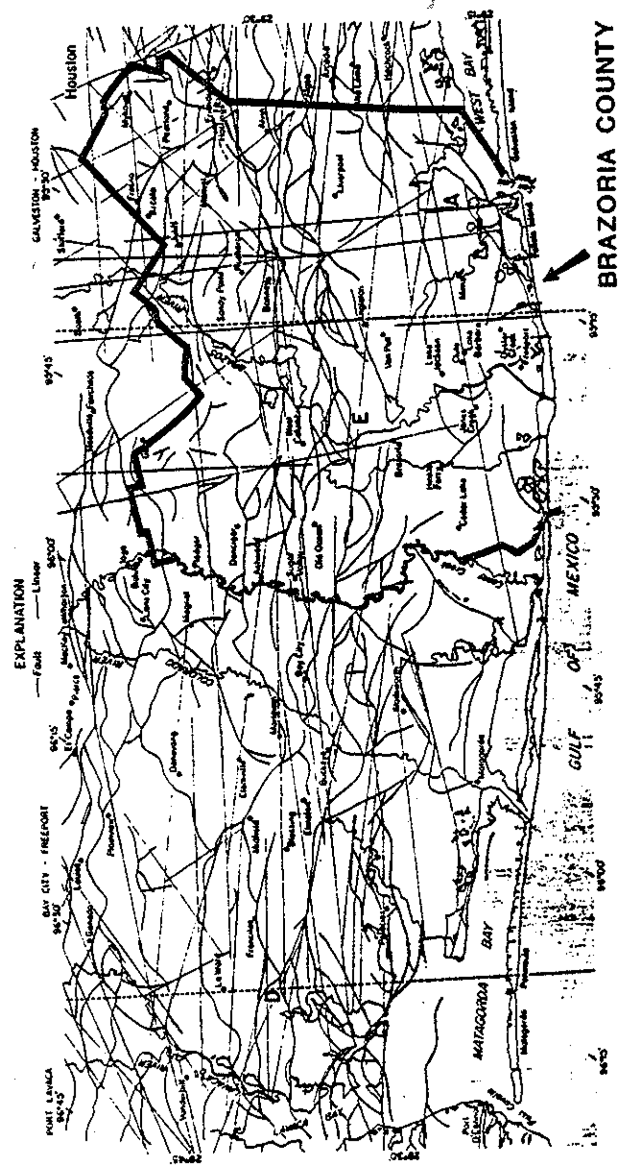

FIGURE 6: Physical properties map showing proposed surface fault linears, Geologic Atlas of the Texas Coastal Zone, Houston-Galveston region, Bureau of Economic Geology, University of Texas at Austin. (Fisher et al., 1972).

location or distribution of surface faults. A difference of opinion is expressed by Kreitler (1976a) who reported the distribution of these regional lineaments agrees favorably with known surface fault locations. His conclusions are based on a statistical analysis which suggests a relationship between the hundreds of lineaments reported, and faults actually mapped at the surface. In most cases it is difficult to see a relationship on which to base such an analysis.

Kreitler (1976b) examined possible fault control on land subsidence and suggested that in areas of little fluid withdrawal, faults are either inactive or moving slowly enough that they act as partial hydrologic barriers which effectively compartmentalize land subsidence. Gabrysch and Holzer (1978) found that the data collection methods used in this study were not reliable. There has been no confirmation of Gulf Coast faults acting as hydrologic barriers to the movement of near-surface groundwater.

As the surface faulting problem gained greater recognition in the Houston area, more effort was made to map surface faults, mostly in connection with geotechnical investigations for construction. Van Siclen (1978) conducted a specific site investigation at the Addicks and Barker Dams on Buffalo Bayou in Harris County. In 1978 and 1979 Verbeek and Clanton documented surface faulting in

parts of the north-central, western and southeastern Houston metropolitan area. These publications are notable for presenting nearly 100 faults mapped at a scale of 1:24,000, and for offering an excellent summary on the many aspects of surface faulting in this region.

Heuer (1979, Master's Thesis) examined 4 faults in northwestern Harris County. He presents a good review of the literature on several mechanisms proposed for growth faulting. He concludes that: differential compaction is not a major factor involved in fault movement; near-surface faults do not act as hydrologic barriers; current data neither confirm nor refute the theory of fault activation generated by lowering of aquifer pressures; and the faults do not follow the concentric fault pattern hypothesized by the radially directed tensional stress theory proposed by Lee and Shen (1969) and advocated by Castle and Youd (1972).

Papers by Elsbury, Van Siclen and Marshall (1980) and Van Siclen (1981) review and update known Houston faults and techniques used in their identification. Verbeek and Clanton (1981) offer another comprehensive review including case histories of modern faulting in the Texas Gulf Coast. They also present a 'photographic portrait' of surface faulting for the Houston metropolitan area (Clanton and Verbeek, 1981). The application of Landsat imagery for identification of Houston area faults is reviewed by Everett and Reid (1981) and a Houston Geological Society Guidebook (1984) includes a road log to locations of subsidence and faulting in East Harris County.

O'Neill and Van Siclen (1984) describe a mechanism by which faults my be reactivated by lowering of the piezometric surface. A procedure for estimating the drawdown necessary for reactivation is presented as well as a procedure to estimate a safe siting distance for structures along fault traces. The authors recognize a link between production of groundwater, ground subsidence, and coincidence of active faulting in space, time and amount.

Finally, a bright note in this review of previous works on surface faulting; Holzer and Gabrysch (1987) document a period of partial recovery of piezometric levels in eastern Houston. The Harris-Galveston Coastal Subsidence District, formed 1976, was authorized by the state legislature to restrict groundwater production. Pumping restrictions imposed by the Subsidence District resulted in partial piezometric level recoveries as early as 1977 and the authors report that fault activity has declined from that time to the present.

Regional Geology and Geologic History

Brazoria County is located on the upper Texas Coastal Plain and extends to the coast in about the middle of the Houston Embayment (Figure 7). Surface deposits consist of very gently coastward-dipping beds of the Pleistocene Beaumont Formation, and sediments of Holocene age along the Brazos and lesser streams and along the shore (Figure 8).

Tectonics

The northern structural rim of the Gulf of Mexico is the Ouachita fold/thrust belt, partly exposed in the Ouachita and Marathon uplifts (Figure 9). This belt formed during Early Pennsylvanian through Early Permian time by the closing of a proto-Gulf, to firmly incorporate North America into the supercontinent of Pangaea (Wickham, et al., 1976). The presence of this structural rim strongly influenced the updip limits, thicknesses and facies of Triassic and younger deposits in the Gulf (Woods and Addington, 1973). The southern edge of this structural rim became the site of major extension and faulting as the present Gulf of Mexico opened along with the Central North Atlantic Ocean.

During the break-up of Pangaea, separation of North and South America began in the Late Triassic with an early

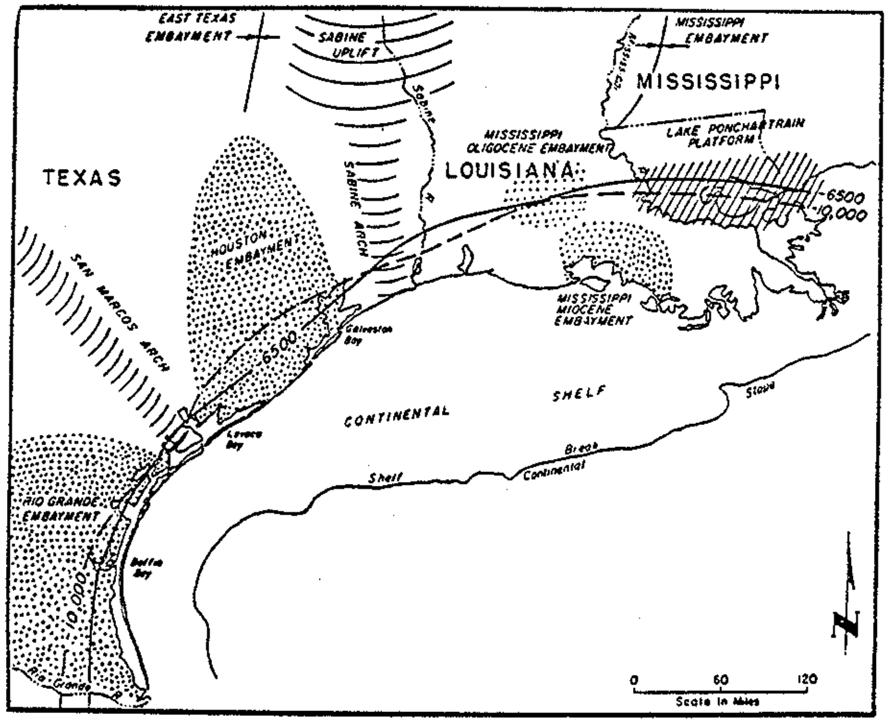

FIGURE 7: Major structural elements within the tectonic framework of the northern Gulf of Mexico Coast. (Modified from Hardin, 1962).

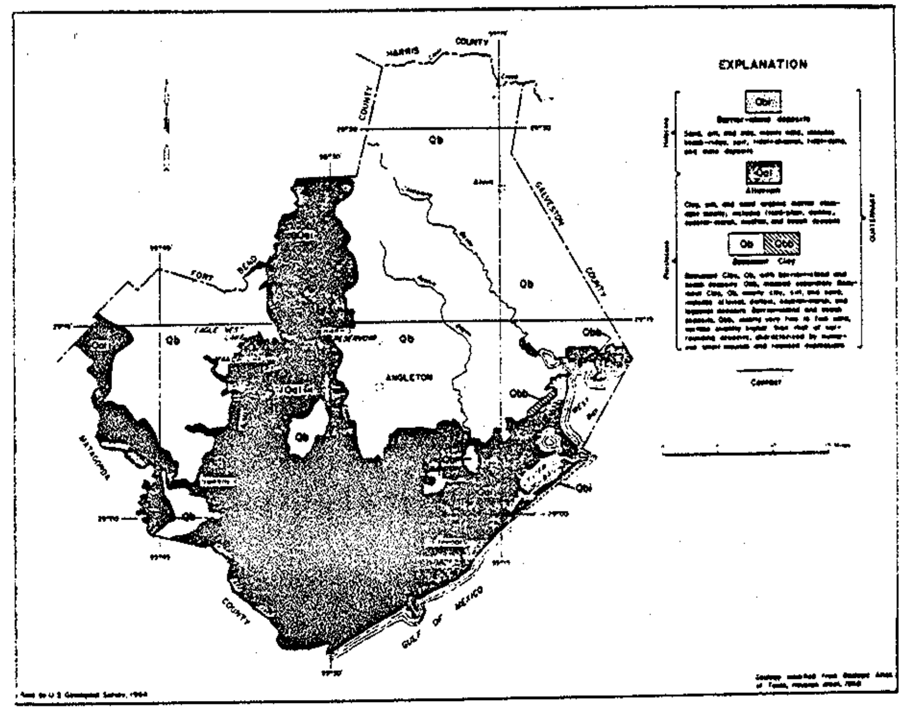

FIGURE 8: Surface deposits, Brazoria County, Texas. (From Sandeen and Wesselman, 1973).

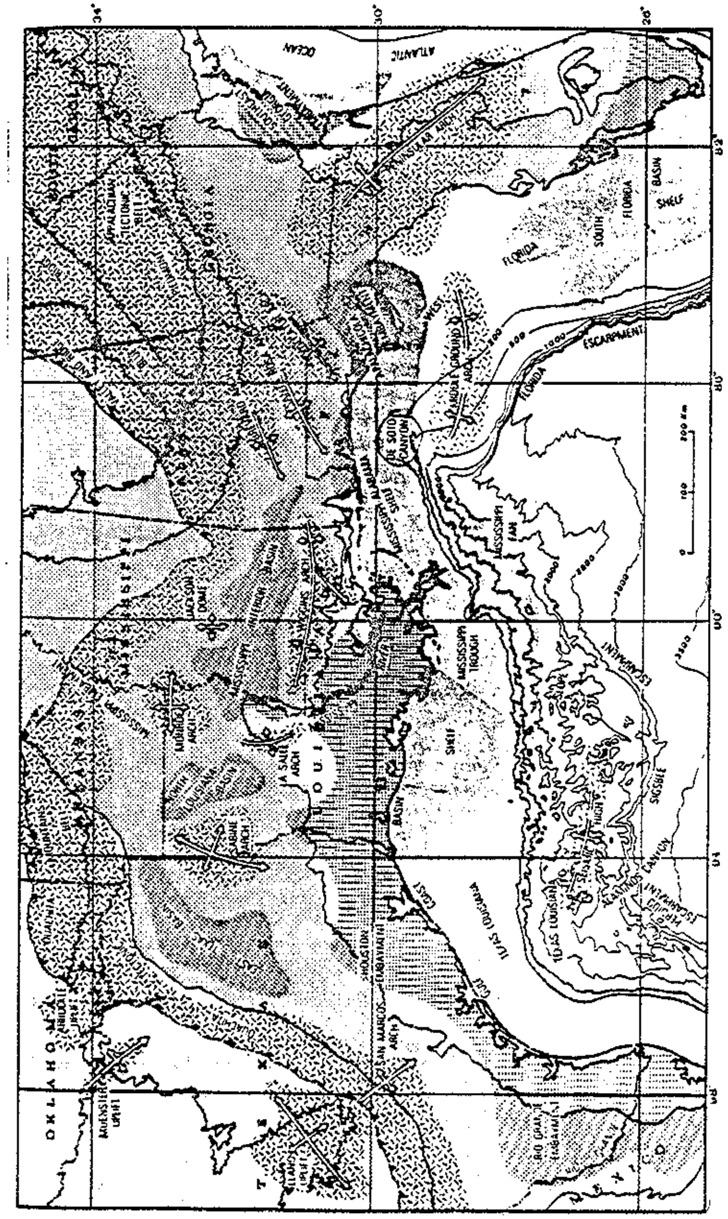

FIGURE 9: Ouachita fold belt and other structurally positive areas and sedimentary basins of the northern and eastern Gulf of Mexico regions. (From Martin, 1978).

period of rifting that opened the Interior basins (Van Siclen, 1984). This extension ended with the opening of a new rift zone farther south, which ultimately developed into the central Gulf of Mexico basin (Van Siclen, 1984, p. 269). By the end of the Triassic the basins were filled with fluvial and deltaic red beds of the Eagle Mills Formation along with some basaltic volcanic rocks. The red beds are considered to be analogous to the Newark Group of eastern North America and are thought to be precursors of the subsequent seafloor spreading (Martin, 1978). With continuing extension the graben basins and narrow, developing ocean basin to the south became flooded with seawater (White and Burke, 1980; Walper, 1980).

By late Middle Jurassic time the Louann and equivalent evaporites began to accumulate on oceanic crust and on the subsiding margins of the continental crust (Walper, 1980). Figure 10 provides a generalized stratigraphic column for the Texas - Louisiana portion of the Gulf Coast for the Paleozoic to Upper Cretaceous. The Louann evaporite deposits locally reach thicknesses up to 10,000 feet and are confined to major salt basins delineated by five prominent structural features oriented perpendicular to the axis of the opening Gulf: the Rio Grande Embayment; the San Marcos Arch; the East Texas Embayment (Houston Embayment downdip);

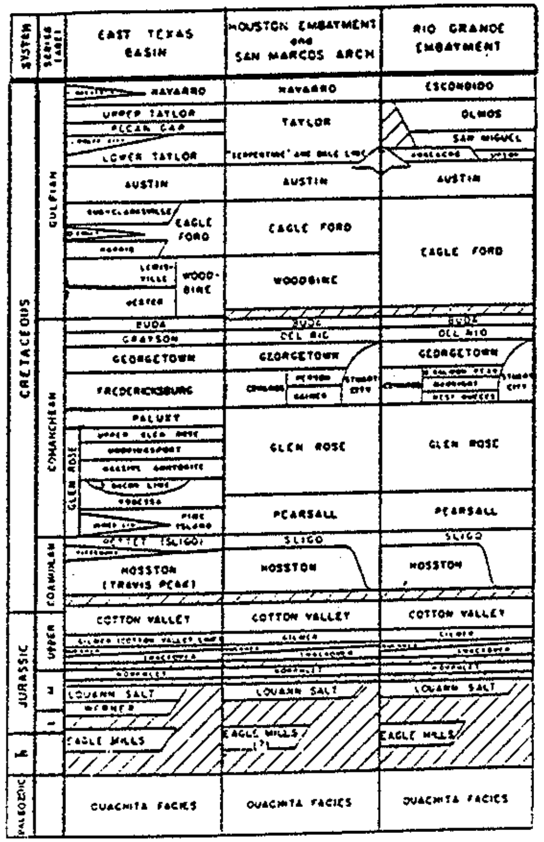

FIGURE 10: Generalized stratigraphic column of the Paleozoic through Upper Cretaceous for the Gulf Coastal region of Texas. (From Galloway and others, 1983).

the Sabine Uplift and Arch; and the Mississippi Embayment (Figures 7 and 9).

With the opening of the Gulf the first marine transgression deposited the upper Jurassic Norphlet Formation over the Louann salt. This was followed by the Smackover Limestone, the accumulation of which was probably controlled by a structural hingeline where deposition kept pace with subsidence (Bishop, 1974).

The Late Jurassic closed with deposition of the Haynesville Formation and the Cotton Valley Group. By this time sea floor spreading had stopped in the Gulf and the basin began the long history of subsidence which would permit the accumulation of over 60,000 feet of Mesozoic and Cenozoic sediments and earn the basin the title of the Gulf Coast Geosyncline (Hardin, 1962).

Sedimentation during the Cretaceous was influenced by frequent eustatic changes in sea level (Mc Farlan, 1977). Early Cretaceous strata in the Gulf are mainly shallow marine carbonate rocks deposited over broad shelf areas. They include the Hosston Formation, Sligo Limestone, Hammet (Pearsell) Shale, Cow Creek Limestone and Hensell Sandstone.

During the Middle Cretaceous sea level was stabilized and gradual subsidence of the carbonate shelf combined with low influx of terrigenous sediment led to an extensive shelf-edge complex known in the subsurface of south Texas as the Stuart City reef trend and in central Texas as the Glen Rose-Edwards Group (Martin, 1978). Upper Cretaceous deposits in the coastal plain reflect the beginning of mountain building in the western United States. At this time carbonate production essentially ended in this portion of the Gulf and mainly sandstones, shale, marl and chalk with some local reef-like carbonate beds were deposited. Formations include the Eagle Ford, Austin Chalk, Taylor and Navarro.

During the Cenozoic a clastic embankment was built out into the Gulf as the result of a tremendous influx of sediments from the western continental interior in response to the Late Cretaceous-Paleocene Laramide Orogeny (Martin, 1978). Sediment supply far exceeded the rate of basin subsidence and resulted in the northern Gulf margin prograding up to 250 miles seaward from the edge of the Cretaceous carbonate shelf (Martin, 1978).

The five prominent structural features that influenced sedimentation during the Jurassic (Rio Grande Embayment, etc.) also had a strong influence on Cenozoic sedimentation in the Gulf (Hardin, 1962). As would be expected, these features allowed the greatest amount of deposition in the negative areas of the embayments while thinner layers were deposited over the positive arches.

Sedimentation rates in the Cenozoic were not uniform throughout the Gulf. Sediments accumulated in depocenters or depoaxes, the locations of which were not related to water depth but to the source of sediment supply, i.e., the mouths of rivers (Figure 11) (Murray, 1961). Thus depocenter sediments are largely deltaic, deposited under marginal marine conditions. Depocenters show not only a seaward, but also an eastward migration during the Cenozoic. This trend was the result of a shift in sediment supply from the ancestral Rio Grande-Nueces River system in southwestern Texas to the Mississippi River system in Louisiana as the western drainage was increasingly captured by the latter (Martin, 1978).

Seaward of the early Cretaceous shelf edge are "flexure" zones which have also modified Cenozoic sedimentation in the Gulf. They trend subparallel to the coast and are defined as zones downdip from which the rate of dip and thickening of beds is accentuated (Hardin, 1962). The flexure zones themselves are accentuated by the formation of regional contemporaneous normal faults. According to Hardin, the origin of flexures can be attributed to deposition across the shelf break in association with the contemporaneous formation of regional faults. It should be noted that each succeeding younger flexure is located seaward (downdip) from the preceding

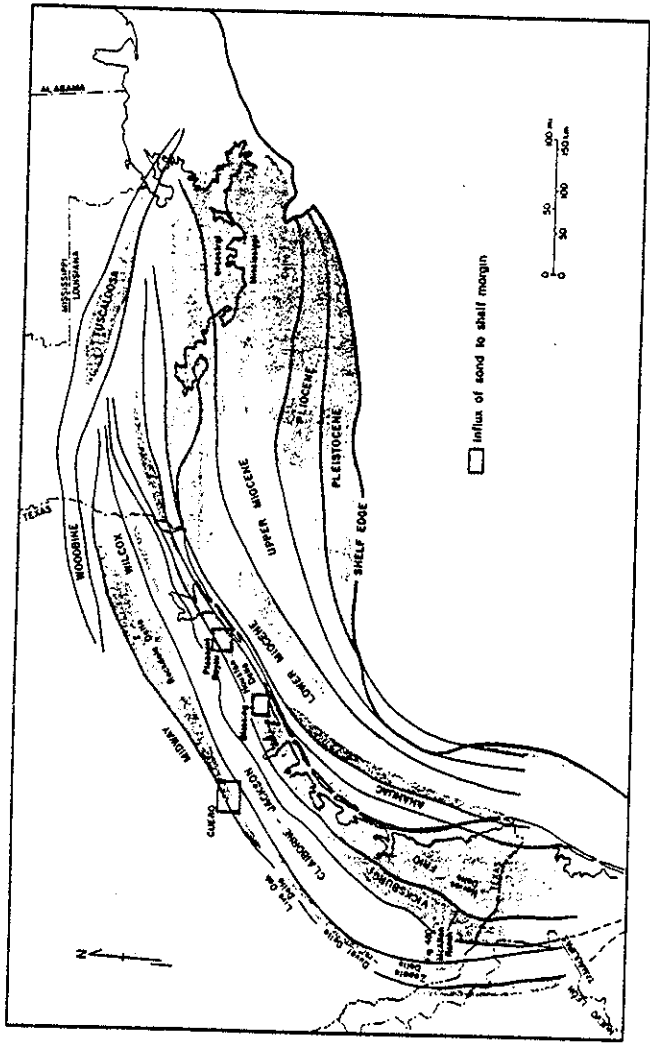

FIGURE 11: Shelf-margin trends and shelf-margin delta complexes (depocenters or areas of major sand influx) in northwestern Gulf of Mexico Basin. (After Winker, 1982).

older one so that the thickest sequence of beds of each succeeding younger stratigraphic unit is downdip of the preceding older unit.

Tertiary sedimentation in the Gulf began with deposition of the transgressive Paleocene Midway Group (Figure 12) consisting of marine clays with interbedded limestone. The regressive fluvial deltaic and lacustrine sediments of the Eocene Wilcox Group were deposited next, followed by the widely fluctuating fluvial, coastal and marine deposits of the Claiborne Group. Fluctuations continued into the Late Eocene with deposition of the marine and fresh water swamp deposits of the Jackson Group. Deposition of the marine unit of the Jackson was in response to a major world-wide transgression. However, the bulk of Jackson sediments are regressive (Dupre, 1987). It has been speculated that the large sediment influx at this time may be in response to the last surge, or rejuvenation phase, of the source area to the west, i.e., the Rocky Mountains and Sierra Madre Oriental (Hardin, 1962).

The thickest accumulation of Eocene and Oligocene deposits in the Gulf can be found in the Rio Grande embayment, indicating that the ancestral Rio Grande and Nueces River systems were the major sediment conduits at this time. A shift in sediment supply back to the northeast would soon begin, however, with the ancestral Brazos,

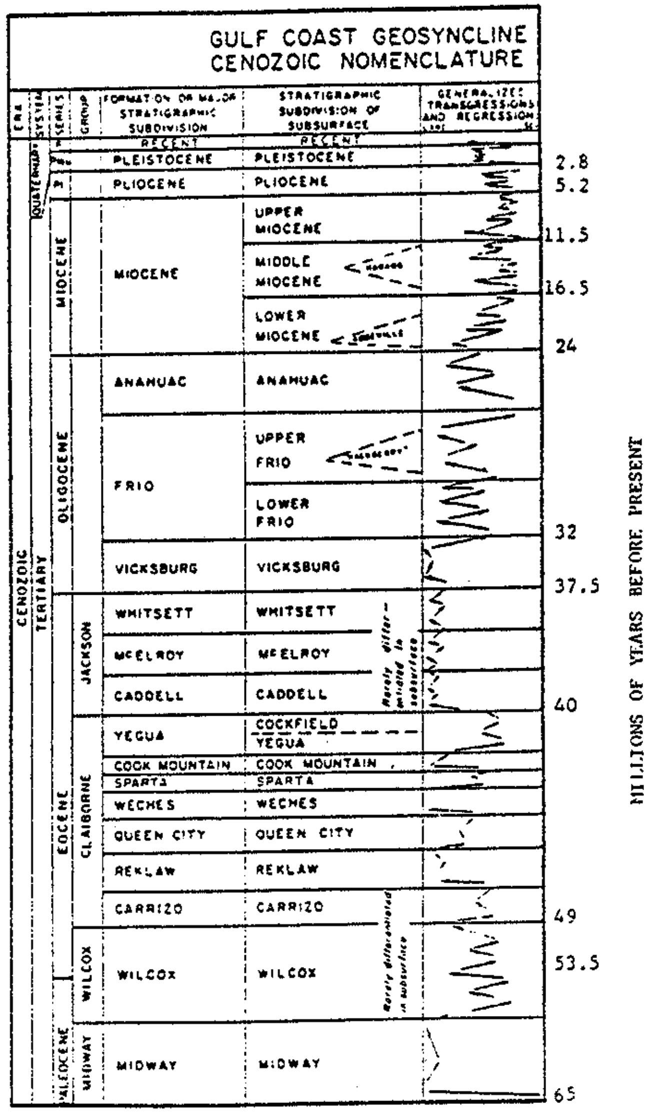

FIGURE 12: Generalized stratigraphic column for the Cenozoic of the Gulf Coastal region of Texas and Louisiana. (From Hardin, 1961).

Colorado, Sabine and Mississippi Rivers beginning to show increased importance in the Late Eocene and Oligocene (Martin, 1978).

The Oligocene began with deposition of the transgressive shales and sands of the Vicksburg Group. Rapid thickening of the Vicksburg occurs across the Vicksburg Fault Zone, which roughly parallels the Texas Coast (Figure 2). Succeeding the Vicksburg is the Catahoula Group, consisting of the Frio and Anahuac Formations of Middle to Late Oligocene age (Dupre, 1987).

A subsurface stratigraphic unit of special interest to this thesis is the Oligocene Frio Formation. Some of the major faults in the county have been traced down into the Frio with the aid of well logs.

The Middle Oligocene Frio Formation consists of transgressive and regressive sands and shales which reach maximum thicknesses of 10,000 feet. Sanwiched between the transgressive shales of the underlying Vicksburg Group and overlying Anahuac Shale, the Frio Formation sands were deposited within aggrading lobate deltas of the Houston Delta System. Logs of wells in northwestern Brazoria County show the formation to be a dominantly sand package 2100 feet thick with thin interbeds of shale. The formation thickens rapidly across the Vicksburg and Frio Fault Zones.

The Late Oligocene Anahuac Shale was deposited during a major marine transgression. It is over 900 feet thick in Brazoria County.

During the Miocene the shoreline remained relatively stable. Miocene sediments in the upper Texas coast were derived principally from the Mississippi River system as sediment supplied to the Rio Grande embayment was drastically reduced. It is believed the reduction was the result of segmentation of the Rio Grande drainage basin into bolsons produced by block faulting. During this time the Mississippi River depocenter was located as far west as the High Island-Sabine Pass area (Woodbury, 1973). In the region that includes Brazoria County, local rivers fed a number of small, wave-dominated deltas forming the shales and thick, vertically-stacked deltaic sands of the Oakville and Lagarto Formations (Dupre, 1987).

Pliocene deposits in the Gulf Coast accumulated in a prograding clastic wedge. In Brazoria County it is represented by the Goliad Formation, which consists of coarse basal sands overlain by more clayey units. Goliad beds are generally the youngest to be displaced by the numerous shallow and deep-seated salt structures that underlie Brazoria County (Sandeen and Wesselman, 1973).

Surface Geology

The surface and near-surface deposits in this area reflect the transgressive and regressive cycles that occurred in response to the glacial stages of the Pleistocene Epoch. During glacial stages when sea level was low, the major rivers in the area, the ancient Colorado, Brazos, and Trinity Rivers, deepened and widened their valleys and deposited their loads at or near the outer edge of the Continental Shelf. During each following interglacial stage, or high-stand of sea level, the river valleys would fill, developing broad flood plains which would continue downstream into broad deltaic plains at the coast that sometimes merged, occupying the entire coast (Van Siclen, Class Notes).

The surface deposits in Brazoria County consist of either Recent alluvial sediments or the very gently gulfward-dipping sediments of the Late Pleistocene Beaumont Formation (Figure 8) (Sandeen and Wesselman, 1973). Often called the Beaumont clay, all three members of this formation, the Oberlin, Almeda, and Eunice, (Van Siclen, 1985), contain few coarse sediments. The present "black gumbo" top soil has developed on the top of these units throughout much of the county.

In Brazoria County, the Beaumont Formation was deposited predominantly during the last major Pleistocene highstand of sea level by the ancient Colorado and Brazos Rivers. During this time the Beaumont alluvial plain formed as a series of coalescing deltas with slight gulfward tilting of the formation occurring after deposition (Winker, 1979).

Le Blanc and Hodgson (1959) report that the glacial advance after Beaumont deposition lowered sea level 300-400 feet below the present level. In response, all the rivers in the region, including the ancient Colorado, Brazos and Trinity Rivers, entrenched their flood plains by channel erosion. The valleys extended out to a shoreline that may have been 50 to 140 miles seaward of the present shoreline. During this time the Colorado and Brazos Rivers built a joint shelf-margin delta and established the present bulge in the shelf edge (Figure 13) (Winker, 1979, p. 441). A few thousand years ago the Colorado River avulsed from its wide alluvial valley, now occupied by Caney Creek and the San Bernard River, to its present location in a narrow alluvial valley to the east (Figure 14) (Le Blanc and Hodgson, 1959). In the early Recent, melting of the Pleistocene glaciers caused the sea level to rise. Streams filled their entrenched valleys and flooded the lower portions of their channels to form estuaries. Some of the larger streams,

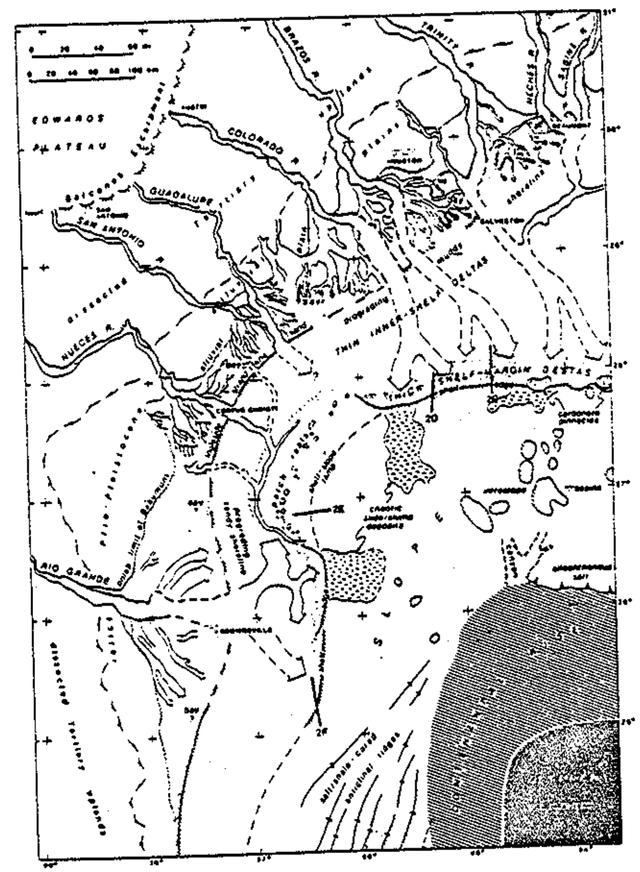

FIGURE 13: After Beaumont deposition a low-stand of sea level (300-400 feet below present levels) caused entrenchment of river valleys and progradation of the shoreline to the shelf edge. (From Winker, 1982).

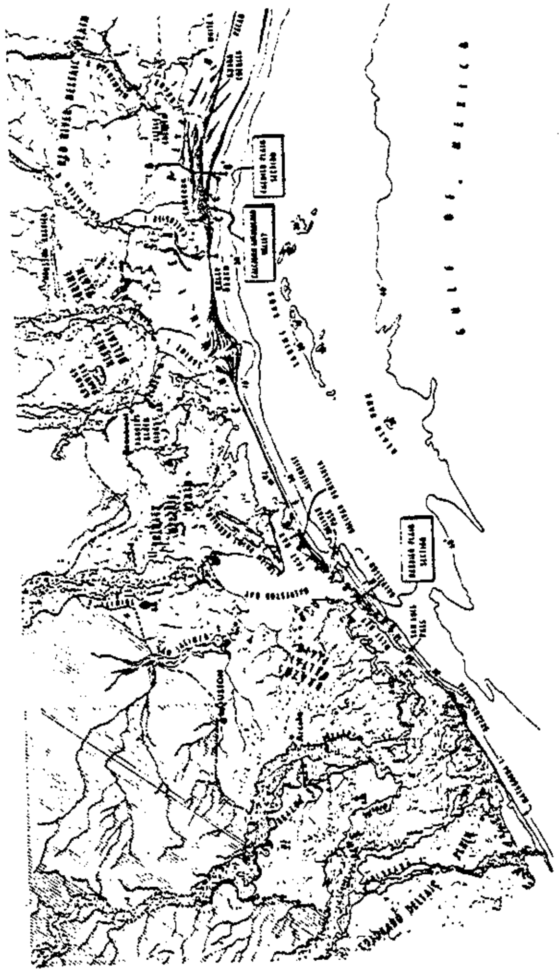

FIGURE 14: The present location of the Colorado River in a narrow alluvial valley is a fairly recent one. A few thousand years ago the Colorado River avulsed from the much wider alluvial valley to the east, now occupied by Caney Creek and the lower portion of the San Bernard River. (After Bernard, LeBlanc and Major, 1962).

like the Brazos and Colorado Rivers, with large alluvial valleys and high sediment load, were able to fill their estuaries and build broad deltaic plains which empty directly into the Gulf of Mexico.

It is apparent that many of the meander-belt ridges east of the present course of the Brazos River represent some fairly late Pleistocene channels of the Brazos (Van Siclen, 1985, p. 526). The youngest of these former meander-belts was occupied by the Brazos as recently as 1000 years ago and was since been inherited by Oyster Creek (Bernard et al., 1970) (Figure 14). Since avulsion of the Colorado River there has been erosion of the delta built jointly by the Colorado and Brazos Rivers. Despite this, the development of the merging deltaic plains of these rivers has had a significant influence on the segment of the Texas coast between Galveston Island and Matagorda Bay (Le Blanc and Hodgson, 1959).

Displacement of post-Goliad beds by salt structures in Brazoria County is generally limited to the area around Damon Mound, West Columbia, Allen, Clemens, Bryan Mound, Stratton Ridge, and Hoskins Mound Domes (Sandeen and Wesselman, 1973). Four of these domes create a distinct rise in the land surface. Damon Mound is the most notable, rising 83 feet above the surrounding land surface; next is Hoskins Mound, rising 25 feet; and finally Bryan Mound and the West Columbia Dome both rising 10 feet above the coastal plain.

Except for a portion of Mustang Bayou above Alvin, present drainage largely occurs in the former back swamp and flood basin areas between the former meander-belt ridges of the Brazos and Colorado Rivers (Van Siclen, 1985), and drain directly to saltwater.

Other surface features in Brazoria County include: a widespread and fairly continuous pattern of relict meander ridges; a portion of the relict Ingleside\barrier island system which extends intermittently from western Louisiana to Corpus Christi, Texas; and two kinds of microrelief features - small depressions and pimple mounds.

Salt Tectonics

The movement of salt has greatly affected the structural fabric of the northern Gulf margin. Salt domes pierce and uplift younger sediments in the interior basins of eastern Texas, northern Louisiana, central Mississippi, and along the Texas and Louisiana coasts from the San Marcos arch to the Mississippi Delta (Figure 15) (Woodbury, et al., 1978). Southern limits of the northern Gulf salt structures are defined by topographic steepening along the Sigsbee and Perdido Escarpments near the center of the Gulf of Mexico.

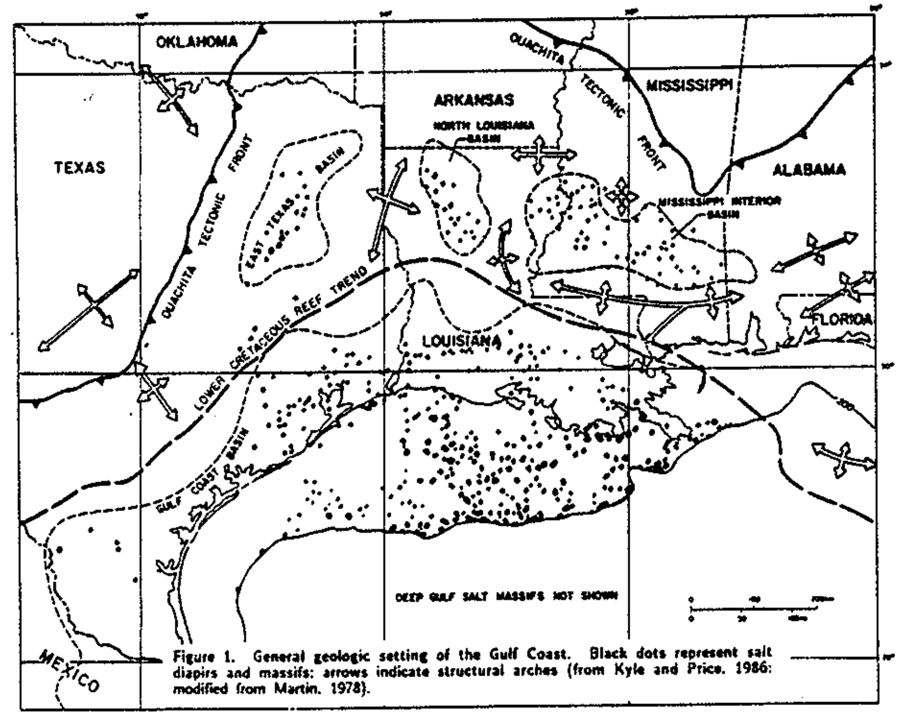

FIGURE 15: Salt basins of the northern Gulf margin; arrows indicate structural arches. (Modified from Martin, 1978).

It has been proposed that salt diapirs form where salt is initially thick and there has been sufficient sediment loading to initiate movement (Humphris Jr., 1978). Jackson and Talbot (1986) feel it is reasonable to assume that the initial geometry of a salt body after deposition is tabular, thinning laterally through facies changes into zones of other evaporites and clastics. In this case average salt thickness would vary only where the basin floor was initially irregular or where basin subsidence was not uniform. Jackson and Talbot (1986) feel these initial geometric variations in the salt body may determine the locale of later salt movement.

The geometric evolution of a salt structure is envisioned to progress from a concordant, low-amplitude structure to a discordant, high-amplitude intrusion and to a salt extrusion in the extreme case. However, evolution or growth of the structure may stop at any stage (Jackson and Talbot, 1986).

The Gulf coastal area is divided into zones characterized by salt structures of similar size, shape and spatial distribution (Martin, 1978). Variations in structural style between zones are attributed to differences in initial salt thicknesses and the amounts and rates of sedimentation.

In Brazoria County, salt diapirs may range in diameter from 1 to 8 kilometers but are normally less than 6 kilometers across.

The Study Area

Brazoria County is located in southeast Texas and is bordered by Harris County on the north, Fort Bend County on the northwest, Wharton County on the west, Matagorda County on the southwest, the Gulf of Mexico on the southeast, and Galveston County on the northeast (Figure 1). This area is covered by all or part of thirty-four USGS 7&1/2 minute topographic quadrangles and contains an area of approximately 1,422 square miles. It is part of the nearly flat Gulf of Mexico Coastal Prairie which rises inland toward the northwest at an average slope of less than 2 feet per mile. Surface material over much of the county consists of Quaternary alluvium and the black gumbo soils of the Beaumont Formation (Figure 8).

Elevations range from sea level to approximately 65 feet to the north and west. There are at least 18 salt domes in the County, 4 of which exhibit surface expressions such as hills, sinks or both. The highest point in the county is Damon Mound, a salt dome, the caprock of which rises 83 feet above the surrounding plain to reach an elevation of 146 feet above sea level.

From the coast to at least five miles inland the land surface consists of coastal swamplands, bays and beaches. The Brazoria National Wildlife Refuge, located landward of

Follet's Island, and the San Bernard National Wildlife Refuge, located in the Cedar Lakes area, are included within this region.

Rivers and streams drain the county from the northwest to the southeast toward the Gulf of Mexico. Major streams include the Linnville Bayou and Cedar Lake Creek along the southwestern boundary of the county; Oyster Creek, San Bernard River and Brazos River in the southern half of the county; Austin and Chocolate Bayous in the northern part of the county; and Clear Creek at the northern boundary.

Since its settlement in the early 1800's, Brazoria County has been an agricultural and cattle producing area. In spite of a large population increase over the last 10 to 15 years, much of the county remains rural with a large percentage of the land still devoted to rice farming and cattle grazing. Substantial tracts of land in the county are currently held by the Texas Department of Corrections which operates the Darrington, Ramsey, Retrieve, and Clemens State Prison Farms.

Mineral resource development began in Brazoria County with the discovery of oil at Damon Mound in 1901 (Sandeen & Wesselman, 1973). Sulphur was first mined at Bryan Mound in 1913. Other natural resources include sand, clay, lime, and natural gas. Major industries are engaged in the production of these natural resources.

The largest city in the county is Freeport, located near the mouth of the Brazos River. In conjunction with a number of surrounding cities, it makes up the Brazosport Industrial Complex. Nine chemical plants located within the complex produce a variety of chemicals and chemical products. Beginning in Freeport in 1939, minerals such as magnesium, salt, iodine, fluorine and bromine have been extracted from sea water at two of the chemical plants. The Department of the Interior runs an experimental sea-water desalination operation in the area which supplies fresh water to the city of Freeport and Dow Chemical Company (Sandeen & Wesselman, 1973).

METHODS OF INVESTIGATION

The primary investigative techniques used in this study include: examination of aerial photographs, including infrared images, to locate lineaments that might arise from fault activity; field investigations to determine the cause of the lineaments; use of borehole electric logs to identify faults, and determine their subsurface geometry; use of seismic reflection profiles to confirm surface faults and examine them in the subsurface; and experimentation with various growth fault models to compare predicted geometries with observed geometries.

Aerial Photographs

Black and white aerial photographs and high resolution false-color infrared aerial photographs were used as reconnaissance tools to locate active and recently active faults throughout the county.

Complete black and white air photo coverage of the county was made available by the Brazoria County Soil Conservation Service office in Angleton. Several generations of black and white air photos were used, including complete sets from 1938, 1952, 1958, 1965, 1974, 1980, 1981, and 1986. Complete false-color infrared aerial photograph coverage was made available by the Department of Civil Engineering at the University of Houston. These 1970 and 1971 photographs were flown by NASA and consist of film positive coverage of large portions of the Texas Gulf Coast. In all, 10 complete sets of aerial photographs spanning nearly 50 years were examined to delineate possible areas of faulting. Appendix A lists the aerial photograph sets used in this study. Appendix B is a compilation of faults for the county which includes the airphoto evidence for each lineament.

Possible fault lineaments identified on aerial photographs were mapped directly onto U. S. Geological Survey (USGS) 7 & 1/2 minute topographic quadrangles at a scale of 1 : 24,000. The quadrangles have been reproduced for the thesis at a scale of 1 : 48,000. Each lineament is assigned a confidence level ranging from 'A' (highest) to 'D' (low) confidence that the feature is a fault. A dashed line is used where fault locations are inferred by interpolation and extrapolation.

Recognition of Faults on Aerial Photographs

In undeveloped areas active faults may appear on both black and white and false-color infrared photos as sharp, curvilinear to rectilinear boundaries between two areas of

tonal contrast (Figure 16). It should be noted that aerial photographs may reveal many such lineaments but the majority of them will not be faults. Features such as abandoned stream channels, meander scars, stream terraces, abandoned dirt roads and trails, underground cables, pipelines, and fence lines may produce lineaments that imitate the appearance of surface faults (Figure 16). Most of these are distinguishable from surface faults under close inspection. However, some features mimic the appearance of fault lineaments so closely that only a thorough field investigation can determine their true nature. Likewise, some faults that do extend to the surface may not produce lineaments on the aerial photos. This may occur for a variety of reasons including heavy vegetation cover, uniformity of soil moisture conditions across the fault, or obliteration of the fault signature by agricultural practices or land development.

The visibility of a surface fault in the Gulf Coast region on both black and white and false-color infrared aerial photos is often due more to 'secondary' features associated with a fault scarp than to the magnitude of the scarp itself.

Fault scarps in Brazoria County are typically less than 0.4 m high. However, the otherwise nearly horizontal ground surface in this region allows the downthrown fault block to

FIGURE 16: Appearance of a surface fault and non-fault linears on black and white aerial photographs. Slop Bowl area east of Stratton Ridge salt dome; Oyster Creek quadrangle (Plate 18).

receive more runoff and retain more moisture than the topographically higher upthrown fault block. This is the primary characteristic which allows faults to be recognized on aerial photographs; soil with a higher moisture content will have a darker hue than the same soil with a lower moisture content. On black and white aerial photos these differences will appear as sharp tonal changes across a linear boundary. These boundaries are sometimes even more pronounced on false-color infrared film.

Reflected infrared energy is primarily reflected solar radiation in the near infrared range. Radiation from 0.7 to 0.9 m wavelength is detectable with film and is called photographic IR (infrared) radiation. The film, first designed for camouflage detection, was originally known as "camouflage detection film", but is now usually referred to as "false-color film", or "IR color film" and is only available as a positive film (Sabins, 1978). As long as some soil moisture variation exists across the fault, the more saturated soils on the downthrown side of the fault will characteristically show as darker tones on both black and white photographs and color infrared film.

The tonal contrast between soils on the down- and upthrown blocks of a fault may be present for a number of weeks after the last rainfall. During extended periods lacking rainfall, however, the surface soils may become uniformly dry and tonal contrasts due to soil moisture content will be lost. When examining different generations of aerial photographs it may therefore be difficult to determine whether absence of a lineament in any one set is due to the absence of a fault, or if a fault is simply not visible because of poor soil moisture conditions. For this reason, reliance on aerial photograph evidence alone to determine the time of initiation of fault movement in an area is an unacceptable practice. If such a determination is desired the appropriate meteorological records for the area should first be consulted.

Periods of prolonged or heavy rainfall commonly cause flooding along the downthrown side of the fault. Often the first indication of an active fault in a suburban area is a section of property that regularly floods during storms. Such areas often continue to sag and pond with water despite efforts to regrade it. The sharply defined edge of such a spot may represent the approximate location of a fault trace with the water ponding directly up against the fault scarp. Ponds are clearly defined as highly reflective surfaces on aerial photographs taken soon after a storm. In many cases an alignment of ponds or puddles can mark the presence of a fault.

Changes in vegetation across a fault are complementary to, and dependent upon, the soil moisture variations across

it. The vegetation contrast itself often appears as a linear feature on aerial photographs. The subtle but relatively constant differences in soil moisture content exert a remarkable influence on the vegetation. As in other portions of the Gulf, prarie grasses and shrubs thrive on the relatively dry upthrown block while marsh-like vegetation such as sedges and rushes occupy the downthrown block (Verbeek & Clanton, 1981). It is common, even in areas where the vegetation type is the same across a fault (such as in lawns and cultivated areas), that rates of growth, maturation and plant health will differ noticibly between plants on the upthrown and downthrown blocks. Such changes in vegetation will be most apparent where the natural vegetation cover has been disturbed, for example, where an overgrown field has been mowed to promote the growth of grasses for grazing, or where a field left fallow is being recolonized by natural vegetation. In contrast, plant communities that have remained relatively undisturbed by man may exhibit few changes across a fault.

In most cases the appearance of a vegetation change across a fault is a more reliable indicator of the fault than soil moisture changes alone. For example, a freshly plowed field will retain soil moisture changes only as long as it takes for the top layers of soil to dry out. Vegetation changes are preferred because the plants remain even through long periods lacking rainfall. However, the ease with which vegetation differences can be recognized will vary with the season in which the photograph is taken. Regardless of the season or recent weather conditions, if a fault has not been active for a few years there is very little chance that it will be detected either on aerial photographs, or by direct observation in the field.

Two additional air photo features associated with surface faults can be recognized across the low profile ground of the Gulf Coastal area: abnormal stream patterns and 'stacked' levees in rice fields. The land surface in Brazoria County slopes toward the coast at regional gradients of 0.4 to 0.7 meters per kilometer. Streams that drain this area show the same low gradients. As a consequence, a fault scarp 0.4 meters or higher may exert some influence on drainage patterns. Rectilinear stream patterns are often fault related. In Brazoria County the scarp of the Moore Road fault (Figure 17) causes 2 right angle bends in the course of Chigger Creek as it flows from the upthrown to the downthrown block, and the Standolind Road fault effects Cowart Creek in a similar manner as it flows from the downthrown to the upthrown block (Figure 18). Numerous examples of fault controlled streams were identified during this study.

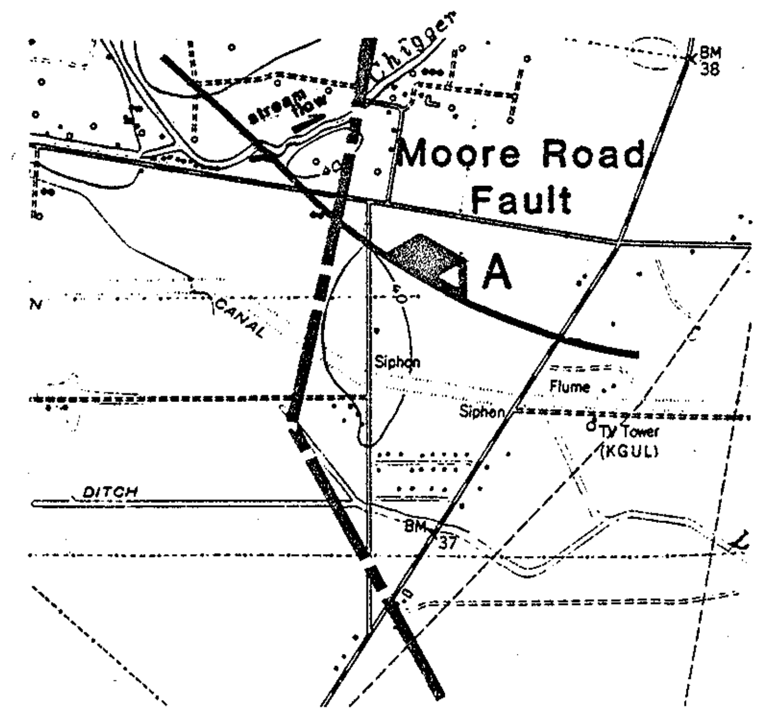

FIGURE 17: Rectilinear stream patterns are often fault related. Here, the Moore Road Fault exhibits control over the course of Chigger Creek near the Brazoria/Galveston County line (Algoa quadrangle, Plate 6).

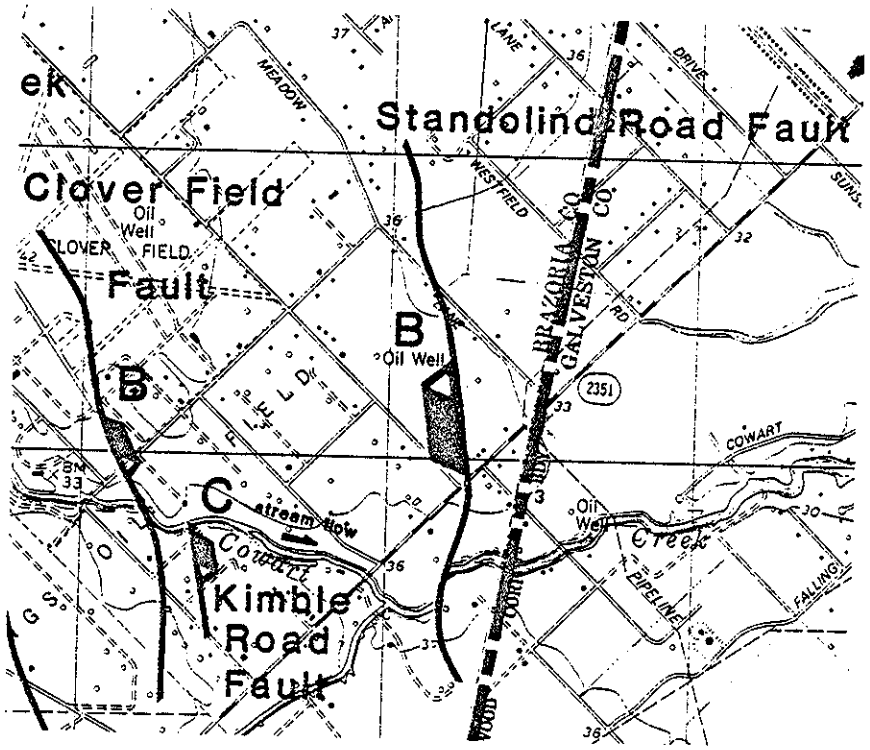

FIGURE 18: Standolind Road (FM 2351) Fault effecting course of Cowart Creek near the Brazoria/Galveston County line (Friendswood quadrangle, Plate 3).

Levees built for the purposes of rice cultivation also can reveal active faults. As aptly described by Verbeek and Clanton, (1981),

> "Prior to planting, irrigation levees - long, sinuous ridges of earth about 0.5 m high - are constructed so as to impound irrigation water to a uniform depth between any two adjacent levees. Each levee, then, is analogous to a contour line in that it maintains a nearly constant elevation along its entire length. Adjacent levees typically differ in elevation by 10 to 15 cm. The pattern of irrigation levees, which is often prominent on aerial photographs, thus reflects the shape of the land surface in much the same way as does a detailed topographic map. Zones of closely-spaced levees that extend across several fields indicate relatively narrow, lengthy topographic slopes, many of which are known to be fault scarps. Scarp heights can be estimated from the number of closely-spaced levees."

So not only do stacked rice levees give an indication of the presence of a fault, they also provide a rough estimate of the displacement of the ground surface.

Field Investigations

Possible fault lineaments identified on aerial photographs have been carefully investigated throughout the 1,422 square-mile area of Brazoria County. The variables involved in mapping surface faults through both rural and urban areas on a county-wide basis are reviewed in the following sections. A complete list of findings from field investigations appear in Appendix B, Fault Descriptions.

Mapping In Developed Areas

In urban areas the primary evidence for a fault is the disturbance of man-made structures including buildings, roads, driveways, fences and parking lots in a linear pattern with a consistent sense of throw. Accurate mapping of faults is facilitated by the close spacing of these man-made structures since each point of disturbance can be marked directly onto a base map. However, only the most active and destructive faults are likely to cause enough cumulative damage to be visible. In addition, mapping in a newly developed area requires special consideration. A fault identified on pre-development aerial photos may not become visible in the new structures for 3 or more years after construction. It is not uncommon for homeowners to be

unaware of any serious problem with their homes for as much as 5 to 10 years after construction. It is the cumulative effects of fault movement over many years which eventually causes visible damage such as broken water mains, ruptured or warped sewer lines, cracked slab foundations, separated brickwork, pitched floors and warped window and door frames (Figure 19).

Mapping In Undeveloped Areas

In rural areas, identification of a fault, particularly a marginally active fault, is usually more difficult than in developed areas because there are fewer man-made structures to reveal the linear pattern of disturbance associated with the fault. Roughly 85 percent of Brazoria County can be considered rural. In such areas all that may be seen of a fault is a gentle topographic scarp in a field. A clearly visible scarp is seldom observed because of the continuous modifications by natural erosion or obliteration by man. Activities such as plowing a field or grading an area for paving or construction may destroy evidence of a scarp. A diffuse ramp may persist but the location of the fault can, at best, be established only within a broad zone over which an abnormally large elevation change occurs (Figure 20). The level of accuracy with which a fault can be positioned

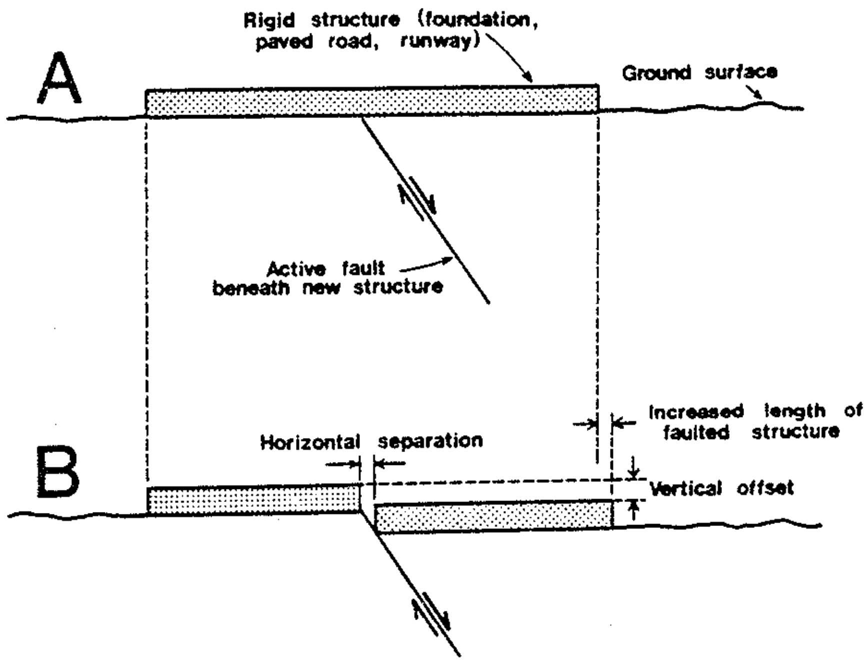

FIGURE 19: Effect of fault movement on a rigid structure built on an active fault. A, original construction; B, structure damaged by fault movement. Both vertical offset and horizontal separation occur. Rigid structures may be pulled apart as faulting proceeds. (From Verbeek, Ratzlaff and Clanton, 1979).

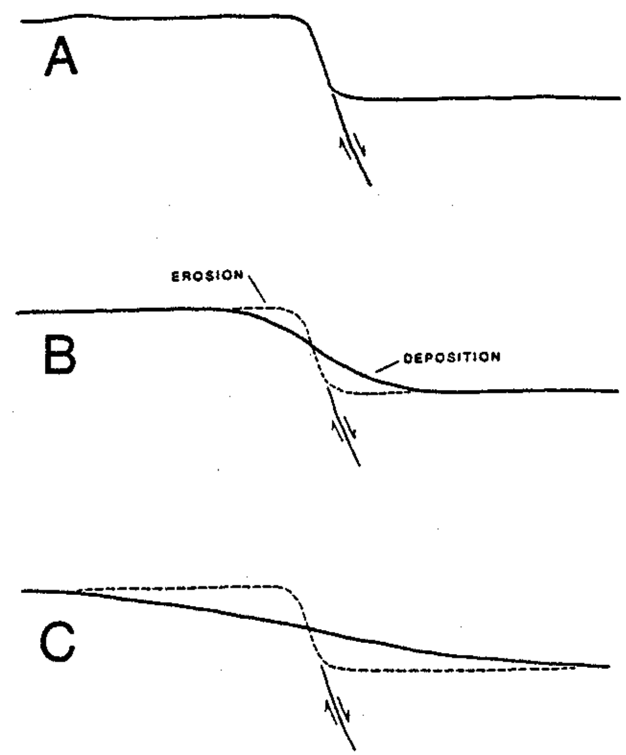

FIGURE 20: Topographic profile across a hypothetical fault. A, shortly after displacement of the land surface. Scarp is sharp and has a steep slope. B, the same fault scarp modified by erosion. Material eroded from the upthrown side is deposited near the base of the scarp. The scarp now has a rounded form and a relatively gentle slope. Location of the fault trace in the absence of structural damage can only be approximated. C, fault scarp after grading for construction or after preparation of a field for cultivation. The scarp is all but destroyed; only a gentle slope remains in its place. The elevation difference between the upthrown and downthrown fault blocks remains, but the location of the underlying fault can only be estimated within broad limits because of extensive modification of the original topography. (From Verbeek, Ratzlaff and Clanton, 1979).

under such circumstances may be no better than a few hundred feet. In an undeveloped area accurate mapping of a fault frequently depends on how closely the present landscape resembles the original topography. To complicate matters, even if a relatively good scarp is found, the paucity of good control points, such as nearby road intersections or buildings, can greatly reduce the accuracy with which a fault scarp can be marked on a map.

In this study the intensity of the field investigation was inversely proportional to the visibility of the feature in the field. That is to say, if, upon investigation in the field, a lineament on the aerial photos was determined to be a 50 cm scarp disrupting pavement and buildings with a uniform sense of motion, the only additional step required was to mark the feature on a base map, trace its extent, and insure it is was the result of natural causes. On the other hand, if there was no obvious topographic scarp or apparent disruption of man-made features associated with a lineament, then a more detailed investigation was necessary to confirm or dismiss the presence of a fault.

Fault scarps in Brazoria County are quite small on the average with heights ranging from 4 to 44 cm and averaging approximately 14 cm. In rural areas such small features are easily and often obscured by high grass and brush.

Therefore, it became necessary to look for indirect evidence of faults. Such indirect evidence might include:

1.) Ponding of water in fields along linear trends or in drainage ditches along the sides of roads;
2.) A change in the physical condition or appearance of vegetation;
3.) Changes in vegetation type;
4.) Linear areas of poor drainage;
5.) Anomalies in courses of streams;
6.) Sections of extensively patched or potholed pavement;
7.) Evidence of repair or regrading of dirt roads at suspected points of fault intersection;
8.) A noticeably higher frequency of crawfish mounds which tend to occur on the soggier downthrown side of a fault.

<u>Levelling Techniques</u>

In cases where subdued scarps were expected, but were not readily visible to the naked eye, a simple method of surveying with a Brunton compass and Jacob staff was used initially. In this method, one person holds a staff marked off in 1 cm increments and placed at consecutive equal distances along a line perpendicular to the scarp while another sights elevations on the staff with a Brunton compass and rod. Elevation profiles were begun on what was expected to be the upthrown side of the fault and carried for a minimum of 100 yards at 50 foot intervals across the scarp toward the downthrown side (Figure 21). In this manner the average topographic gradient for the area could be established and the probable position of the fault noted where there was a significant increase in gradient.

Although the Brunton compass-Jacob staff method was adequate in most cases, a more reliable method was later used which could achieve higher levels of accuracy. The instrument consisted of a 20 foot (6.1 m) section of plastic tubing filled with water and corked at both ends. The tube is used in conjunction with two rods, both scaled in 1 cm intervals. The ends of the tubes are held alongside the rods, which are held vertically at measurement points. When the tubing is uncorked, the water at the two ends will stand at a common level. If the ground surface is level, the water will stand at equal levels on both rods. If the surface is not level, a higher value will be read at the rod that is lower in elevation (Figure 22). With this method, readings to an accuracy of 0.5 cm could be made. Thus it became possible to identify scarps with heights of only a few centimeters. At no time was the presence of a scarp taken as the solitary piece of evidence of a fault. Rather, it is the combination of evidence gathered throughout the

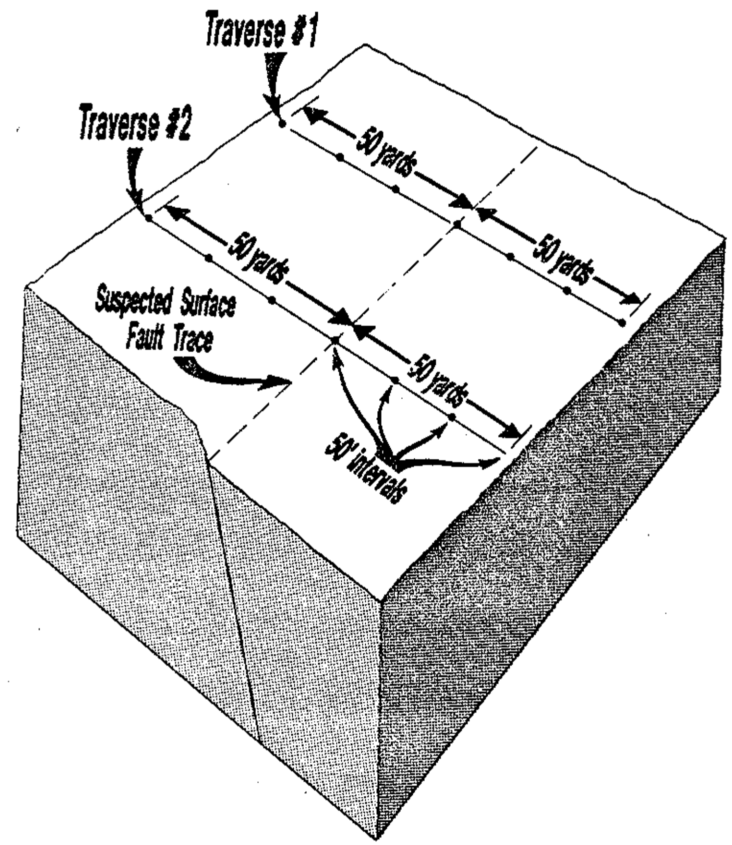

FIGURE 21: When a surface fault scarp could not be detected by eye in the field, multiple traverses, 1, 2, etc., were conducted over the area suspected to be faulted.

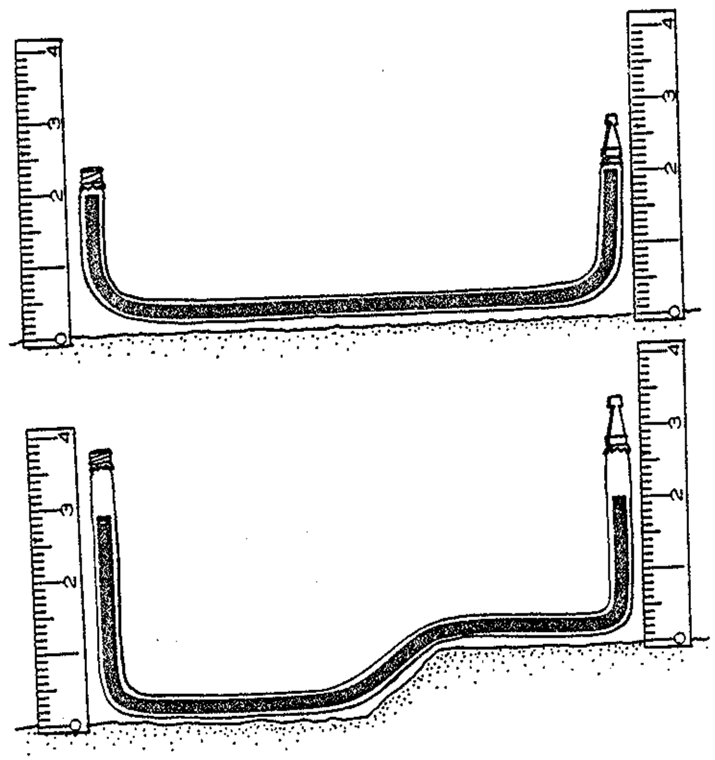

FIGURE 22: A simple water-level measurement system was used which allowed measurement of fault scarps to within 0.5 cm accuracy.

study, including air photo lineaments, field evidence, and subsurface evidence, etc., that have been used jointly to establish the presence or absence of a fault.

During the field investigation both geologic maps and soils maps produced by the Soil Conservation Service (SCS) were consulted. The SCS maps served not only as base maps but also as maps of changes in soil type or landforms which could have some bearing on the features being examined in the field.

The field investigation was an iterative process of repeated field checks, measurements, and consultation of aerial photos. Every accessible lineament was investigated. Access to property was obtained from private citizens, industrial complexes, and governmental agencies. Unfortunately, there were some areas along the marshy expanse of the coast that could not be reached. Special swamp vehicles or boats would be necessary to explore these areas. Even if reached, it is doubtful that useful information on surface faults could be obtained without the drilling of exploratory holes. In extensive swamplands, it should be assumed that the designation of a fault is based solely on strong photographic evidence, unless otherwise noted.

Electric Logs and Subsurface Fault Modeling

An intensive study of borehole electric logs from northwestern Brazoria County near Arcola, Texas serve to answer a number of provoking questions about surface faults and to test predictive fault shape models. Electric logs were obtained from the Gulf Coast Geological Library and the Geological Data Library in Houston, Texas. These log libraries graciously made their logs and facilities available to me for this study.

In the Arcola area good well control is available close to 2 well-known surface faults. Questions to be answered are whether the features appearing at the earth's surface extend as faults into the subsurface, and if so, how deep do they extend? Are they shallow faults that have been active only in the Holocene, or are they older, showing evidence of movement since the Cenozoic? Are the faults truly listric in shape? Do they exhibit true growth fault character? Are there hanging-wall roll-over structures associated with them?

Finally, with the information gleaned from electric logs, predictive models for expected fault geometry at depth could be tested. Predictive models investigated include the Gibb's model (1983) which predicts fault geometry and depth-to-detachment from measured amounts of rollover, and

the Xiao/Suppe model (1986) which predicts fault geometry from known stratigraphy and compaction gradients.

Appendix D lists all the electric logs used in the Arcola study.

Seismic Reflection Profiles

Permission was obtained from various petroleum industry firms to examine seismic profiles. In all, 44 seismic profiles, comprising nearly 400 miles of data, were examined. These data provided positive confirmation for a large number of surface faults identified from airphoto linears and field investigations. About half of the profiles were viewed on a one-time, 'quick-look' basis. However, three companies agreed to allow use of selected lines in this thesis.

Seismic profiles also provided a means to examine the subsurface geometry of the faults. With the use of velocity surveys, time-depth conversions were made and amounts of displacement with depth were calculated for many of the faults. These measurements appear in Appendix B, and illustrate the growth character of these faults. A few of the seismic profiles used in the study, and an average velocity curve derived from down-the-hole velocity surveys appear in Appendix C.

Road Repair Records

Brazoria County is divided into 5 county road repair precincts. Each precinct is exclusively responsible for maintenance of paved and upaved roads within its boundaries. State highways and roads within incorporated city limits are excluded. Initially it was thought that county precinct road repair records could serve as a means to confirm points of disturbance related to surface faulting. Theoretically, a specific section of road requiring frequent regrading, resurfacing or patching would be a likely place to investigate for a surface fault. It was found, however, that road repair records are not sufficiently detailed to provide much help in confirming the existence of surface faults. For example, records for a 20 mile length of road may list repair dates, amount of material used, man hours involved and costs, but will not state where along the 20 mile stretch the repairs were made. Occassionally a road repair foreman would confirm that certain trouble spots coincided with mapped air photo lineaments. These verbal confirmations helped lend credibility to some of the features mapped.

BRAZORIA COUNTY FAULT TRENDS

Surface Fault Patterns

As many as 105 lineaments that may represent previously unknown active surface faults have been identified in Brazoria County. Confidence levels for these 105 lineaments range from definite to possible. The addition of these lineaments raises the total number of surface faults that might be present in the county to 130 (Figure 23 and Plate 24). The approximate cumulative length of the 105 newly identified lineaments is 140 miles (225 km). Adding this to the 30 mile total length of the 25 previously known faults raises the possible cumulative length of surface faults in the county to 170 miles (273 km).

Measured heights of surface fault scarps in the county currently range from 2-3 cm (.79 - 1.18 inches) to a maximum of 40 cm (approximately 16 inches), averaging slightly less than 14 cm (5.5 inches). Maximum scarp heights and, therefore, highest rates of movement, are located along the central portions of the surface faults. Scarp heights decrease progressively toward the ends of a fault.

Geophysical logs and seismic profiles indicate surface faults in Brazoria County are the surface expression of much larger faults that continue deep into the subsurface. The

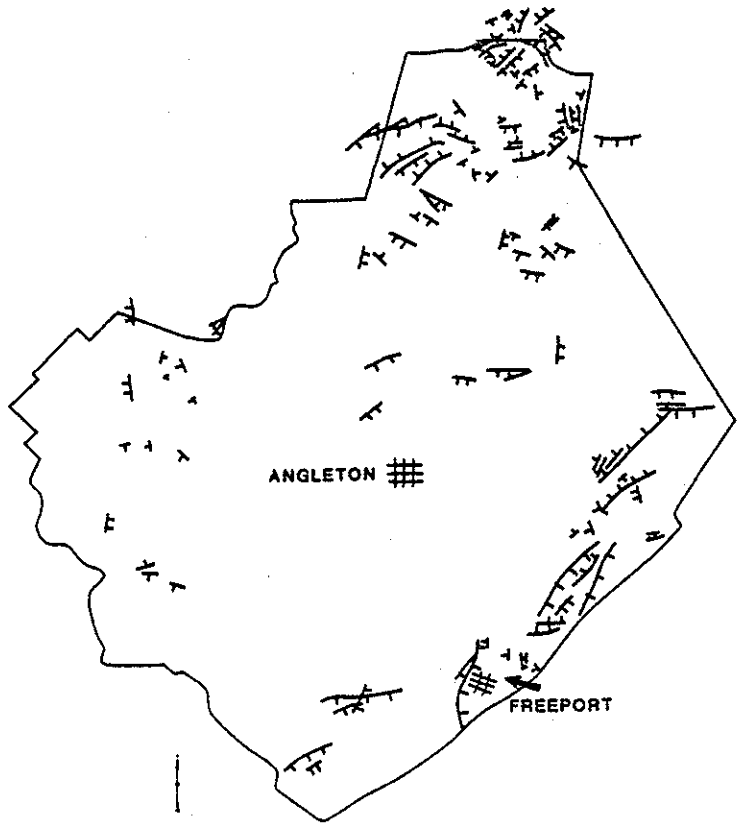

FIGURE 23: Brazoria County surface faults as mapped in this study. As many as 105 lineaments that may represent previously unknown active surface faults have been identified. Scale is approximately 1" = 6.5 miles. In some areas faults are too small, or too numerous, to be shown at this scale.

faults demonstrate increased displacement with increasing depth confirming their growth character and long movement history which extends well into the Cenozoic. The movement history indicates these faults existed and were active long before the influence of man, thus the faults in Brazoria County are naturally occuring geologic phenomena.

Surface faults are not evenly distributed throughout Brazoria County. Most of the surface faults in Brazoria County lie within two distinct areas: 1.) The northernmost neck of the county, and; 2.) Along the coastal regions of the county (Figure 23 and Plate 24).

The northernmost region of high fault density contains approximately 1/10 of the land area and over 35% of the surface faults in the county. This highly faulted portion of the county corresponds to a region of high salt dome density. At least six salt domes influence faulting in this region including two in Fort Bend County (Blue Ridge and Thompsons), one in Harris County (Mykawa), one in Galveston County (Webster), and two in Brazoria County (Manvel and Hastings).

The second highly faulted area of Brazoria County is along the coastal regions where slightly more than 1/10 of the county land area contains 25% of the surface faults. In examination of this pattern it should be noted that the Texas Coastal Plain built seaward from the north and west as a series of aggrading delta plains. Thus, sediments become younger toward the coast, as do the growth fault systems. These younger growth fault systems are naturally more active and, therefore, may account for the concentration of active surface faults in this area. Another factor involved is the high visibility of surface features in this coastal region. Except for the city of Freeport, the coastal wetlands of the county represent an area virtually untouched by land development or agricultural practices. Also, the land surface is extremely flat, thus even very small scarps become visible. In addition, vegetation consists largely of salt marsh grasses; trees and brush are not present to obscure a clear view during field and aerial photographic investigations.

There are few visible surface faults in the west central and south central portions of the county. These areas of low surface fault occurrence roughly coincide with the distribution of Recent sediments deposited in the Brazos/Oyster Creek and San Bernard/Caney Creek alluvial valleys (Figure 8). These wide alluvial valleys contain an intricate and pervasive pattern of meander belt ridges and scars which create a strong signature on aerial photographs. In the field, this uneven and scarred topography may easily obscure a very subtle fault scarp. In areas covered by recent alluvium a surface fault must be very active and

produce a reasonable scarp in order to be recognized in a county-wide investigation of this type.

The orientation of surface faults in Brazoria County also is not uniform, however, a large percentage do have a trend which is roughly parallel to the regional trend, i.e., parallel to the coast. Nearly 70% of the surface faults in the county have a roughly regional strike, trending between 0 and 90 degrees east of north (Figure 24). This compares favorably with a similar pattern in Harris County where 69.4% of the surface faults have a northeasterly strike (Figure 25). Narrowing the trend even further, nearly 20% of Brazoria County surface faults strike between N 41 E and N 60 E along a strongly regional (coast parallel) trend. In Harris County a full 30% of the surface faults reflect this strongly regional trend.

Approximately 31% of Brazoria county surface faults have strike directions at high angles to the regional trend. These faults, striking 0 to 90 degrees west of north, represent the minimum percentage of surface faults that are salt dome related. In Harris County 30% of the surface faults are salt dome related and strike at high angles to the regional trend.

The orientation and distribution of faults in Brazoria County are very similar to the fault patterns thus far identified in Harris County. Although no county-wide map of

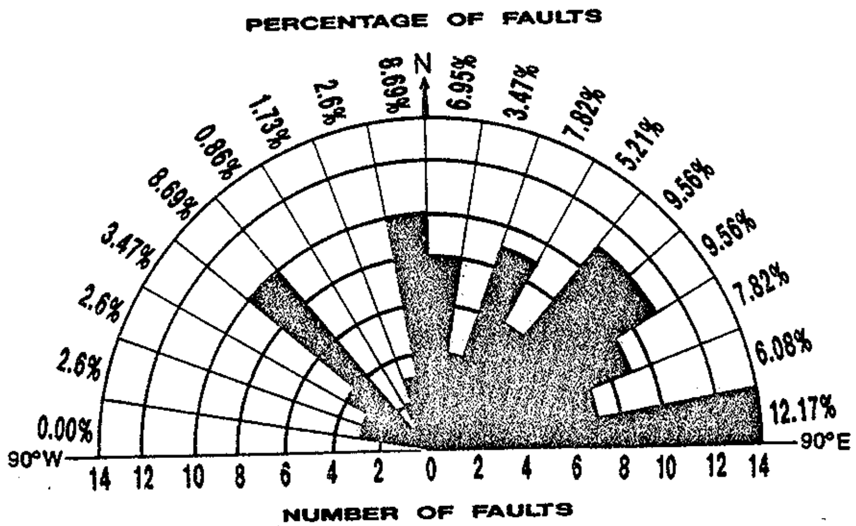

FIGURE 24: Orientation of surface lineaments, Brazoria County, Texas. One hundred fifteen lineaments are represented. Nearly 70% of surface faults in Brazoria County have a roughly regional, coast sub-parallel strike trending between 0 and 90 degrees east of north. Approximately 31% of Brazoria County surface faults strike at high angles to the regional trend, these are salt dome related faults.

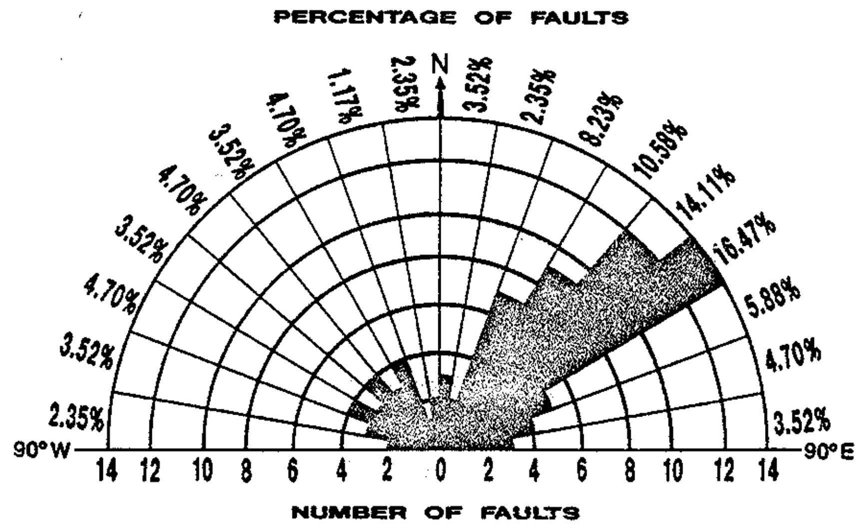

FIGURE 25: Orientation of surface lineaments, Harris County, Texas. Eighty-five lineaments are represented. Nearly 70% of published surface faults in Harris County have a roughly regional, coast sub-parallel strike trending between 0 and 90 degrees east of north. At least 30% of Harris County surface faults strike at high angles to regional trend, these are salt dome related faults.

surface faults is available for Harris County, a large portion of the county has been mapped in separate investigations, especially the area in and around the Houston metropolitan area (Figure 3).

In both Harris and Brazoria Counties there emerges two distinct components to the pattern of surface fault distribution. In both counties, regional, roughly coast parallel faults, make up one component consisting of approximately 70% of the surface faults, while salt dome related faults represent the remaining 30% of the surface faults.

In Brazoria County surface faults of regional trend are most evident along the coast, away from areas of salt dome concentration. In Harris County regional surface faults are located in the northern and western sectors of the county, also away from areas of high salt dome concentration. Harris County is not a coastal county so the locality of regional faults differs, but like Brazoria County, regional faults comprise nearly 70% of all surface faults and they are most evident in areas away from salt domes.

Salt domes and salt dome related surface faults are concentrated in the northern portion of Brazoria County, this area borders the southeastern portion of Harris County where the same pattern exists.

Subsurface Geometries of Selected Faults

Introduction and Aims

Attempts to trace surface faults into the subsurface were undertaken to:

a) Determine if the faults continue into the deep subsurface, and if they do, to what depths.
b) Describe the structural features associated with the faults and the geometric shape of the faults by construction of structure contour maps, fault plane maps and cross-sections.
c) Determine whether the faults show growth characteristics by the construction of isopach maps and calculation of expansion indicies (the ratio of the thickness of sediments on the downthrown block divided by the thickness of sediments on the upthrown block).
d) Investigate patterns of sedimentation associated with the faults by interpretation of isopach maps.
e) Describe the movement history of selected faults by the interpretation of isopach maps and expansion indicies.

f) Test models designed to predict fault shape at depth (Chapter 4).

Only a few of the active surface faults in Brazoria County have sufficient subsurface data available in their immediate vicinity to accomplish these goals. At the outset of this study, the only available sources of data were logs of water wells and oil wells. Some seismic profiles became available late in the study, but these data were largely used to verify the results of the surface mapping and photo interpretation.

Water-well logs are not sufficient in number, spacing or depth to permit adequate subsurface mapping of the faults. Consequently, the primary data base for this part of the study is a suite of oil-well logs.

In Brazoria County most oil fields are located on the flanks of salt domes. The high concentration of deep faults associated with the domes would make the tracing of a single surface fault very difficult. For this reason regional faults were chosen for the study, recognizing that fewer logs would be available away from the intensively drilled salt domes. At the Arcola Oil Field, three good surface faults appear where considerable exploitation drilling has been done since the early 1930's. Figure 26 locates the Arcola Oil Field area of special interest. Surface faults

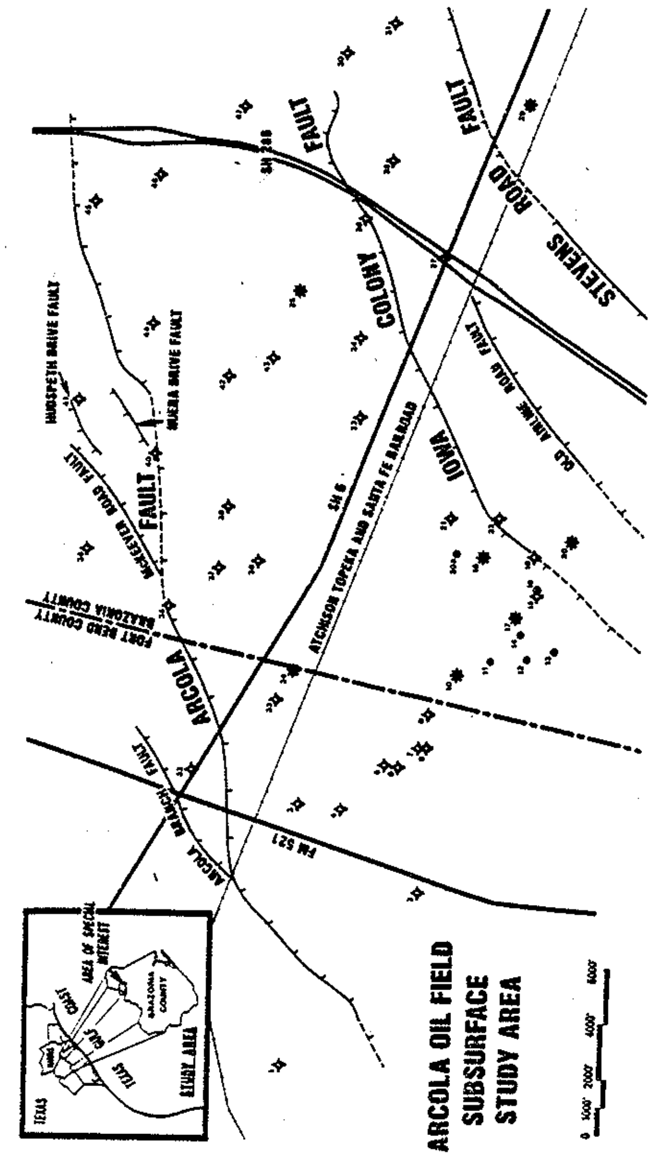

FIGURE 26: Location of the Arcola Oil Field subsurface investigation. The enlarged area of special interest displays surface faults in relation to cultural features and the distribution of well control used in the study. The boundaries of the enlarged area are the same as those used for all subsequent fault plane, structure and isopach maps.

are shown in relation to cultural features. Wells used for the subsurface study are numbered on the figure and identified in Appendix D. The boundaries of the enlarged area coincides with those of all subsequent fault plane, structure and isopach maps.

Subsurface Mapping Techniques

In the Arcola Oil Field two types of well logs are available to the virtual exclusion of all others: the spontaneous potential (SP) log, and the resistivity log (generally consisting of two induction curves and a shallow-focus log).

The SP log measures the electrical potential created between the three electrolytes found in the borehole: the naturally occurring waters in the shales; the naturally occurring waters in the sands; and the drilling fluids. The resistivity tool measures the electrical resistivity (in ohm-meters) of the formation to a constant induced current. The response of both logs is largely a function of the salinity of the connate fluids. Variations in these curves are utilized to recognize the type of fluid present in the formation, e.g., freshwater, saltwater, or hydrocarbons. One of the main purposes of running these logs, however, is to facilitate stratigraphic correlation between boreholes.

Correlation of borehole logs is essentially an exercise in pattern-recognition; the patterns, or shapes, of the curves are a function of lithology, fluid type and bed thickness. For example, the shape of the SP curve in saltwater saturated formations will vary with changes in grain size and bed thickness; the shallow and deep focus resistivity curves are identical in shales, but deviate from one another in sands containing saltwater. This effect decreases as the formation water becomes fresher because the separation is a function of the differences in salinity of the formation fluids and the freshwater drilling fluid. Bed thickness influences these curves because each tool has a minimum thickness resolution.

Lithology, bed thickness, and sequence of beds will tend to be similar in adjacent boreholes, therefore, lithostratigraphic correlations can be established. These correlations can be used to extract data for subsurface mapping.

The presence of a normal fault on a well log can be inferred from the sudden absence of a section of strata, and from a sudden change in elevation between correlative strata in adjacent wells (Figure 27). Unconformities may also produce "missing section" in adjacent wells, but can be differentiated on the basis of the areal distribution of the missing section. In the case of faulting, the distribution

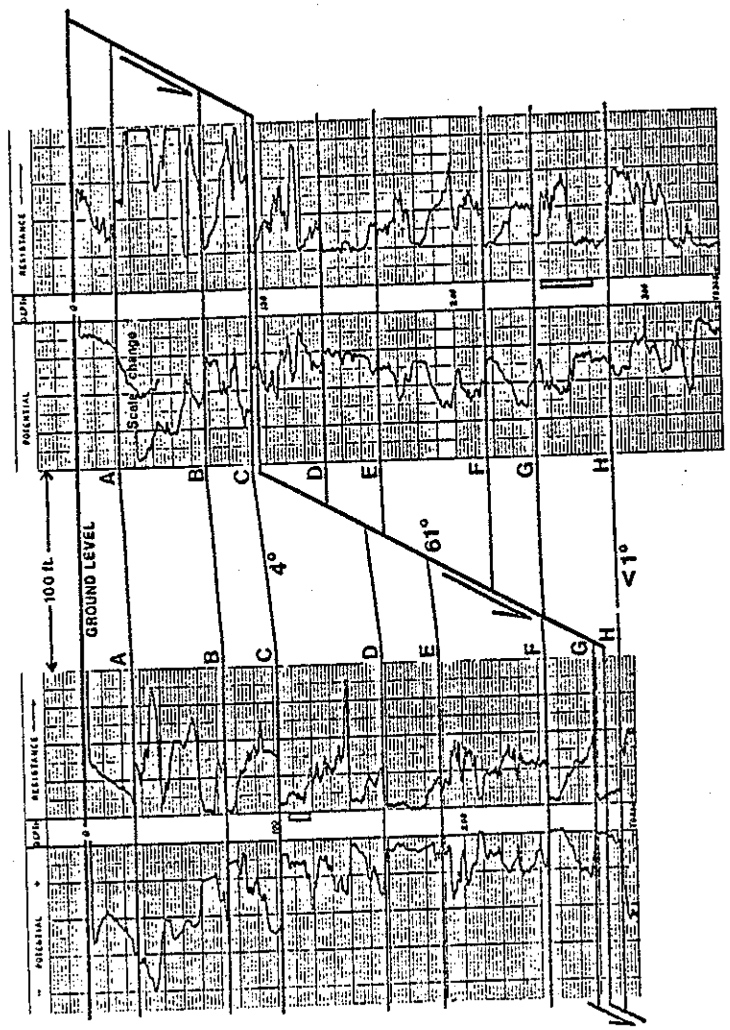

FIGURE 27: Spontaneous potential (SP) and resistivity logs of two closely spaced boreholes cutting a fault. Box in center of each log indicates the section of strata faulted out of the opposite log. (From Van Siclen, 1981).

of a missing section does not occur at the same stratigraphic level when wells are located different distances from the surface trace of the fault.

Three types of maps were constructed using well log data: fault plane maps, structure contour maps, and isopach maps. Figure 28 illustrates the major structural features to be discussed in this section. Note that the axis of the Arcola-Stevens Road anticline is located along the surface trace of the Iowa Colony Fault. On the maps to follow, the faults will be identified with the following abbreviations: ARC = Arcola Fault; IC = Iowa Colony Fault; STV = Stevens Road Fault; ARC B = Arcola Branch Fault; MKV = McKeever Road Fault; OA = Old Airline Fault.

The Fault Plane Map

Figure 29 is a fault plane map depicting the geometry of the Arcola and Iowa Colony faults and six smaller ones nearby. In construction of this map the contours are kept as closely parallel as possible to the strike of the surface fault trace.

The most pronounced fault in the Arcola-Iowa Colony system is the Arcola Fault. Throw on this fault exceeds 600 feet at depths of 8000 feet. The Arcola Fault is listric, i.e., the dip of the fault plane decreases progressively

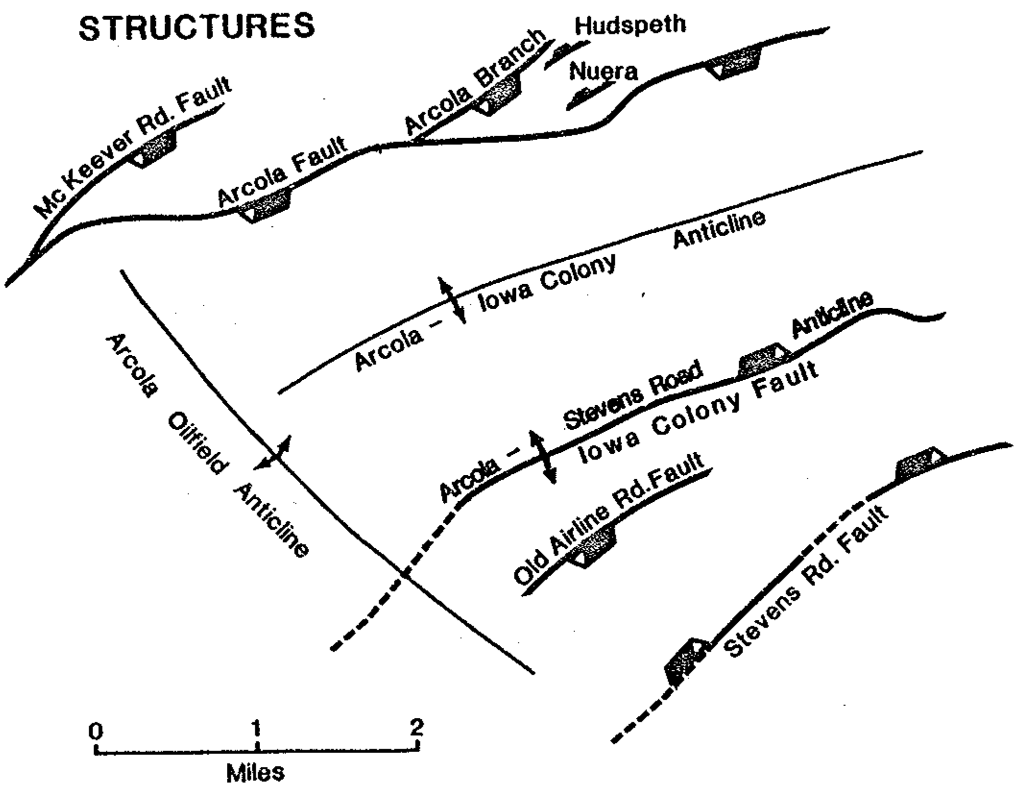

FIGURE 28: Major structural features defined in the Arcola Oil Field. Note, the axis of the Arcola - Stevens Road Anticline lies along the surface trace of the Iowa Colony Fault.

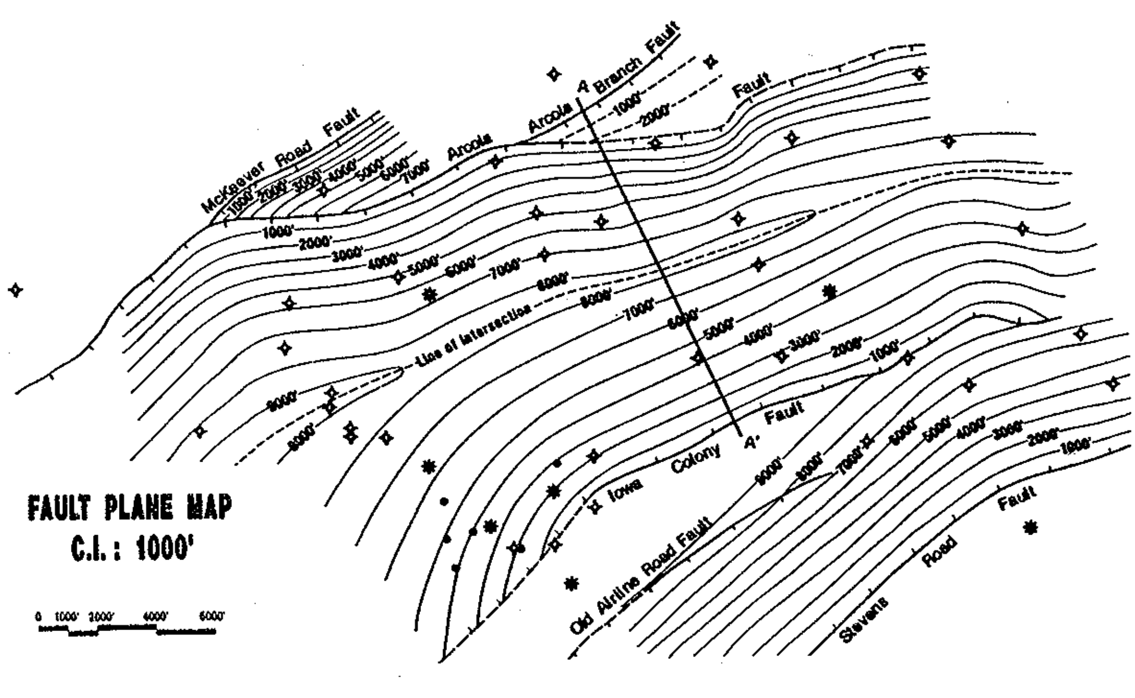

FIGURE 29: Fault plane map, Arcola Oil Field. In some areas lack of adequate well control prevents fault plane determination.

with depth. The Stevens Road and Iowa Colony Faults are large up-to-coast faults, both antithetic to the Arcola Fault.

Figure 30 is a cross-section through the Arcola area constructed from the fault plane map along section line A-A'. Increasing amounts of stratigraphic offset with depth can be seen on both the Arcola and Iowa Colony Faults, as well as decreasing dips with depth. Throw is measureably greater on the down-to-coast Arcola fault with reverse drag and rollover also apparent.

Four short faults occur on the upthrown side of the Arcola Fault: The Arcola Branch Fault (downthrown to the southeast); the Hudspeth Drive and Neura Drive Faults (downthrown to the northwest); and the McKeever Road Fault (downthrown to the southeast). Only 'probable' missing stratigraphic sections could be identified in boreholes penetrating these faults. It is likely that the throw across these faults is very small. Isopach maps (Figures 36, 39 and 40), do show thickened stratigraphic section on the down-thrown side of the Arcola Branch and McKeever Road Faults, suggesting active movement for at least part of their history.

Seismic profiles indicate that the Arcola and Iowa Colony Faults extend well beyond the average 8000 ft. depth of the well logs available for this study. Dips on the

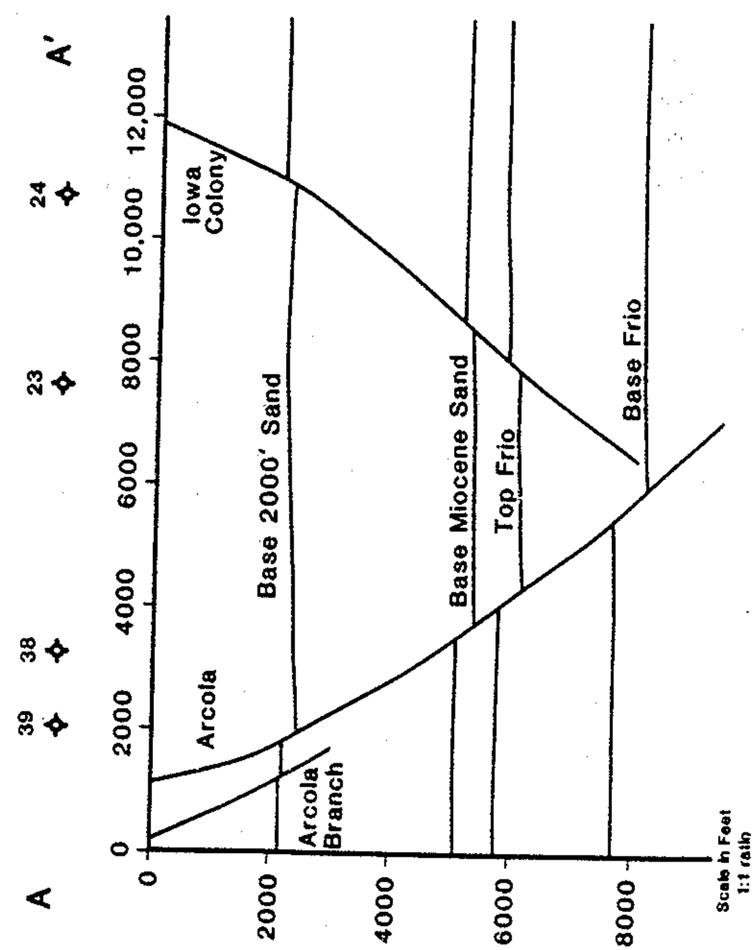

FIGURE 30: Cross-section A - A' constructed from the fault plane map. Numbered wells are projected into the line of cross-section.

faults are still relatively steep at this depth. In fact, on seismic profiles, the Arcola Fault can be recognized to depths of at least 13,000 feet, the data are of poor quality beyond this point. In the next chapter fault models are used to predict the shape of the Arcola and Iowa Colony Faults from the surface to beyond 8000 foot depths.

Figure 31 lists depth versus dip angle for these faults. The dip angles decrease progressively with depth as prescribed by listric fault models. The Stevens Road Fault has the shallowest dip angle of 60 degrees at 1000 feet decaying very little within the next 7000 feet. An interesting relationship appears between the dip angles on the regional down-to-coast Arcola Fault and its two antithetic up-to-coast partners. The near-surface dip angle of the down-to-coast Arcola Fault is 5 to 13 degrees greater than that of the up-to-coast Iowa Colony and Stevens Road Faults. Moreover, the average dip of the Arcola Fault from 1000 to 8000 feet is 66 degrees while that of the Iowa Colony and Stevens Road Faults is 59 degrees. It is not known whether these relationships are common to fault systems throughout the Gulf.

Depths at which the individual fault planes intersect may be estimated from the fault plane maps. The Iowa Colony Fault intersects the Arcola at a depth of about 8000 feet,

	ARCOLA FAULT	IOWA COLONY FAULT	STEVENS ROAD FAULT
DEPTH	DIP	DIP	DIP
1000'	73	68	60
2000'	71	63	59
3000'	68	61	59
4000'	67	60	59
5000'	65	58	59
6000'	63	56	57
7000'	62	55	57
8000'	60	54	58

FIGURE 31: A listing of depth versus fault dip angle (in degrees) for the Arcola, Iowa Colony and Stevens Road Faults.

but the Stevens Road Fault, located more distant from the Arcola, intersects it below 15,000 feet.

The rather small Old Airline Fault (Figure 29) is antithetic to the Stevens Road Fault. Lack of well control precludes interpretation of this fault.

Structure Contour Maps

Correlation of Arcola area well logs led to the selection of 5 distinctive horizons to use in the construction of structure contour maps. Theses five horizons are readily identifiable and laterally continuous throughout the Arcola Oil Field. Mapping the structures of successive horizons will aid in deciphering the movement history of the major faults in the Arcola area. Figure 32 is a type log for the Arcola area marked with the following horizons:

a) The base of the Frio Formation ranging between 7700 and 8200 feet labelled "Base Frio Formation".
b) The top of the Frio Formation at about 6000 feet labelled "Top Frio Formation".
c) The base of an extremely consistent Miocene sand at an average 5300 feet depth labelled

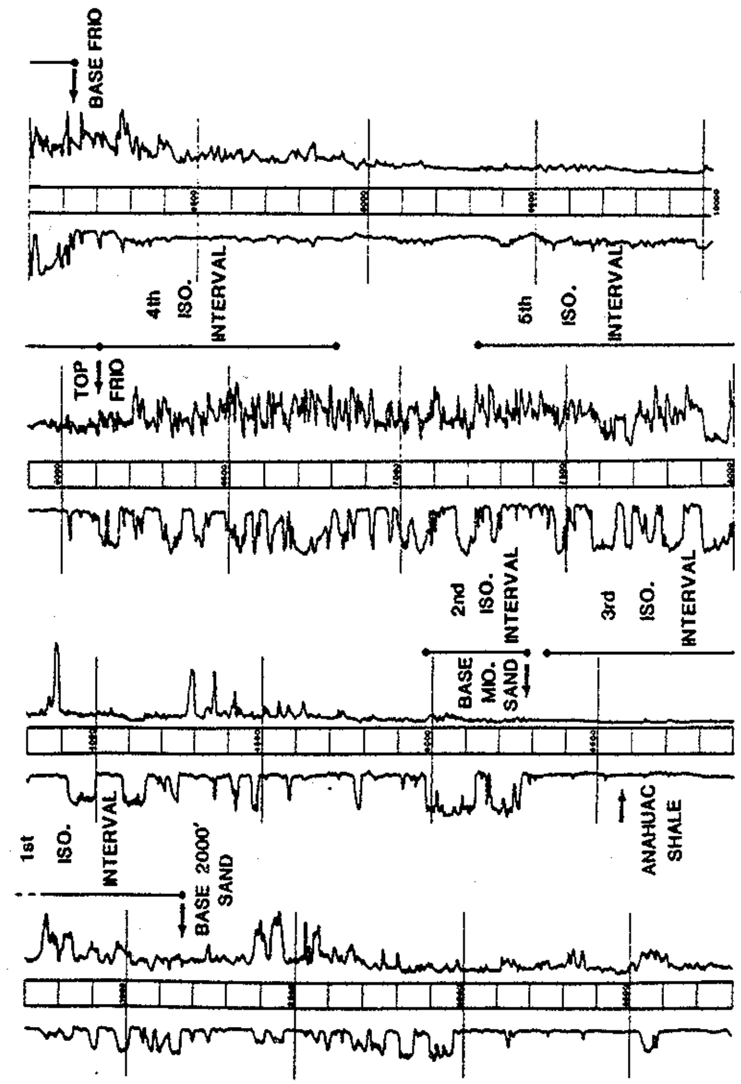

FIGURE 32: Type log for the Arcola Oil Field area. This log has the greatest depth of any used in the study. Well Log #7: The Navidad Oil & Gas & Davidson Geochemical, Hall Etter #1.

"Base Miocene Sand".

d) The base of a near surface, persistent sand labelled "Base 2000' Sand". The base of this sand is at, or very near, the Plio-Pleistocene boundary.

Structure contour maps of the above horizons will also show the geometries of structures associated with the Arcola Fault system and give insight into their structural evolution.

Base Frio Structure

Three structurally distinct areas appear at the base of the Frio Formation (Figure 33): North and west of the Arcola Fault an area of gentle regional dip toward the fault; within the Arcola - Stevens Road Fault graben a central structural high, striking northeast, the Arcola - Stevens Road Anticline; and southeast of the Stevens Road Fault, an area influenced by growth of the Manvel Dome.

At the base of the Frio Formation, the most striking feature is the rollover anticline between the Arcola and Stevens Road Faults. Within this downfaulted block, closure along the southwestern part of the anticline trapped hydrocarbons in the Lower and Middle Frio Formation, the

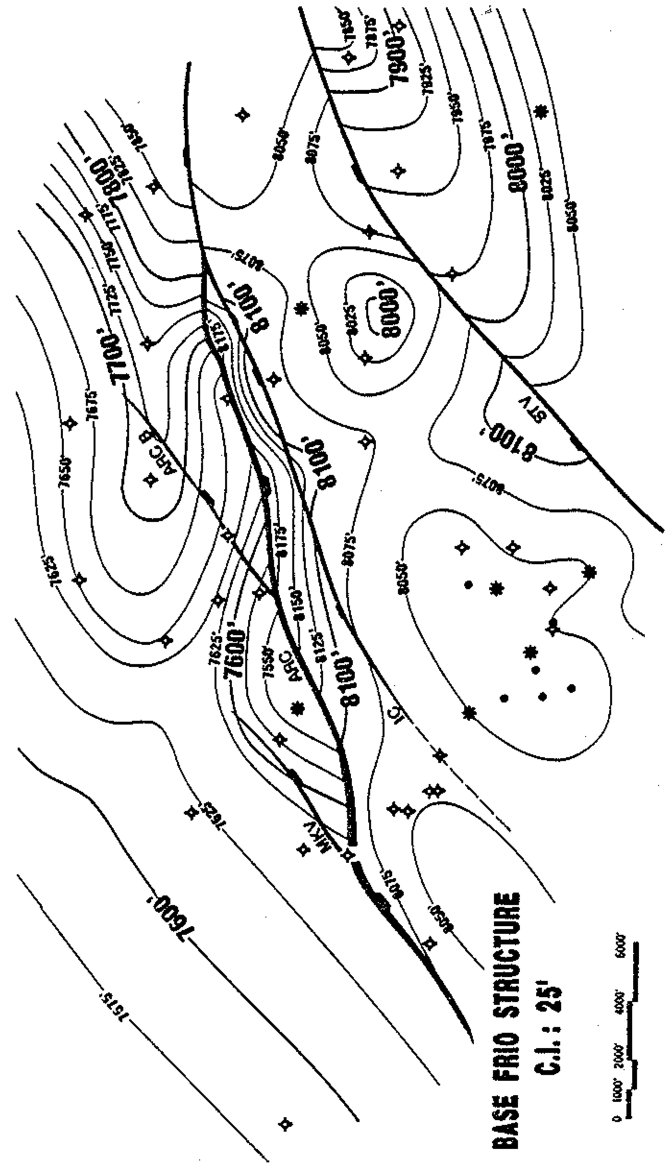

FIGURE 33: Base of Frio structure. Three structurally distinct areas appear: Gentle regional dip in the northwest; a central high developed along the Arcola - Stevens Road Fault graben with the Iowa Colony exhibiting no control over structure; and to the southeast, beds plunge to the southwest.

producing horizons of the Arcola Oil Field. The entire producing portion of the field is enclosed by the 8050′ contour.

In conjunction with excellent rollover development, small lows appear along the sides of the Stevens Road - Arcola graben, these lows are the result of reverse drag associated with active movement along the faults.

It should be noted that the Iowa Colony Fault does not exert a discernable influence on structure at the base of the Frio Formation. The Iowa Colony Fault may have been inactive or moving very slowly at this time. Also, at these depths the Iowa Colony Fault is approaching intersection with the Arcola Fault plane making throw at this horizon difficult to resolve.

Top Frio Structure

The structure map drawn on the Top Frio (Figure 34) is substantially different from that at the base of the Frio. One similarity is that the area northwest of the Arcola Fault is still an area of gentle regional dip. However, the Iowa Colony Fault is now exhibiting a strong influence on the structure of the downthrown block of the Arcola Fault. At this horizon, the position of the Iowa Colony Fault trace roughly follows what was the crest of the Arcola - Stevens

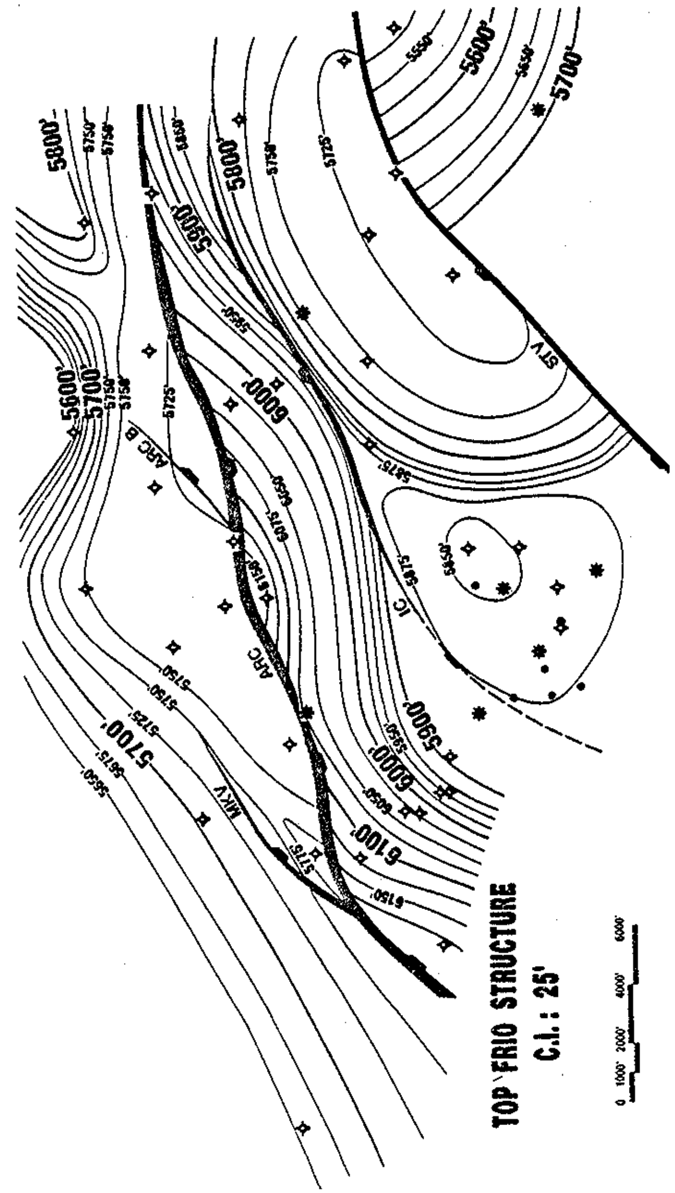

FIGURE 34: Top Frio structure. At this level regional dip persists to the northwest. Within the Arcola - Stevens Road Fault graben the Iowa Colony now exhibits some control over structure. Southeast of the Stevens Road Fault, beds continue to plunge to the southwest.

Road Anticline described on the previous map. It is not uncommon for successive antithetic faults to form along the crests of rollover anticlines (Ellis and McClay, 1988).

The Arcola - Iowa Colony Fault graben dips toward the Arcola Fault disturbed by a large high to the southwest. This northwest trending high, the Arcola Oil Field Anticline, has 250 feet of relief at this level. Its cross-trend suggests that it may be underlain by a deep seated salt mass. In the area between the Iowa Colony and Stevens Road Fault the Arcola - Stevens Road Anticline plunges to the southwest. Southeast of the Stevens Road Fault continued growth on Manvel Dome is indicated by closely spaced contours rising 250 feet to the northeast.

Base Miocene Sand Structure

Broad structural patterns apparent at the top of the Frio Formation are also present at the base of a distinctive Miocene Sand (Figure 35).

The upthrown block of the Arcola Fault remains an area dominated by regional dip. Within the Arcola - Iowa Colony graben dip remains northwest toward the Arcola Fault. The Arcola Oil Field Anticline has less relief at this horizon, 160 feet versus 250 feet at the top of the Frio Formation.

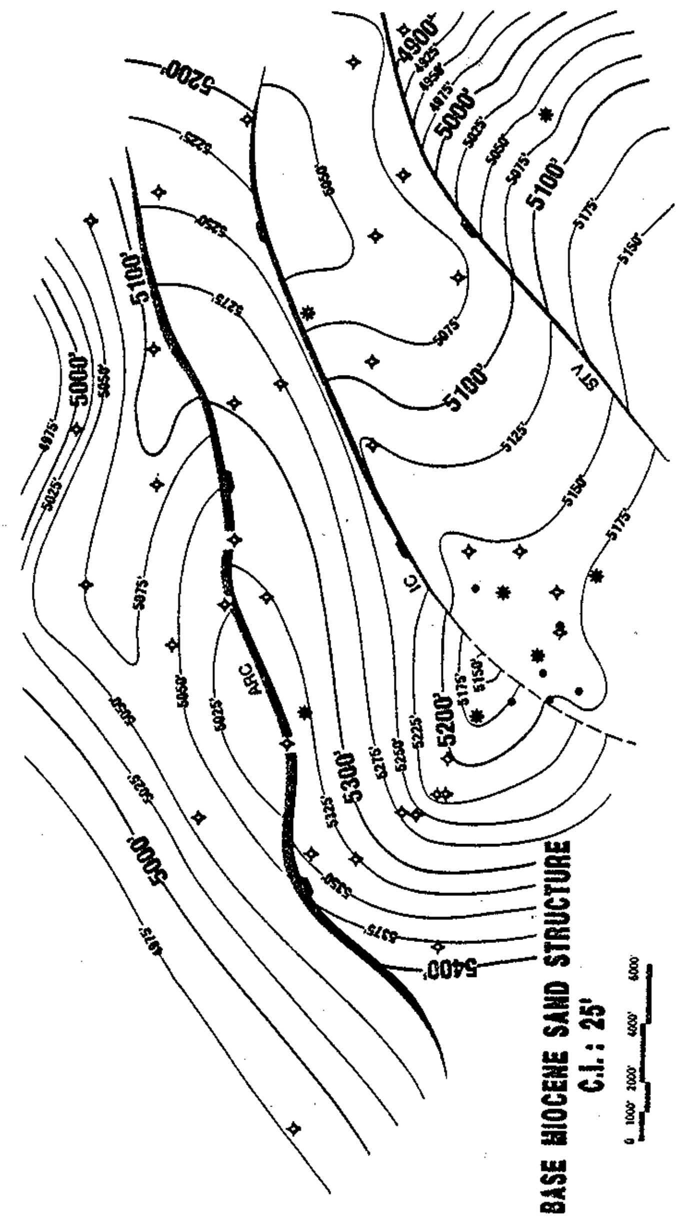

FIGURE 35: Base Miocene Sand structure. Three structural provinces persist: Regional dip to the northwest; a prominent high (the Arcola Oil Field Anticline) trending northwest within the Arcola - Stevens Road Fault graben; and southwest plunging beds in the southeast.

South of the Iowa Colony Fault, the gently southwest plunging Arcola - Stevens Road Anticline is still in evidence. Southeast of the Stevens Road fault contours continue to rise toward the Manvel Dome.

2000′ Sand Structure

At the base of the 2000′ Sand (Figure 36) the upthrown block of the Arcola Fault remains an area of regional dip, only slightly interrupted by the McKeever Road and Arcola Branch Faults and shallow basins developed on their downthrown sides. At this horizon, movement on the Arcola and Iowa Colony Faults has resulted in pronounced reverse drag and rollover between them, creating a central high with over 200 feet of structural relief (the Arcola-Iowa Colony Rollover Anticline) bounded by lows adjacent to the faults.

The Arcola Oil Field Anticline has much less relief at this shallow level. Relief on this structure is approximately 75 feet, less than half of what occurs at the base of the Miocene Sand. Less relief on this structure at younger horizons further suggests a deep seated salt mass origin. South of the Iowa Colony Fault, the influence of the Manvel Dome is also diminishing. Only 100 feet of relief occurs at the base of the 2000′ Sand versus 250 feet at the base of the Miocene Sand. Also, south of the Iowa

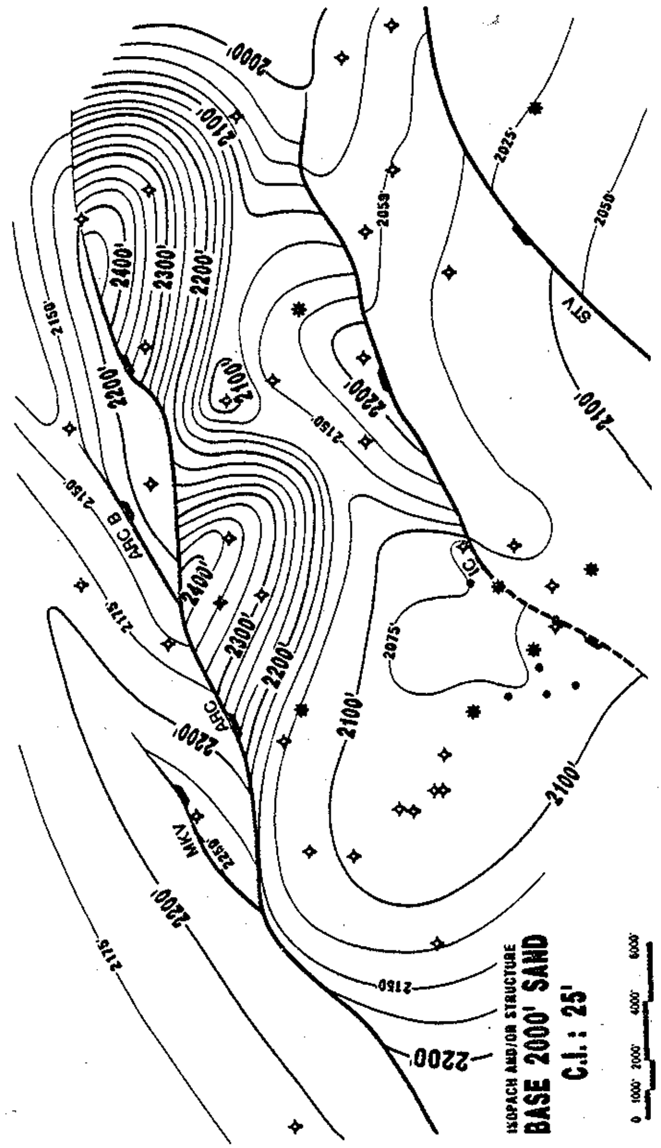

FIGURE 36: Because the 2000' Sand isopach is from the surface to the base of this distinctive sand body, this map can be viewed as both a structure and an isopach map.
a.) Base 2000' Sand structure. Regional dip is still dominant in the northwest; the main structural graben now occurs between the Arcola and Iowa Colony Faults; in the southeast, beds plunge gently to the southwest.
b.) 2000" Sand isopach. Substantial thickening of sediments within the Arcola - Iowa Colony Fault graben is evident during this interval. Sediment thickness increases across the slowly moving Stevens Road Fault are just over 50 feet.

Colony Fault there is very little, if any, expression of the Arcola - Stevens Road Fault Anticline which was a prominent feature on previous horizons. The decline of this feature occurs in conjunction with a near cessation of movement on the Stevens Road Fault.

Little has been said about the structural influence of the small faults in the Arcola area, the Old Airline Road Fault, Hudspeth Drive and Nuera Drive Faults in particular. These faults are visible on aerial photographs, have field expression and are recognized on seismic profiles but poor well control precludes an understanding of their movement history.

Isopach Maps

Isopach maps are drawn to illustrate patterns and trends in the thickness of stratigraphic intervals. Such patterns are often related to the movement histories of growth faults and other structural features present or developing during deposition of the interval.

Thickness data is obtained from well logs. Fault locations are approximated for each interval and the thickness data contoured accordingly. The completed isopach maps are used to calculate fault expansion indices at points along the fault trace. The fault expansion index is

determined by dividing the contour value on the downthrown block by the contour value on the upthrown block. A value greater than 1.00 indicates some degree of expansion across the fault.

As noted on Figure 32, isopach maps of the following five intervals are presented:

a) The lower Frio Formation of Middle Oligocene age.
b) The upper Frio Formation of Middle Oligocene age.
c) The Anahuac Shale of Late Oligocene age.
d) The Lower Miocene Sand.
e) Base of the 2000′ Sand through Holocene isopach. (Since the top of the Holocene is nearly horizontal this map is essentially equivalent to the 2000′ Sand structure map showing thickness variations of the entire Late Miocene through Holocene interval.

Lower Frio Isopach

The thickness of this interval varies from 750′ to 950′ (Figure 37). Sediments north of the Arcola Fault gradually thin toward the fault trace without interruption from the McKeever Road or Arcola Branch Faults. There is evidence of significant displacement and rollover development along the

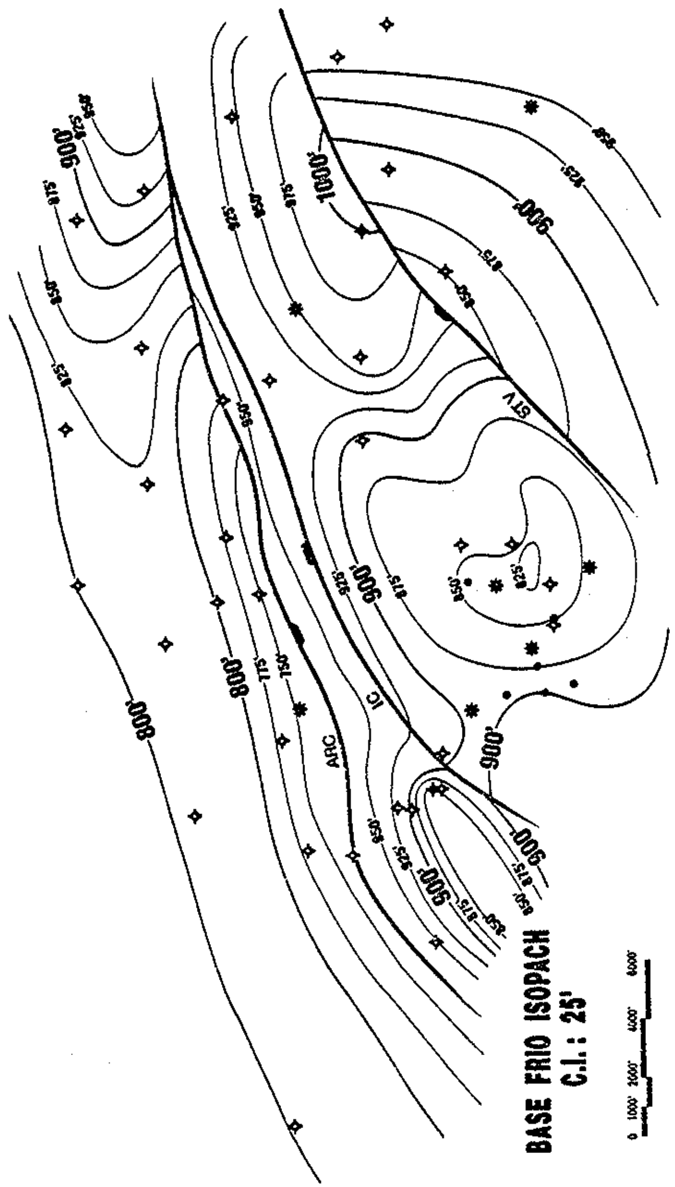

FIGURE 37: Lower Frio isopach. Sand thicknesses and expansion indices demonstrate that the Iowa Colony Fault was not active during deposition of this interval.

Arcola Fault (expansion indices 1.09 to 1.30) and Stevens Road Faults (expansion indices 1.00 to 1.20). The wide range of expansion indices posted along the length of one fault trace indicates the variable rates of movement along the fault during deposition of the interval. This demonstrates portions of the fault experience active movement while other portions are virtually "locked" in position.

Lower Frio sediments in the Arcola - Stevens Road Fault graben thin over the Arcola - Stevens Road Fault Anticline. Stratigraphic thinning over the Arcola Oil Field Anticline is most prominent and reflects a possible salt mass at depth.

The Iowa Colony Fault does not appear to exert an influence on Lower Frio depostion. Southeast of the Stevens Road Fault sediments thicken southeast away from the fault trace.

Upper Frio Isopach

The Upper Frio interval is between 600′ and 800′ thick (Figure 38). North of the Arcola Fault sediments thicken southeast toward the fault without disruption from the McKeever Road or Arcola Branch Faults. High rates of movement are indicated along both the Arcola Fault

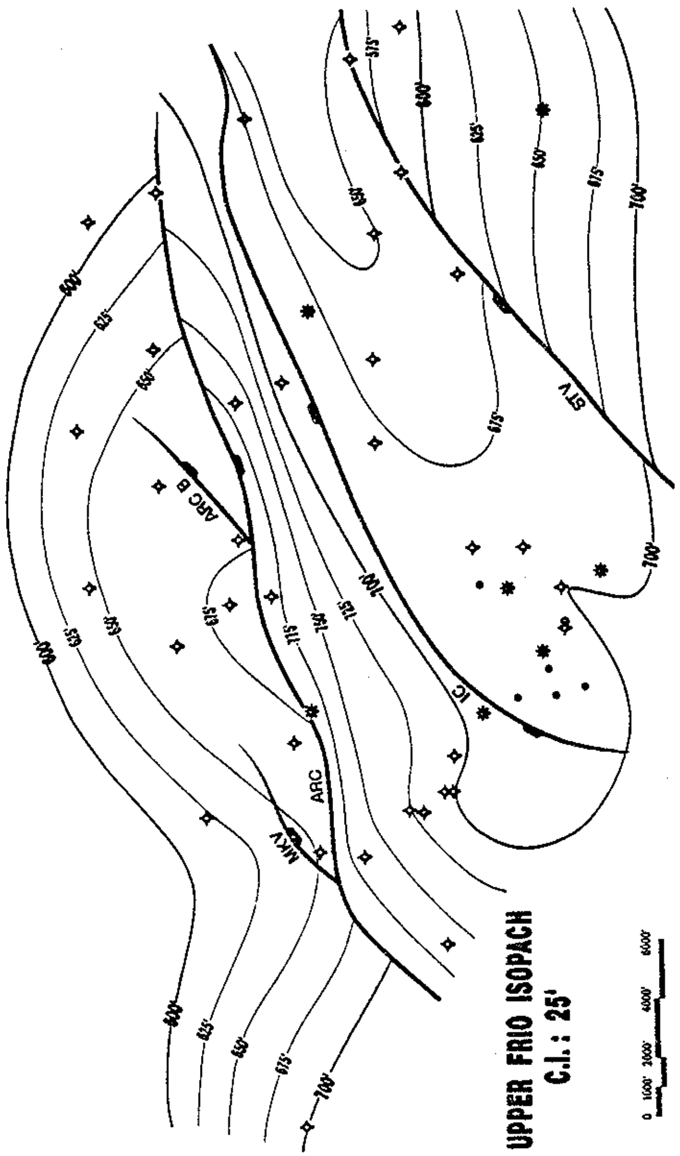

FIGURE 38: Upper Frio isopach. Ratios of sediment thicknesses on the upthrown versus downthrown block (expansion indices) indicate some of the highest rates of movement recorded in this study occured on the Arcola and Stevens Road Fault during the Upper Frio interval. Once again the Iowa Colony shows no influence on sedimentation.

(expansion indices 1.15-1.24) and the Stevens Road Fault (1.00-1.14). Rollover between these faults is accompanied by significant thinning over the anticlinal axis.

Little if any movement is indicated along the Iowa Colony Fault. Expansion indicies range from 1.00 - 1.01, and isopach contours are not deflected by the fault. South of the Stevens Road Fault sediments thin toward the rising Manvel Dome.

Anahuac Shale Isopach

This interval encompasses strata between the base of the Miocene Sand and the top of the Frio Formation (Figure 39). Important points to note on this map are: 1.) Continued slow growth across the Iowa Colony Fault. Expansion indices range between 1.00 and 1.01, and isopach contours remain uninterrupted across the fault trace; 2.) A drop in activity along the Arcola Fault (expansion indices 1.06-1.17) and; 3.) Very slow movement along the Stevens Road Fault (expansion indices 1.00-1.04) as compared to earlier intervals.

North of the Arcola Fault sediments thicken toward the fault trace and for the first time movement is indicated on the McKeever Road Fault, expansion index 1.07, and the Arcola Branch Fault, expansion index 1.02.

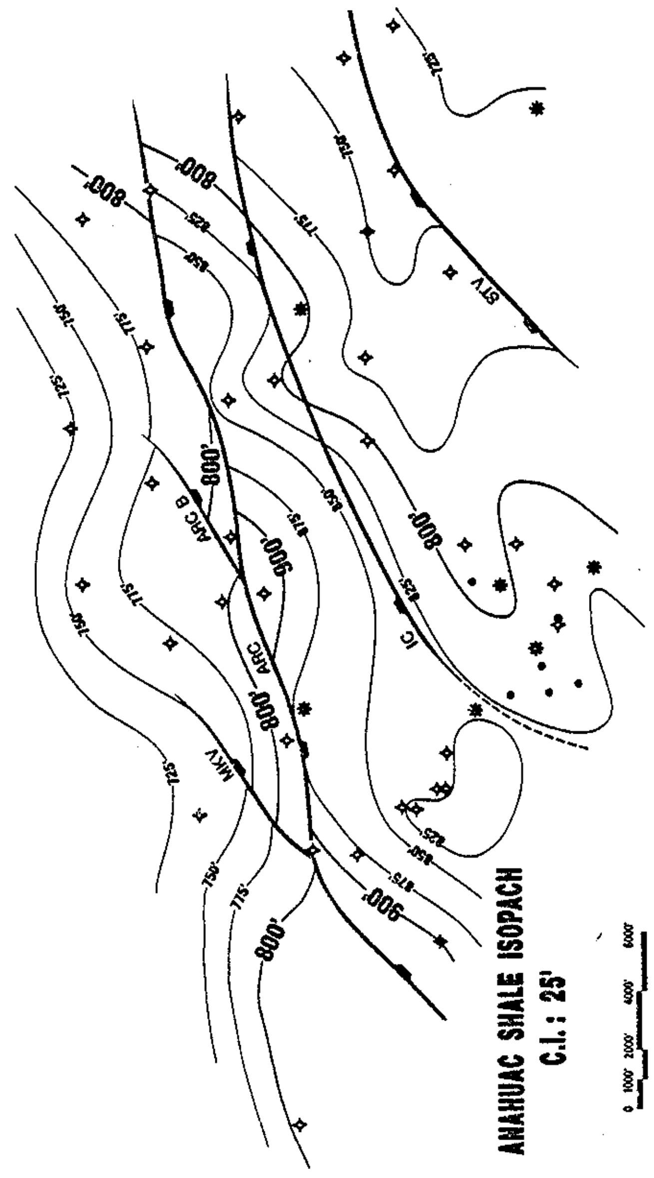

FIGURE 39: Anahuac Shale isopach. A dramatic decrease in rate of movement on the Arcola and Stevens Road Faults occurs during this interval with the Iowa Colony showing little if any influence on sedimentation.

Anahuac sediments are thickest on the downthrown block adjacent to the Arcola Fault. To the southeast, within the Arcola - Stevens Road Fault graben, sediments thin along the Arcola - Stevens Road Fault Anticline and over the Arcola Oil Field Anticline. South of the Stevens Road Fault sediments thin slightly toward the Manvel Dome.

Miocene Sand Isopach

Lower rates of fault movement are evident during deposition of this interval (Figure 40). North of the Arcola Fault sediments thicken toward the fault trace with very little interruption from the McKeever Road or Arcola Branch Faults. Expansion indices along the Arcola Fault (1.00-1.11) suggest slow continued growth along its length. The Stevens Road Fault shows moderate movement with expansion indices ranging from 1.00-1.08. The only fault showing an increased rate of movement is the Iowa Colony Fault with expansion indices ranging from 1.00 to 1.19.

Within the Arcola - Iowa Colony Fault graben, thinning of the Miocene Sand interval over the active Arcola Oilfield Anticline is particularly noticeable, coupled with localized rollover into the Arcola and Iowa Colony Faults. South of the Iowa Colony Fault sediments thin northeast, toward the Manvel Dome.

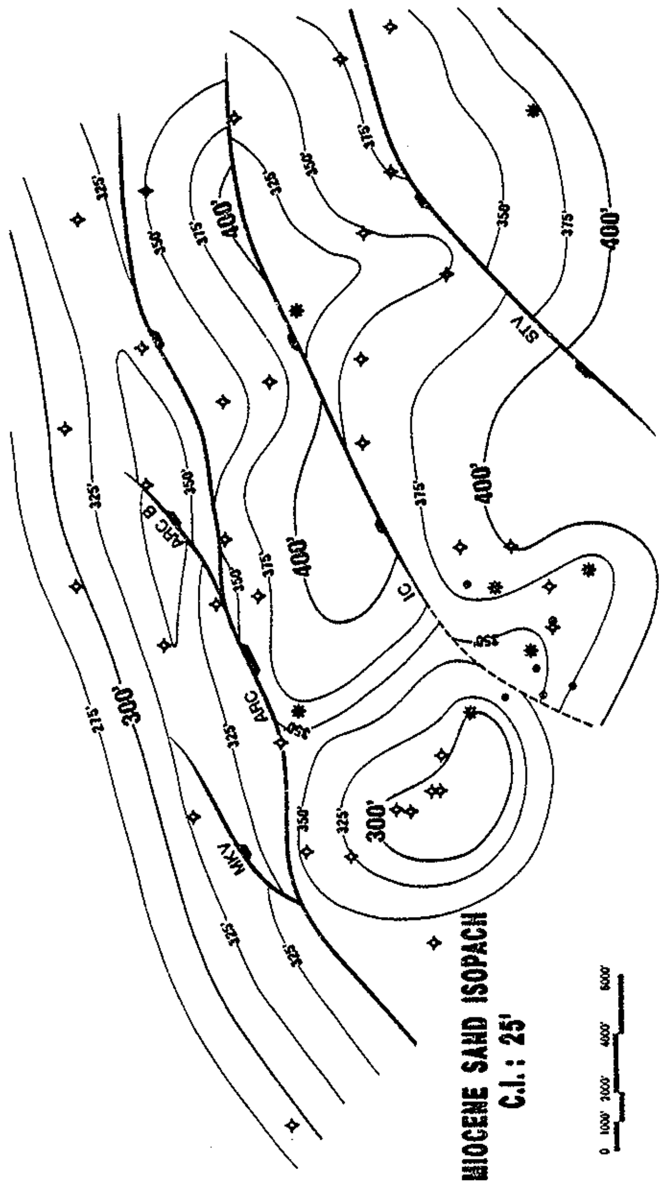

FIGURE 40: Miocene Sand isopach. For the first time the Iowa Colony Fault demonstrates a marked influence on sedimentation patterns.

2000′ Sand - Present Isopach

Expansion indices suggest widespread fault activity during deposition of this interval (Figure 36). North of the Arcola Fault the McKeever Road and Arcola Branch Faults influence deposition with expansion indices ranging up to 1.02. Expansion indices of the Arcola Fault range from 1.00 to 1.12, indicating movement rates similar to those of the Anahuac interval. Within the Arcola - Iowa Colony Fault graben, 250 feet of stratigraphic thinning occurs over the Arcola - Iowa Colony Rollover Anticline. South of the Iowa Colony Fault, sediments thin northeast toward the Manvel Dome with very little interruption from the Stevens Road Fault.

Summary

Figures 41-43 illustrate the expansion index data for the Arcola, Stevens Road and Iowa Colony Faults in summary form. Each figure represents the movement history of a single fault. The bars represent the range of expansion index values for the fault during each time interval. A

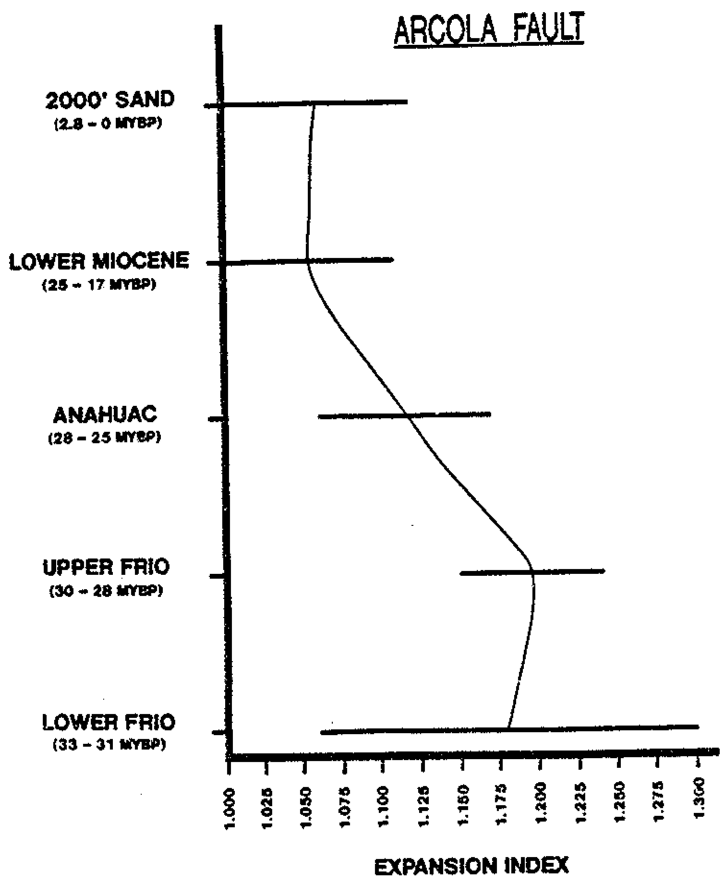

FIGURE 41: Movement history of the Arcola Fault. Each bar represents the range of expansion indices calculated for the fault during the corresponding time interval. The curved line connecting their midpoints represents the average movement rate of the fault through time.

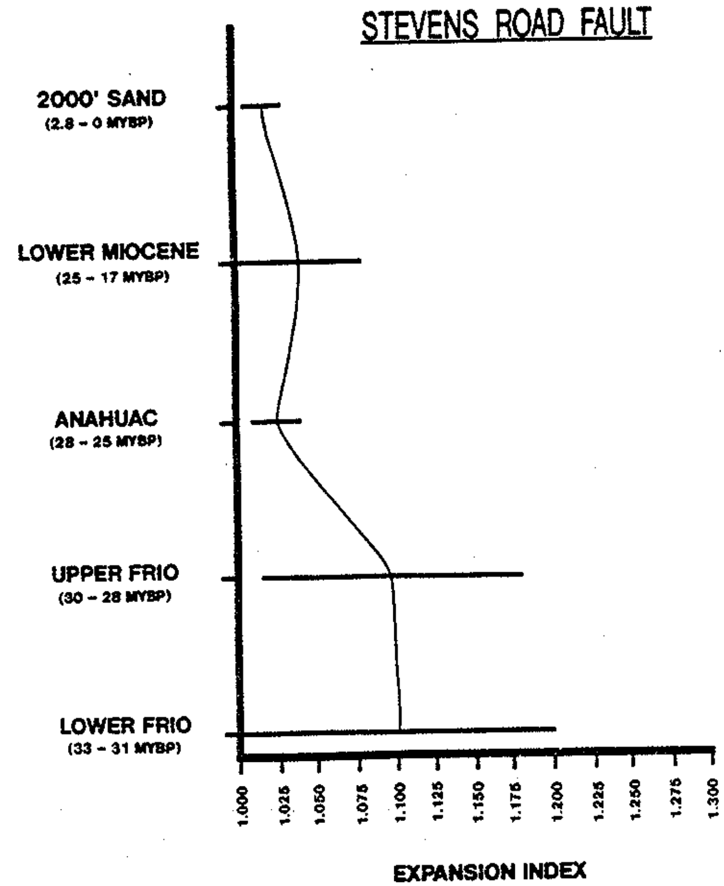

FIGURE 42: Movement history of the Stevens Road Fault. Each bar represents the range of expansion indices calculated for the fault during the corresponding time interval. The curved line connecting their midpoints represents the average movement rate of the fault through time.

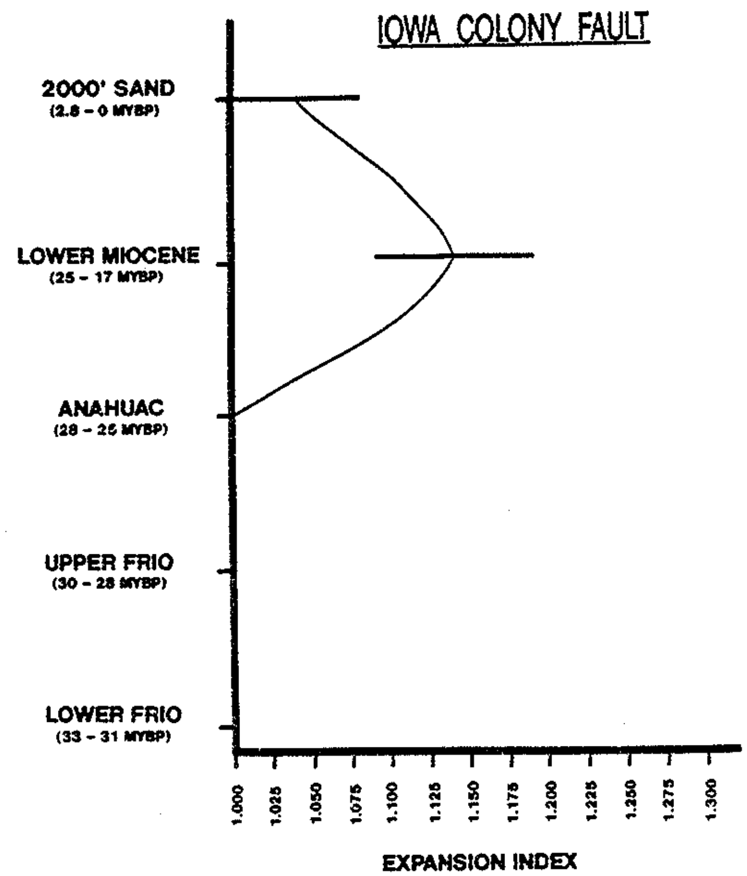

FIGURE 43: Movement history of the Iowa Colony Fault. Each bar represents the range of expansion indices calculated for the fault during the corresponding time interval. The curved line connecting their midpoints represents the average movement rate of the fault through time.

curve connecting their midpoints is drawn to show long-term trends in the movement history of the fault.

Figure 44 is designed to summarize all the data presented in the preceding structure and isopach map discussions. A bar graph appears for each structure and its width represents the relative amount of movement it underwent during the corresponding time period; the wider the bar, the higher the movement rate.

The most striking structural feature in the area is the Arcola Fault. It is a growth fault that has been active since at least the Early Oligocene. However, its rate of motion has decreased progressively from the Oligocene to the present. Expansion indices indicate that from the early Oligocene to the Miocene, movement took place along nearly the entire length of the fault. From the Miocene to the present, however, portions of the fault appear to have "locked up" while others continued to move.

The Stevens Road Fault formed antithetic to the Arcola Fault no later than Vicksburg time, and it remained the primary antithetic fault until Anahuac time. Expansion indices suggest renewed movement of the fault in the Miocene, but it remained a subordinate feature. Since Miocene rejuvenation, the Stevens Road Fault also shows a general pattern of decreasing rates of movement to the present.

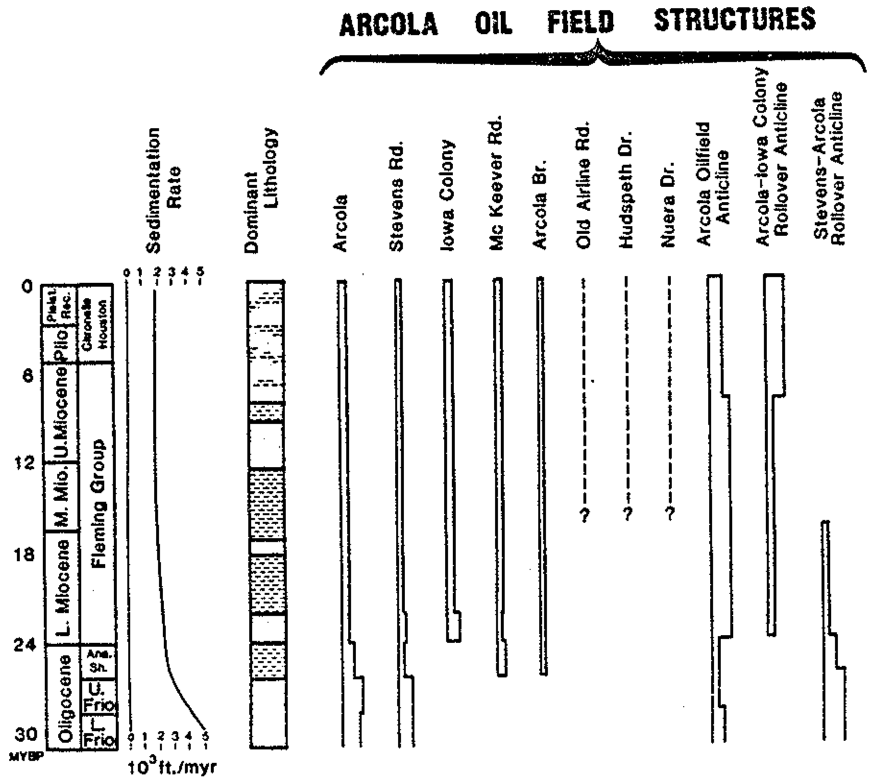

FIGURE 44: Generalized geologic history of Arcola Oil Field faults and structures in graphic form. The width of the bar graph for each structure represents the relative amount of activity of that structure during the corresponding time period.

The fault with the highest level of recent activity is the Iowa Colony Fault. It first experienced high rates of movement in the Early Miocene corresponding in time to the deposition of a basal Miocene sand package suggesting it may have formed in response to sediment loading. Although it is antithetic to the Arcola, it shows greater expansion indices than that fault from the Lower Miocene to the present. Like the Arcola, rates of movement on the Iowa Colony Fault decreased since the Miocene, but the prominent surface lineament associated with this feature strongly suggests it is currently more active than the Arcola.

Explanations for the development of the Iowa Colony, Stevens Road and Old Airline Road Faults may be found in listric fault studies by Ellis and McClay (1988). Their fault model demonstrates that a rollover anticline with associated antithetic faults develops in response to extensional movement along a primary listric fault. When rollover development reaches a critical point, a graben forms along the crest of the rollover anticline. The first antithetic fault forms at some distance from the primary listric fault and subsequent antithetic faults develop in stepwise fashion increasingly closer to it. According to this model, the following scenario would explain the interrelated geometry of four of the Arcola area faults: Movement along the Arcola Fault initiated rollover development along which a crestal graben formed. The Stevens Road Fault was the first antithetic to develop, probably in conjunction with the Old Airline Fault to create the graben structure. As movement on the Arcola Fault continued, the Iowa Colony Fault developed antithetic to it in the expected position, closer to the primary listric fault than the previous antithetic.

Development of the McKeever Road, Arcola Branch, Hudspeth Drive and Nuera Drive Faults is probably related to the sinuous nature of the Arcola Fault. These subordinate faults appear along portions of the Arcola where bends appear in its surface trace. These bends exist because of the regional stresses present; however, it is possible that movement along the sinuous portions of the fault induces local stresses which require development of subsidiary features to absorb them. The earliest evidence of movement on the McKeever Road and Arcola Branch Faults corresponds to decreased activity on both the Arcola and Stevens Road Faults during Late Oligocene time. Decrease in activity along the McKeever Road Fault during the Early Miocene corresponds to the earliest evidence of substantial movement on the Iowa Colony Fault and increased activity on the Stevens Road Fault.

The pattern of development of the Arcola Oil Field Anticline shows no direct correspondence to that of the

faults in the area. Its axis is nearly perpendicular to the strike of the faults. The development of this unusual feature is most likely related to the evolution of a deep-seated salt structure which appears at great depth on seismic profiles.

Earliest development of the Arcola-Iowa Colony rollover anticline occurred in the earliest Miocene in response to active movement on the Iowa Colony Fault. Within the data constraints of this study, the Stevens Road - Arcola Rollover Anticline shows most vigorous activity in Middle Oligocene times, decreased activity in Late Oligocene and Early Miocene time, and a cessation of growth by the Middle Miocene.

FAULT MODELING

The aim of this chapter is to describe models which have been proposed for the prediction of fault geometry and to test these models using the data from the Arcola Oil Field area.

On the basis of excellent well control, and available seismic data, it is evident that the Arcola Fault is a major down-to-coast, syndepositional, listric fault. The Iowa Colony and Stevens Road Faults are major antithetic up-to-coast, syndepositional, listric faults associated with the Arcola Fault. Other faults in the vicinity are minor synthetic features. Movement on the major faults is accompanied by differential rotation of the faulted strata, and all the major faults exhibit growth character during at least part of their movement history. Although there are several theoretical and empirical models that describe the initiation (Kehle, 1970; Carver, 1968; Ode, 1962; etc.) and subsequent geometric evolution (Bradshaw and Zoback, 1988; Ellis and McClay, 1988; Wheeler, 1987; Bruce, 1984) of growth faults, none, except those described by Gibbs (1983) and Xiao & Suppe (1986), are directly amenable to testing.

The Gibbs construction predicts listric fault shape from rollover shape and calculates the depth to detachment. In Figure 45 (Jackson and Galloway, 1984) the horizontal

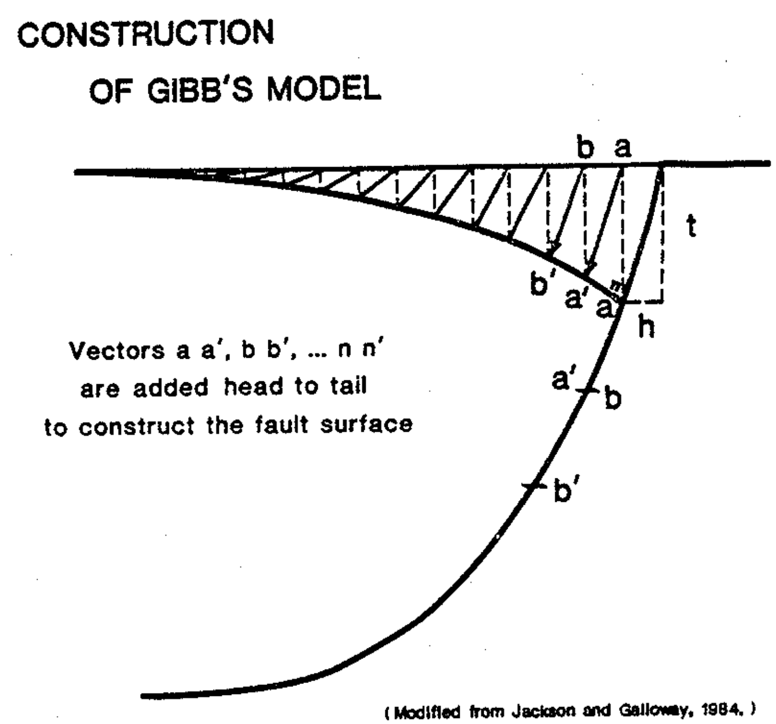

FIGURE 45: The Gibb's model predicts listric fault shape from rollover shape.

line is the pre-rollover position of a sedimentary horizon. The Gibbs model is based on a consideration of the path of motion of particles within the defined stratigraphic layer from pre- to post-rollover positions, assuming constant volume. To apply the model one must have two knowns: the near surface dip of the fault; and the final rollover shape. It is assumed that the rollover bed was initially horizontal.

In this model the shape of the rollover reflects the cumulative movement on the fault below. The displacement vector aa′ is the result of the throw, t, and the heave, h, for that portion of the fault. Likewise, the displacement of a to a′′ on the rollover is the result of the same throw and heave. If the displacement vectors for the rollover are defined, they may be projected down to construct the curving fault plane in segments.

Construction of the listric fault shape is accomplished by dividing the rollover into blocks with equal width, h, starting from the fault plane. Next, the diagonal is drawn to each heave block so that it is plunging away from the fault. This diagonal is the throw-heave resultant, or displacement vector (Jackson and Galloway, 1984). Each displacement vector is then added graphically to construct the listric fault shape. The horizontal component, heave (h), must be kept constant if there is to be no change in

cross-sectional area. Throw, (t), will decrease as the crest of the rollover anticline is approached, causing both the plunge and magnitude of the displacement vectors to decrease with distance from the fault. This causes the dip of the fault to decay toward a horizontal detachment plane whose depth is proportional to the relief of the rollover anticline and the near-surface dip of the fault.

Figure 46 illustrates the cross-sectional geometry of the Arcola and Iowa Colony Faults as determined from well logs and as predicted by the Gibbs model from rollover on the 2000′ Sand. It is obvious that the Gibbs model predicts fault dip angles that are much too low and a detachment surface at much too shallow a depth.

A reason behind the failure of the model may be the existence of antithetic faults in the area. The Gibbs model considers only a single listric fault. The effects of antithetic faulting are not accounted for. The "potential void" created by slip on a listric fault can be filled either by reverse drag (rollover development), or by antithetic faulting. Antithetic faults will act to decrease the relief of the rollover anticline and thus cause the model to fail.

Another reason for its failure when applied to the Arcola and Iowa Colony Faults is that it is a "constant

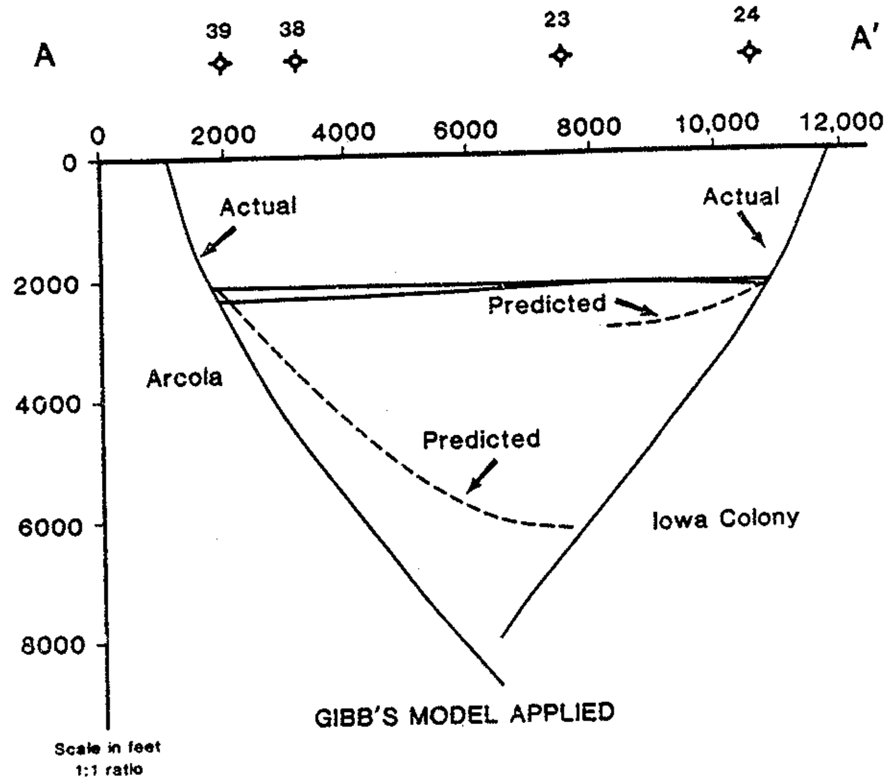

FIGURE 46: The Gibb's model applied to the Arcola and Iowa Colony Faults. The model predicts much too shallow dip angles and flattening at much too shallow depth. (Refer to Figure 29 for location of cross-section line A - A').

volume" model which does not consider the effects of sediment compaction.

A model proposed by Xiao and Suppe (1986), considers compaction of sediments to be the principal cause of listric fault shape. They propose that, "In the Gulf Coast area the dip of a normal fault will decrease with depth due to compaction in response to increasing overburden pressure" (Xaio and Suppe, 1986, p. 4), (Figure 47).

Consider the diagonals of rectangles A and B to be fault planes. Before burial and compaction, rectangles A and B were the same size and shape; and 0o, the initial dip angle, was equal in both rectangles. It is assumed that as vertical compaction proceeds porosity decreases. In addition, the height of rectangle B, and the fault dip decrease while the solid volume remains unchanged. This idea is expressed in the following way:

$$\frac{\tan \theta}{\tan \theta_0} = \frac{1 - \phi_0}{1 - \phi}$$

Where: θ_0 and θ are the initial and present fault dip angle; and ϕ_0 and ϕ are the initial and present porosity, respectively.

In order to apply the model, the compaction gradient for sandstone and shale must be determined. A linear porosity

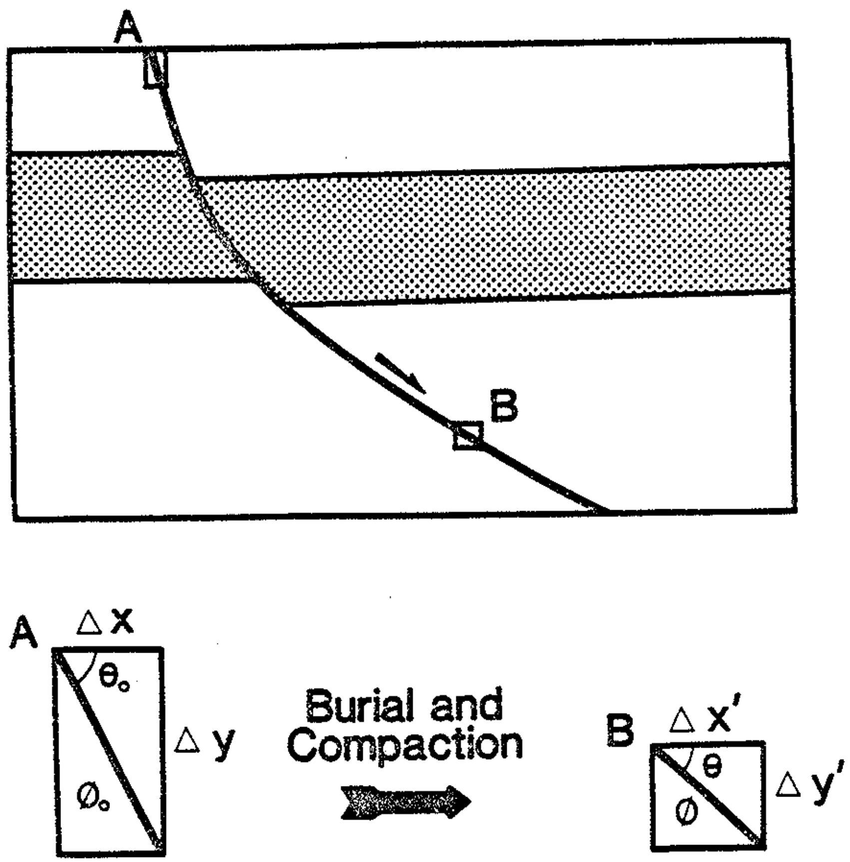

FIGURE 47: In the Xaio/Suppe model listric fault shape is obtained by the processes of burial and compaction.

versus depth relationship is assumed and expressed in the equation:

$$\phi = aY + b$$

Where: b is the initial porosity; a is a regression coefficient; and Y is depth.

Xaio and Suppe (1986) originally applied their model to a south Louisiana growth fault. During derivation of the fault shape equations I found that two coefficients had been transposed in their written progress report. The transposition has been corrected in this study and porosity data specific to Brazoria County has been used in the equations. A "best fit" regression line for sand and shale were determined from porosity data from the Pleasant Bayou Oil Field, Brazoria County. When the porosity versus depth equations for pure sand and pure shale are substituted into Equation 1, and integrated, the following predicted fault shape equations are obtained in terms of X (horizontal) and Y (vertical) coordinates:

For pure sand: $$X = \frac{Y}{k}\left(1 - b - \frac{aY}{2}\right)$$

For pure shale: $$X = \frac{Y}{k}\left(1 - d - \frac{c}{\ln 10}\ln Y + \frac{c}{\ln 10}\right)$$

Appendix E outlines the derivation of these equations.

Using the above equations, two separate fault shapes are produced (Figure 48); one for homogeneous sandstone, and one for homogeneous shale. Since the Arcola-Iowa Colony area consists of interbedded sandstone and shale, the corresponding fault shapes are spliced together to form a continuous, but uneven fault shape.

The type log for the Arcola area (Figure 32) was used to represent the average stratigraphic section. Figure 49 shows clearly that the modified Xaio-Suppe model describes the geometry of the Arcola and Iowa Colony Faults very well. The Iowa Colony may show some greater deviation from the predicted curve than does the Arcola, but this could be due to inaccuracies in the assumed sand-shale ratio in the immediate vicinity of the fault and the assumption of a linear porosity decrease.

It should be noted that the predicted profiles are 'best-fits'. To plot the profiles, it had to be decided what initial fault dip values to use. At depths of 1000 feet, the fault plane map indicates dips of 73 and 68 degress, respectively, for the Arcola and Iowa Colony Faults. When these fault dips are used as initial dips, the predicted fault shapes do not achieve a 'best-fit'. If a

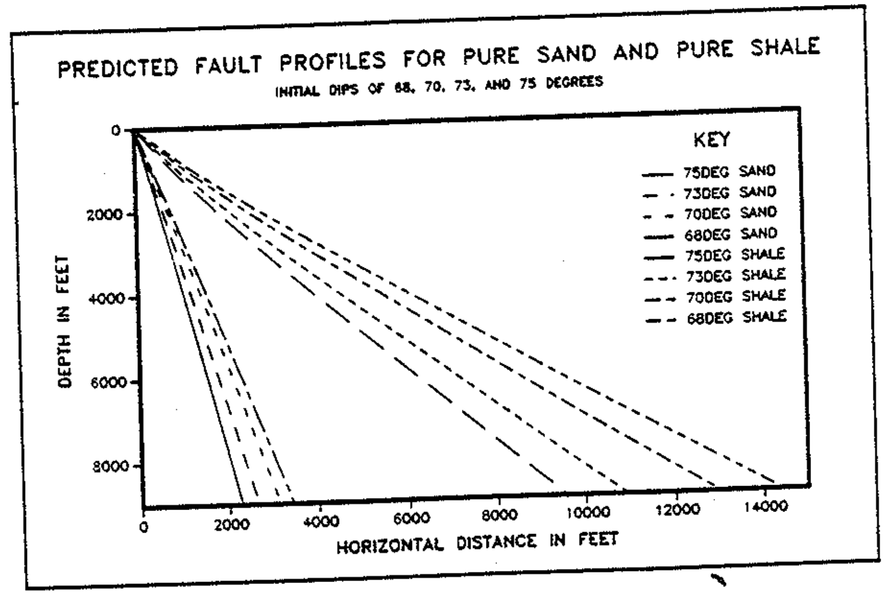

FIGURE 48: In the Xaio/Suppe model two separate fault shapes are calculated and spliced together to construct the predicted fault shape. The homogenous sandstone curves are much steeper than the homogeneous shale curves. Several initial dip angles are illustrated for each curve.

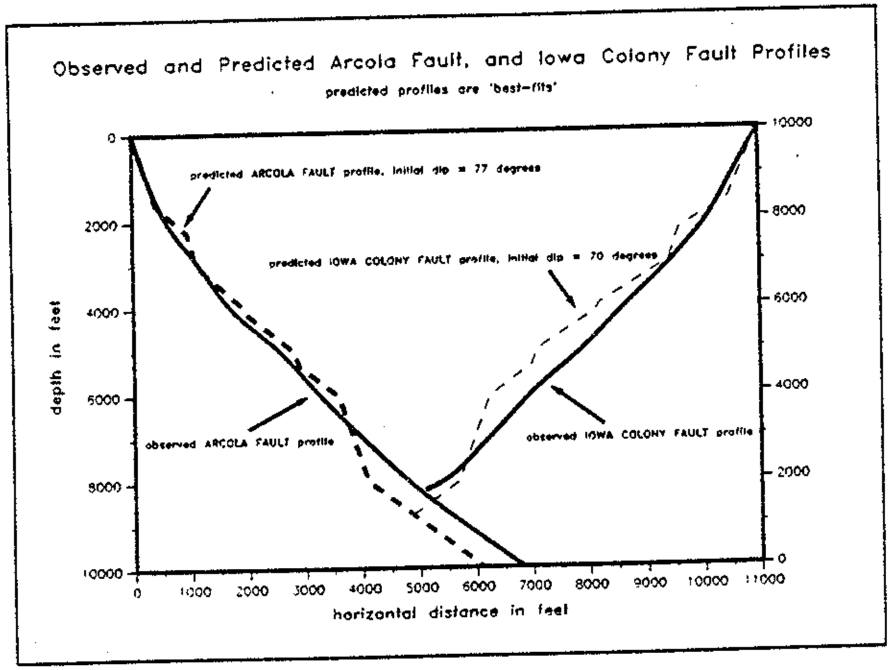

FIGURE 49: The Xaio/Suppe model applied to the Arcola and Iowa Colony Faults. The compaction model describes the geometry of the faults very well.

cross-section of the fault planes is constructed with no vertical exaggeration, near surface dip angles of 77 and nearly 70 degrees are measured for the Arcola and Iowa Colony Faults. These steeper initial dip values of 77 and 70 degrees were used for the Arcola and Iowa Colony Faults, respectively, and a 'best-fit' was obtained. This result is reasonable since the dip of a growth fault characteristically increases toward the surface.

An additional growth fault model, or hypothesis, is proposed by Bruce (1984). In a paper focusing on smectite/illite diagenesis, Bruce explains that the water released in this process increases pore pressures in the host shale creating an overpressured zone. Bruce proposes that overpressured zones cause the angle of dip of a growth fault to be greatly reduced as it passes through the zone. "Development of this pressure preceded or was simultaneous with fault development, otherwise the fault would have maintained a more normal dip through the interval of diagensis" (Bruce, 1984, p.680). In the same paper Bruce defines the zone of smectite diagenesis as occuring between 11,300 and 14,400 ft. in the Texas Gulf Coast (Bruce, 1984, p. 680).

It is reasonable that smectite diagenesis and the development of overpressured zones may contribute to the deformation of pre-existing growth faults. Bruce claims that the overpressured zones control, "The depths to which growth faults can penetrate," and also that the, "... dip that these faults assume at depth are largely dependent on fluid pressure in the sedimentary section at the time of faulting" (Bruce, 1984, p. 673). Bruce is applying his theory to the development of a fault through an existing overpressured section. Growth faults are syndepositional, meaning they are active at the earth's surface during sedimentation. Stratigraphic layers offset by growth faults exhibit increased vertical offset with depth and have expanded stratigraphic section on the downthrown block. The expanded stratigraphic section attests to the fact that the fault was active at the earth's surface during sedimentation. As the fault is buried to great depths, its original near-surface dip angle may be altered by any of a number of post depositional events including structural deformation and diagenetic alteration. As noted above, in the Gulf Coast, overpressured zones form at great depth, not at the earth's surface. It would seem most probable that this later development of overpressured zones would contribute to the eventual deformation of the growth fault angle of dip, but not control the development of initial fault dip near the earth's surface.

The Bruce (1974) hypothesis should be testable if fault dip information is available outside, and within the zone of

overpressure, and if pore pressure data are available within the overpressured zone. The effects of other diagenetic processes such as compaction plus local stress variations should also be determined and removed. The Bruce (1974) theory has not been applied in this study because overpressured zones were not encountered in the Arcola Oil Field. The depth of Arcola Oil Field well logs used in this study averaged 9,000 feet. This put most of the well logs at or near the base of the Frio Formation. In the Gulf Coast geopressure is often encountered in the Frio Formation or underlying Vicksburg Formation. However, the absence of overpressure in the Frio Formation in this portion of Brazoria County is confirmed by Bebout et al., (1976, p. 41) who state, "Wells drilled into the thick Tertiary section along the Upper Texas Gulf Coast encounter normal hydrostatic subsurface fluid pressure of .464 pounds per square inch per foot (psi/ft) for the upper 8,000 to 10,000 feet", and, "The top of geopressure occurs within the Frio Formation only within a 30-mile-wide band along the coast where it lies between 9,000 and almost 12,000 feet below sea level" (Figure 50).

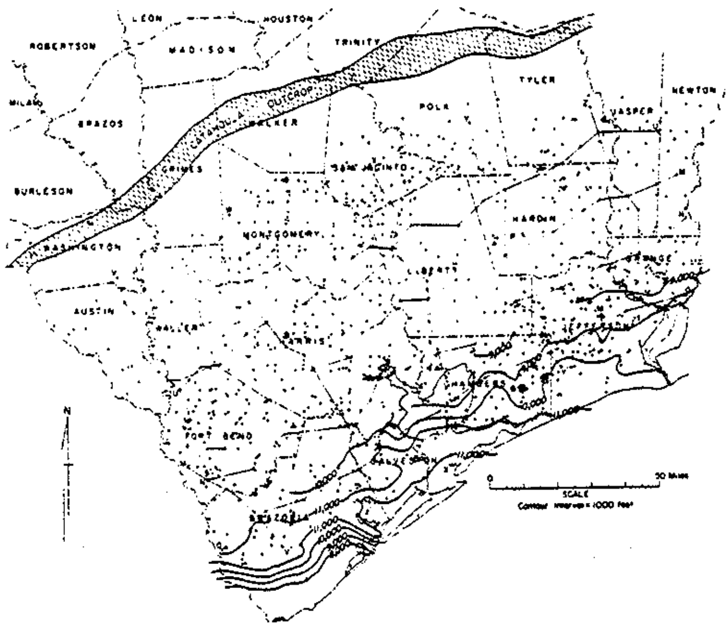

FIGURE 50: Top of geopressure, Upper Texas Gulf Coast. (From Bebout et al., 1976).

SUMMARY AND CONCLUSIONS

This study was undertaken to learn about surface faulting in Brazoria County, Texas. Information for this study was gathered primarily from examination of aerial photographs, field investigations, geophysical logs and seismic profiles. The combined interpretation of these data lead to the following conclusions:

1.) As many as 105 lineaments that may represent previously unknown active surface faults have been identified in Brazoria County, Texas. This raises the count of the total number of faults that might be present in the county to 130 (Figure 23 and Plate 24). The approximate cumulative length of the 105 new lineaments is 140 miles (225 km). Adding this to the 30 mile total length of the 25 previously known faults raises the possible cumulative length of faults to 170 miles (273 km).

2.) Roughly 70% of Brazoria County surface faults follow a regional, coast subparallel trend. Salt tectonics have imposed a pattern of radial faulting comprising a minimum 30% of surface faults in the county (Figure 24). The same pattern of surface faulting occurs in

Harris County with 69.4% of the faults having a regional, or coast subparallel strike, and a full 30% trending at high angle (between 1 and 90 degrees west of north) to the regional trend (Figure 25). The continuity of this surface fault pattern across such a large region indicates a wide-spread and ultimately natural origin for these features.

3.) Most of the surface faults in Brazoria County lie within two distinct areas: a.) The northernmost neck of the county where there is a high density of salt domes, and; b.) along the coastal regions of the county where it is expected that younger growth fault systems are more active, and where there is high visibility of such features (Figure 23).

4.) As interpreted from geophysical logs and seismic profiles, surface faults in Brazoria County are indeed the surface expression of much larger faults that continue deep into the subsurface. The surface faults also demonstrate increased displacement with increasing depth indicating their growth fault character.

5.) The movement history of faults in the Arcola Oil Field has been established through interpretation of

expansion indices plus fault plane, structure and isopach maps. These data indicate high rates of sedimentation and high rates of fault movement during the Early Oligocene. Sedimentation and fault movement rates decreased in the Middle and Late Oligocene and have followed a decreasing trend to the present. A break in this pattern occurred in the Early Miocene with a period of accelerated fault movement coinciding with deposition of a thick sand layer (Figures 42 and 43).

6.) The documented movement history of faults in the Arcola Oil Field since Frio deposition 33 million years ago, and the established growth character of other Brazoria County faults indicate these features are naturally occuring geologic phenomena of ancient origin with movement histories extending well into the Cenozoic (Figures 41 - 43).

7.) In establishing the heirarchy of faults in the Arcola Oil Field, the Arcola Fault is found to be the primary regional, down-to-coast, normal, listric growth fault which has been active since at least the early Oligocene. Structure and isopach data (Figures 33 - 40) indicate the Stevens Road Fault was the primary antithetic to the Arcola during the Oligocene through Anahuac deposition and the rollover anticline formed between these two faults had greatest expression during Frio deposition. In Earliest Miocene, a slow-down of movement on the Stevens Road Fault and accelerated movement on the Iowa Colony Fault established the Iowa Colony as the primary antithetic to the Arcola.

8.) Near-surface dip angles for the Arcola Fault are 5 to 13 degrees greater than those of the antithetic Iowa Colony and Stevens Road Faults (Figure 31).

9.) The Gibbs constant volume listric fault model is a poor predicter of the listric shape of the Arcola and Iowa Colony Faults (Figure 46).

10.) The Xaio and Suppe compaction model predicts very well the listric shape of both the Arcola and Iowa Colony Faults (Figure 49).

In the 1970's the population of Brazoria County increased 50 - 60%. Due to the sagging oil economy, population increases for the 1980's are not expected to be as dramatic, however, the rural character of Brazoria County is definitely changing. Along with increased population

come increased needs for construction of roads, highways, private homes, apartment complexes, schools, businesses and industry. Also needed will be new sites to dispose of the increased volume of waste produced. Location of any of these structures or facilities over an area of active surface faulting may, with time, have detrimental effects.

One of the primary uses of this study should be as a land-use planning guide. 130 "possible" active surface faults are mapped and documented. In terms of present and future land development in Brazoria County, the following findings and conclusions are made:

11.) Evidence of current movement of surface faults in Brazoria County include:

a.) Bending and cracking of streets, highways, parking lots and driveways.

b.) Warping, tilting and cracking of buildings and their foundations.

c.) Topographic anomalies such as scarps, right angle bends in streams, aligned ponds and marshes.

12.) No dollar amount for existing fault damage in the county is available. Although large, it is not expected to approach the millions of dollars in damages that have occurred in the Houston metropolitan area. However, as development in Brazoria County proceeds, substantial dollar amounts in damages will occur unless the proper steps are taken. When construction of permanent structures or facilities is planned, a geologic investigation should be conducted before tens, or hundreds of thousands of dollars are invested in the purchase and development of a piece of land. A geologic investigation undertaken by qualified individuals will determine if the property is affected by active surface faulting. A site specific, geologic investigation is the only way to ensure that an investment will not be lost due to the effects of surface faulting.

13.) Movement of faults in Brazoria County is most likely to be related to a combination of the following:

a.) Regional extensional stresses caused by basinward creep of the Cenozoic clastic wedge.

b.) Development of salt domes and ridges imposing local control over surface fault patterns.

c.) Possible reactivation and/or increased activity of faults due to extraction of subsurface fluids.

Even with future research, it may be difficult to determine the relative importance of each of these mechanisms as a cause of surface faulting in Brazoria County.

14.) The probability of future movement of a particular fault will be related to:

a.) The activity level of the fault as measured by its current surface expression.

b.) The movement history of the fault in the geologic past as determined by the increased throw of correlative beds with depth.

c.) The character and structural relationship of the fault, e.g., whether it is a regional down-to-coast fault, an antithetic fault or salt dome related fault. Salt dome related faults may be expected to remain active as long as the salt is still mobile. Large down- to-coast faults may remain active at varying rates indefinitely into the future. Movement on antithetic faults is directly related to movement on the primary down-to-coast fault. Movement on an antithetic fault some distance from the primary fault may dissipate with activation of younger antithetics closer to the primary fault. If this relationship of early and later stage antithetics can be determined, the relative probability of active movement on one of these faults versus movement on the other could be determined.

d.) The depth and rates of subsurface fluid production in the vicinity: It has been shown that production of subsurface fluids at depths greater than 3000 - 4000 feet generally does not cause surface subsidence and associated fault reactivation. The elastic properties of the overlying strata are such that reductions in pore fluid pressure in the producing layer are compensated for well before they affect surface layers; production of subsurface fluids even at shallow depths may not cause surface subsidence and fault reactivation if rates of production are very low. Very low production rates may eliminate the risk of severe

piezometric level declines which induce compaction of both the reservoir and the over/underlying shale layers, which is ultimately the cause of surface subsidence.

REFERENCES

Amery, G.B., 1978, Structure of continental slope, northern Gulf of Mexico, in: A.H. Bouma, G.T. Moore, and J.M. Coleman, (eds.), Framework, facies, and oil-trapping characteristics of the continental margin: American Association of Petroleum Geologists, Studies in Geology, no. 7, p. 141-153.

Aronow, S., 1981, Surface geology, in: Soil survey of Brazoria County, Texas: U.S. Dept. Agriculture, Soil Conservation Service, p. 79-83.

Bally, A.W., 1981, Atlantic type margins, in: Geology of passive continental margins. History, structure and sedimentological record: American Association of Petroleum Geologists, Education Course Note Series 19, p. 1/1-1/48.

Bally, A.W., Bernoulli, D., Davis, G.A., and Montadert, L., 1981, Listric normal faults: Oceanologica Acta, Proceedings 26th International Geology Congress, Paris, 1980, p. 87-101.

Barton, D.C., 1930, Surface geology of coastal southeast Texas: American Association of Petroleum Geologists Bulletin, v. 14, no. 10, p. 1302-1320.

Barton, D.C., 1936, Surface fracture system of South Texas, in: Gulf Coast oil fields: American Association of Petroleum Geologists, p. 25-269.

Bernard, H.A., LeBlanc, R.J., and Major, C.F., 1962, Recent and Pleistocene geology of southeast Texas, in: Geology of the Gulf Coast and Central Texas: Houston Geological Society, p. 175-224.

Bernard, H.A., Major, C.F., Jr., Parrott, R.S., and Le Blanc, R.J., Sr., 1970, Recent sediments of Southeast Texas - a field guide to the Brazos alluvial and deltaic plains and the Galveston Barrier Island complex: University of Texas at Austin, Bureau of Economic Geology, Guidebook No. 11.

Bevier, G.M., 1926, The Damon Mound Oil Field, Brazoria County, Texas, in: Geology of Salt dome oil fields: American Association of Petroleum Geologists Bulletin, p. 613-643.

Bishop, W.F., 1973, Late Jurassic contrmporaneous faults in North Louisiana and South Arkansas: American Association of Petroleum Geologists Bulletin, v. 57, no. 5, p. 858-877.

Bishop, W.F., 1974, Geology of a Smackover stratigraphic trap: American Association of Petroleum Geologists Bulletin, v. 55, no. 1, p. 51-63.

Bishop, R.S., 1977, Shale diapir emplacement in South Texas: Laward and Sherriff examples: Gulf Coast Association of Geological Societies Transactions, v. 27, p. 20-31.

Bott, M.H.P., 1979, Subsidence mechanisms at passive continental margins, in: J.S. Watkins, L. Montadert, and P.W. Dickerson, (eds.), Geological and geophysical investigations of continental margins: American Association of Petroleum Geologists Memoir 29, p. 3-9.

Bradshaw, G.A. and Zoback, M.D., 1988, Listric normal faulting, stress refraction, and the state of stress in the Gulf Coast basin: Geology, v. 16, p. 271-274.

Braunstein, J. and O'Brien, G.D., (eds.), 1968, Diapirism and diapirs: American Association of Petroleum Geologists Memoir 8, 444 p.

Bruce, C.H., 1973, Pressured shale and related sediment deformation; mechanism for development of regional contemporaneous faults: American Association of Petroleum Geologists Bulletin, v. 57, no. 5, p. 878-886.

Bruce, C.H., 1984, Smectite dehydration - its relation to structural development and hydrocarbon accumulation in northern Gulf of Mexico basin: American Association of Petroleum Geologists Bulletin, v. 68, no. 6, p. 673-683.

Buffler, R.T., Watkins, J.S., Shaub, F.J., and Worzel, J.L., 1980, Structure and early geologic history of the deep central Gulf of Mexico basin, in: R.H. Pilger, (ed.), Proceedings of Symposium, The origin of the Gulf of Mexico and the early opening of the central North Atlantic Ocean, p. 3-16.

Carver, R.E., 1968, Differential compaction as a cause of regional contemporaneous faults: American Association of Petroleum Geologists Bulletin, v. 52, no. 3, p. 414-419.

Castle, R.O. and Youd, T.L., 1972, Discussion: The Houston fault problem: American Association of Petroleum Geologists Bulletin, v. 9, no. 1, p. 57-68.

Christensen, A.F., 1983, An example of a major syndepositional listric fault, in: A.W. Bally, (ed.), Seismic expression of structural styles: American Association of Petroleum Geologists, Studies in Geology, no. 15, v. 2, p. 36-40.

Clanton, U.S., and Amsbury, D.L., 1975, Active faults in southwestern Harris County, Texas: Environmental Geology, v. 1, no. 3, p. 149-154.

Clanton, U.S. and Verbeek, E.R., 1981, Photographic portrait of active faults in the Houston metropolitan area, Texas, in: Houston area environmental geology: Houston Geological Society, p. 70-85.

Cloos, E., 1968, Experimental analysis of Gulf Coast fracture patterns: American Association of Petroleum Geologists Bulletin, v. 52, no. 3, p. 420-444.

Collins, E.W., Hobday, O.K., and Kreitler, C.W., 1980, Quaternary faulting in East Texas: University of Texas at Austin, Bureau of Economic Geology Cirular 80-1, 20 p.

Cox, S.J.D. and Scholz, C.H., 1988, On the formation and growth of faults: An experimental study: Journal of Structural Geology, v. 10, no. 4, p. 413-430.

Crans, W., Mandl, G., and Harembourе, J., 1980, On the theory of growth faulting: a geomechanical delta model based on gravity sliding: Journal of Petroleum Geology, v. 2, p. 265-307.

Crenwelge, G.W., Crout, J.D., Griffin, E.L., Golden, M.L., and Baker, J.K., 1981, Soil survey of Brazoria County, Texas: U.S. Department of Agriculture, Soil Conservation Service, in cooperation with Brazoria County Commissioners Court and the Texas Agricultural Experiment Station, 140p., 116 plates.

Dailly, G.C., 1976, A possible mechanism relating progradation, growth faulting, clay diapirism and

overthrusting in a regressive sequence of sediments: Canadian Petroleum Geology Bulletin, v. 24, no. 1, p. 92-116a.

Doering, J.A., 1956, Review of Quaternary surface formations of Gulf Coast region: American Association Petroleum Geologists Bulletin v. 40, p. 1816-1862.

Dupre, W.R., 1987, An introduction to the Cenozoic geologic history of the Texas Gulf Coast: Houston Geological Society, 106 p.

Edwards, M.B., 1981, Upper Wilcox Rosita delta system of South Texas: growth-faulted shelf-edge deltas: American Association of Petroleum Geologists Bulletin, v. 65, p. 54-73.

Ekimov, R., 1980, Bibliography on subsidence, faulting, and groundwater of southeast Texas with special emphasis on the Houston-Galveston area (1892-1979): Houston Geological Society, p. 146-164.

El-Ashry, M.T., (ed.), 1977, Air photography and coastal problems: Benchmark Papers in Geology, v. 38, Dowden, Hutchinson and Ross, Inc., Stroudsburg, PA, 425 p.

Ellis, P.G. and McClay, K.R., 1988, Listric extensional fault systems- results of analogue model experiments: Basin Research (1988)1, p. 55-70.

Elsbury, B.R., Van Siclen, D.C., and Marshall, B.P., 1980, Engineering aspects of the Houston fault problem: American Society Civil Engrs. - Fall Mtg. Texas and New Mexico Sections, 39 p.

Etter, E.M., (ed.), 1978, Field trip ot Damon Mound: Houston Geological Society, 67 p.

Everett, J.R. and Reid, W.M., 1981, Active faults in the Houston, Texas area as observed on Landsat Imagery, in: Houston Area Environmental Geology, Houston Geological Society, p. 13-27.

Ewing, T.E., 1983, Growth faults and salt tectonics in the Houston diapir province - relative timing and exploration significance: 33rd Ann. Gulf Coast Association Geological Societies Transactions, p. 83-90.

-----1986, Structural styles of the Wilcox and Frio growth-fault trends in Texas: Constraints on geopressured reservoirs: University of Texas at Austin, Bureau of Economic Geology, Rept. of Invest. No. 154, 86 p.

Finley R.J., 1979, Landsat analysis of the Texas coastal zone: University of Texas at Austin, Bureau of Economic Geology, Rept. of Invest., No. 93, 71 p.

Fisher, W.L. and McGowan, J.H., 1972, Environmental geologic atlas of the Texas coastal zone - Galveston-Houston area: University of Texas at Austin, Bureau of Economic Geology, 91 p.

Freed, R.L., 1982, Clay mineralogy and depositional history of the Frio Formation in two geopressured wells, Brazoria County, Texas: Transactions Gulf Coast Association Geological Societies v. 32, p. 459-463

Gabrysch, R.K., and Bonnet, C.W., 1975, Land-surface subsidence in the Houston-Galveston region, Texas: Texas Water Development Board, Rept. 188, 19 p.

Gabrysch, R.K., and Holzer, T.L., 1978, Fault control of subsidence, Houston, Texas: Discussion of a paper by C.W. Kreitler, Ground Water, v. 16, no. 1, p. 51-55.

Galloway, W.E., 1986a, Growth faults and fault-related structures of prograding terrigenous clastic continental margins: Transactions Gulf Coast Association of Geological Societies, v. 36, p. 121-128.

-----, 1986b, Reservior facies architecture of microtidal barrier systems: American Association of Petroleum Geologists Bulletin, v. 70, p. 787-808.

Galloway, W.E. and Hobday, D.K., 1983, Terrigenous clastic depositional systems: Applications to petroleum, coal, and uranium exploration: Springer-Verlag, Inc., New York, 416 p.

Galloway, W.E., Hobday, D.K., and Magara, K., 1982, Frio Formation of the Texas Gulf Coast Basin - depositional systems, structural framework, and hydrocarbon origin, migration, distribution, and exploration potential: University of Texas at Austin, Bureau of Economic Geology, Rept. of Invest. 122.

Galloway, W.E., Jirik, L.A., Morton, R.A., and DuBar, J.R., 1986, Lower Miocene (Fleming) depositional episode of the Texas Coastal Plain and continental shelf: Structural framework, facies, and hydrocarbon resources: University of Texas at Austin, Bureau of Economic Geology, Rept. of Invest. No. 150, 50 p.

Galloway, W.E., and others, 1983, Atlas of major Texas oil reserviors: University of Texas at Austin, Bureau of Economic Geology, 139p.

Gardner, F.J., 1952, The oil and gas fields of the Texas Upper Gulf Coast: Railroad Commission, District 3, p. 45-74.

Gibbs, A.D., 1983, Balanced cross-section construction from seismic sections in areas of extensional tectionics: Journal of Structural Geology, v. 5, no. 2, p. 153-160.

Gregory, A.R., 1980, Study effects of geopressured-geothermal subsurface environment on elastic properties of Texas Gulf Coast sandstones and shales using well logs, core data, and velocity surveys: Prepared for the United States Department of Energy, Division of Geothermal Energy, by the University of Texas at Austin, Bureau of Economic Geology, Contract No. DE-AS05-78ET-28468, 35 p.

Halbouty, M.T., 1979, Salt Domes - Gulf Region, United States and Mexico: Gulf Publishing Co., Houston, Texas, 425 p.

Hanor, J.S., 1982, Reactivation of fault movement, Tepetate Fault Zone, South Central Louisiana: Transactions Gulf Coast Association Geological Societies, v. 32, p. 237-242.

Hardin, F.R. and Hardin, G.C., 1961, Contemporaneous normal faults of Gulf Coast and their relation to flexures: American Association of Petroleum Geologists Bulletin, v. 45, p. 238-248.

Hardin, G.C., Jr., 1962, Notes on Cenozoic sedimentation in the Gulf Coast geosyncline, U.S.A., in: Geology of the Gulf Coast and Central Texas: Geological Society of America Annual Mtg. and Houston Geological Society, p. 1-15.

Hesemann, T., Healy T., and Soled, B., 1982, Surface faulting in the Houston metropolitan area of Texas: A guide to literature and other information: Bulletin, Houston Geological Society, 25(3), p. 6-8.

Heuer, W.C., 1979, Active faults in the northwestern Houston area: University of Houston, Master's Thesis, 172 p.

Holzer, T.L. and Bluntzer, R.L., 1984, Land subsidence near oil and gas fields, Houston, Texas: Groundwater, v. 22, no. 4, p. 150-159.

Holzer, T.L. and Gabrysch, R.K., 1987, Effect of water-level recoveries on fault creep, Houston, Texas: Ground Water, v. 25, no. 4, p. 392-397.

Houston Geological Society, 1984, Environmental geology of East Harris County: Houston Geological Society Guidebook, (D.C. Dale, Chair), Environmental Committee, 46 p.

Humphris, C.C., 1978, Salt movement on continental slope, northern Gulf of Mexico, in: A.H. Bouma, G.T. Moore, and J.M. Coleman, eds., Framework, facies, and oil-trapping characteristics of the upper continental margin: American Association of Petroleum Geologists, Studies in Geology 7, p. 69-86.

Jackson, M.P.A. and Galloway, W.E., 1984, Structural and depositional styles of Gulf Coast Tertiary continental margins: Application to hydrocarbon exploration: American Association of Petroleum Geologists Continuing Education Course Note Series No. 25, 226 p.

Jackson, M.P.A. and Talbot, C.J., 1986, External shapes, strain rates, and dynamics of salt structures: Geological Society of America Bulletin, v. 97, p. 305-323.

Kehle, R.O., 1970, Analysis of gravity sliding and orogenic translation: Geological Society of America Bulletin, v. 81, p. 1641-1664.

Kreitler, C.W., 1976a, Lineations and faults in the Texas Coastal zone: University of Texas at Austin, Bureau of Economic Geology, Rept. of Invest. No. 85, 32 p.

-----1976b, Fault control of subsidence, Houston-Galveston area, Texas: University of Texas at Austin, Bureau of Economic Geology, Research Note 5, 17 p.

Le Blanc, R.J., and Hodgson, W.D., 1959, Origin and development of the Texas shoreline: Gulf Coast Association of Geological Societies Transactions, v. 9, p.197-220.

Lee, K.L. and Shen, C.K., 1969, Horizontal movements related to subsidence: Journal of the Soil Mechanics and Foundations Divisions, Proceedings American Society Civil Engineers, 95, no. SM-1, p. 139-166.

Lehner, P., 1969, Salt tectonics and Pleistocene stratigraphy on continental slope of northern Gulf of Mexico: American Association of Petroleum Geologists Bulletin, v. 53, p. 2431-2479.

Lerche, I. and O'Brien, J.J., 1987, Dynamical geology of salt and related structures: Academic Press, Inc., New York, 832 p.

Loucks, R.G., 1978, Sandstone distribution and potential for geopressured geothermal energy production in the Vicksburg Formation along the Texas Gulf Coast: Transactions Gulf Coast Association of Geological Societies, v. 12, p. 27-37.

Lowell, J.D., 1984, Sructural styles in petroleum exploration: OGCI Publications, Tulsa, 460 p.

McClelland Engineer, 1966, Land surface subsidence and surface faulting (Appendix C), in: Turner, Collie, and Braden, Inc., A comprehensive study of Houston's municipal water system for the city of Houston, Phase I, Basic studies, 50 p.

McFarlan, E., Jr., 1977, Lower Cretaceous sedimentary facies and sea level changes, U.S. Gulf Coast: University of Texas at Austin, Bureau of Economic Geology, Rept. of Invest. No. 89, p. 5-11.

McNaughton, D.A., (ed.), 1953, Guidebook, field trip routes, oil field geology: American Association of Petroleum Geologist, Society of Economic Paleontologists and Mineralogists, Society of Exploration Geophysicists, 168 p.

Martin, R.G., 1978, Northern and eastern Gulf of Mexico continental margin: Stratigraphic and structrual framework, in: A.H. Bouma, G.T. Moore, and J.M. Coleman, (eds.), Framework, facies, and oil- trapping characteristics of the upper continental margin: American Association of Petroleum Geologists Studies in Geology No. 7, p. 21-42.

-----1980, Distribution of salt structures, Gulf of Mexico: U.S. Geological Survey Map MF - 1213.

Minor, H.E., 1925, Goose Creek Oil Field, Harris County, Texas: American Association of Petroleum Geologists Bulletin, v. 9, no. 2, p. 286-297.

Murray, G.E., 1961, Geology of the Atlantic and Gulf coastal province of North America: Harper and Bros., New York, 692 p.

Murray, G.E., 1968, Salt structures of Gulf of Mexico basin - a review, in: Diapirism and Diapirs: American Association of Petroleum Geologists Memoir 8, p. 99-121.

Norman, C.E., 1987, Surface faults in West Harris County, in: Environmental Geology - West Harris County: Houston Geological Society Guidebook, Environmental Committee, November 14, 1987, p. 22-28.

Ocamb, R.D., 1961, Growth fautls in South Louisiana: Transactions Gulf Coast Association Geological Societies, v. 11, p. 139-175.

O'Neill, M.W. and Van Siclen, D.C., 1984, Activation of Gulf Coast faults by depressuring of aquifers, an engineering approach to siting structures along their traces: Association of Eng. Geologists Bulletin, v. 2, no. 1, p., 73-87.

Poland, J.F. and Davis, G.H., 1983, Land subsidence due to withdrawal of fluids, in: Physical Hydrogeology, Benchmark Papers in Geology, 72, p. 384-397.

Pratt, W.E. and Johnson, D.W., 1926, Local subsidence of the Goose Creek Oil Field: Journal of Geology, v. 34, p. 577-590.

Prokopovich, N.P., 1983, Neotectonic movement and subsidence caused by piezometric decline: Bulletin of Association of Engr. Geologists v. 20, no. 4, p. 393-404.

Quarles, M., Jr., 1953, Salt-ridge hypothesis on origin of Texas Gulf Coastal type faulting: American Association of Petroleum Geologists Bulletin, v. 37, p. 489-508.

Reid, W., 1973, Active faults in Houston, Texas: PhD Dissertation, University of Texas at Austin, 122 p.

Roberts, W.H., III, 1982, Gulf coast magic: Transactions Gulf Coast Association Geological Societies, v. 32, p. 205-216.

Sabins, F.F., Jr., 1978, Remote sensing principles and interpretation: W.H. Freeman and Co., San Francisco, 426 p.

Sandeen, W.M. and Wesselman, J.B., 1973, Ground-water resources of Brazoria County, Texas: Texas Water Development Board, Rept. 163, 199 p.

Seni, S.J., and Jackson, M.P.A., 1983, Evolution of salt structures, East Texas diapir province, part I. Sedimentary record of halokinesis: American Association of Petroleum Geologists Bulletin, . 1219- v. 67, p. 1219-1244.

Sheets, M.M., 1971, Active surface faulting in the Houston area, Texas: Houston Geological Society Bulletin, v. 13, no. 7, p. 24-33.

-----1976, Subsidence and active surface faulting in the Houston vicinity: Houston Geological Society Guidebook, 9 p.

-----1979, Oil fields and their relation to subsidence and active surface faulting in the Houston area: Houston Geological Society Guidebook, 20 p.

Shelton, J.W., 1984, Listric normal faults: An illustrated summary: American Association of Petroleum Geologists Bulletin, v. 68, p. 801-815.

Stude, G.R., 1978, Depositional environments of the Gulf of Mexico South Timbalier Block 54: Salt dome and salt dome growth models: Transactions Gulf Coast Association Geological Societies, v. 28, p. 627-646.

Turner, Collie and Braden, Inc., Consulting Engineers, 1966, Comprehensive study of Houston's municipal water system for the city of Houston, Phase I, Basic studies, 50 p.

Van Siclen, D.C., 1966, Active faulting and its relation to subsidence in the Houston area, Report to McClelland Engineers, Inc., in: Turner, Collie and Braden, Inc., Comprehensive study of Houston's municipal water system for the city of Houston, Phase I, Basic studies, 50 p.

-----1967, The Houston fault problem: American Inst. Prof. Geologists, Texas Section, 3rd Ann. Mtg., Proceedings, p. 9-31.

-----1978, Geologic study of faulting at Addicks Dam, Buffalo Bayou, Harris County, Texas: U.S. Army Corps of Engineers, Galveston Engineer District, 76 p.

-----1981, Land development and fault investigations in the Houston, Texas area, in: Houston area environmental geology: Houston Geology Society, p. 1-12.

-----1984, Early opening of initially closed Gulf of Mexico and central North Atlantic Ocean: Transactions Gulf Coast Association Geology Society, v. 34, p. 265-275.

-----1985, Pleistocene meander-belt ridge patterns in the vicinity of Houston, Texas: Transactions Gulf Coast Association Geological Societies, v. 35, p. 525-532.

Verbeek, E.R., 1979, Surface faults in the Gulf Coastal Plain between Victoria and Beaumont, Texas: Tectonophysics, no. 52, p. 373-375.

Verbeek, E.R., and Clanton, U.S., 1978, Map showing surface faults in southeastern Houston metropolitan area, Texas: U.S. Geological Survey Open File Report 78-797, 20 p.

Verbeek, E.R. and Clanton, U.S., 1981, Historically active faults in the Houston metropolitan area, Texas, in: Houston area environmental geology: Surface faulting, ground subsidence, hazard liability: Houston Geological Society, p. 28-69.

Verbeek, E.R., Ratzlaff, K.W., and Clanton, U.S., 1979, Faults in parts of north-central and western Houston

metropolitan area, Texas: U.S. Geology Society, Misc. Field Studies Series, Map MF - 1136.

Walper, J.L., 1980, Tectonic evolution of the Gulf of Mexico, in: The Origin of the Gulf of Mexico, Proceedings of a Symposium, p. 87-98.

Weaver, P. and Sheets, M.M., 1962, Active faults, subsidence, and foundation problems in the Houston, Texas area, field excursion no. 5, in: Geology of the Gulf Coast and central Texas and guidebook of excursions: Houston Geological Society, p. 254-265.

Wernicke, B. and Burchfiel, B.C., 1982, Modes of extensional tectonics: Journal of Structural Geology, v. 4, no. 2, p. 105-115.

Wheeler, J., 1987, Variable-heave models of deformation above listric faults: The importance of area conservation: Journal of Structural Geology, v. 9, no. 8, p. 1047-1049.

White, G.W. and Burke, K.C., 1980, Outline of the tectonic evolution of the Gulf of Mexico and Caribbean region: Houston Geological Society Bulletin, v. 22, no. 10, p. 8-13.

Wickham, J., and Roeder, D., 1976, Plate tectonic models for the Ouachita fold belt: Geology, v. 4, p. 173-176.

Winker, C.D., 1979, Late Pleistocene fluvial-deltaic deposition Texas Coastal Plain and shelf: Master's Thesis, University of Texas at Austin, 187 p.

-----1982, Cenozoic shelf margins, northwestern Gulf of Mexico: Transactions Gulf Coast Association Geological Societies, v. 32, p. 427-448.

Withjack, M.O. and Scheiner, C., 1982, Fault patterns associated with domes - an experimental and analytical study: American Association of Petroleum Geologists Bulletin, v. 66, p. 302-316.

Woodbury, H.O., et al, 1973, Pliocene and Pleistocene depocenters, outer continental shelf of Louisiana and Texas: American Association of Petroleum Geologists Bulletin, v. 57, p. 2428-2439.

Woodbury, H.O., Spotts, J.H., and Akers, W.H., 1978, Gulf of Mexico continental-slope sediments and sedimentation, in: A.H. Bouma, G.T. Moore and J.M. Coleman, eds., Framework, Facies and oil- trapping characteristics of the upper continental margin: American Association of Petroleum Geologists, Studies in Geology No. 7, p. 117-138.

Woodruff, C.M., Jr., and Caran, S.C., 1984, Lineaments of Texas: Technical Papers ACSM-ASP, American Society Photogrammetry, p. 741-750.

Woods, R.D. and Addington, J.W., 1973, Pre-Jurassic geologic framework northern Gulf: Transactions Gulf Coast Association Geological Societies, v. 23, p. 92-108.

Xaio, H. and Suppe, J., 1986, New techniques for predicting growth-fault geometry from well-log analysis, Caillou Island Field, South Louisiana: In House Progress Report, 37 p.

Yerkes, R.F. and Castle, R.O., 1969, Surface deformation associated with oil and gas field operations in the United States, in: Land subsidence, Proceedings of the Tokyo Symposium, Sept. 1969, Joint Publication of the International Association of Scientific Hydrology and UNESCO, v. 1, p. 55-66.

APPENDIX A

AERIAL PHOTOGRAPH LISTING

The following is a listing of the aerial photography used in this study. Both false-color infrared and black and white imagery was used.

DATE	SCALE	SOURCE
Various Months, 1938	1"=1320'; 4" = 1 mile	1
March 8, 1952	1"=660'; 8" = 1 mile	1
May 5, 1958	1"=660'; 8" = 1 mile	1
October 31, 1965	1"=1320'; 4" = 1 mile	1
January 29, 1974	1"=1667'; 3" = 1 mile	1
Nov./Dec., 1980	1"=400'; 13.2" = 1 mile	1
October, 1981	1"=1000'; 5.28"= 1 mile	1
October 28, 1987	1"=2000'; 2.64"= 1 mile	2

DATE	MISSION/ROLL#	SCALE	SOURCE
Nov. 3, 1970	145/69	1" = 1 mile	3
Nov. 11, 1971	191/11	1" = 1 mile	3

1. B&W aerial photographs: U.S. Department of Agriculture, Soil Conservation Service (SCS), available at the County SCS Office and Engineer's Office, Angleton, Texas.

2. B&W aerial photographs: Texas Department of Highways and Public Transportation, available at their offices on 7721 Washington, Houston, Texas.

3. False-color infrared aerial photographs: NASA, available from EROS data center, Sioux Falls, SD. Made available for this study by the Department of Civil Engineering, University of Houston.

APPENDIX B

SURFACE FAULT DESCRIPTIONS

This section provides a written description of the surface faults mapped in Brazoria County. Aerial photographic evidence, field evidence and subsurface evidence are presented for each of the 112 surface faults mapped for the study.

Fault descriptions are organized by topographic quadrangle. Each of the quadrangles containing surface faults have been numbered sequentially starting from the northwest corner, left to right, to the southeast corner and are labelled Plates 1 - 23. (See index map, Figure 51). Portions of some quadrangles may cover areas outside the study area. Typically, only faults located within the study area have been mapped and described.

Quadrangles which do not contain surface faults are so indicated on the index map by N/F, 'No Fault'. Within the quadrangles each fault is located on a 9 block grid system designating its general location, for example; (NE) = northeast, (NC) = north-central, (C) = central, etc. (Figure 52). The designations are noted in parentheses with each fault title. A composite map of all surface faults mapped in Brazoria County is presented in Plate 24.

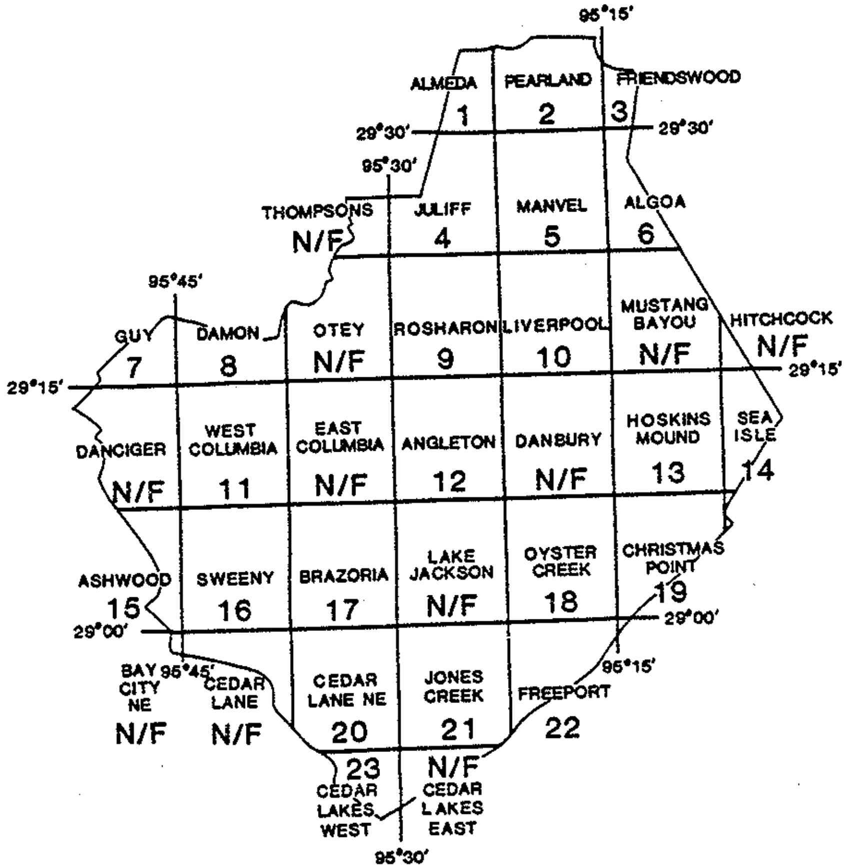

FIGURE 51: Index map to USGS 7½' topographic quadrangles. Quadrangles with faults correspond to Plates #1-23. Quadrangles that do not contain faults are designated 'N/F' (No Faults).

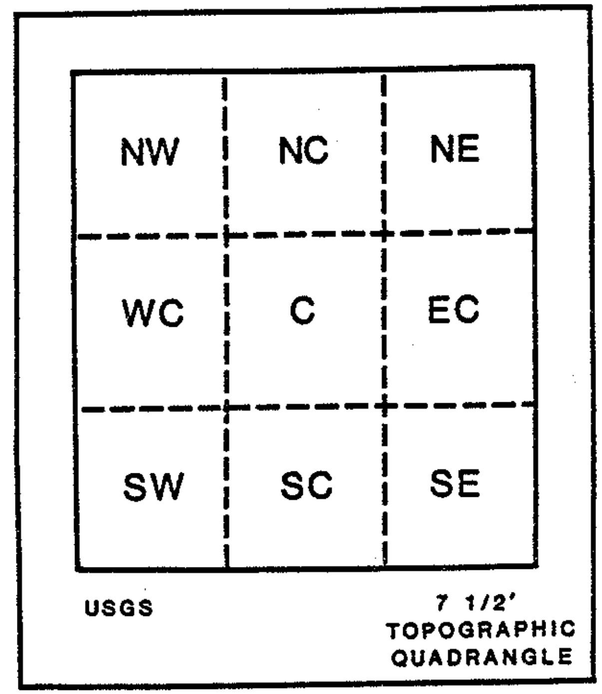

FIGURE 52: Locations of surface faults within the topographic quadrangles are referred to on a 9-block grid, NC = northcentral; SE = southeast; etc.

Each fault description should be reviewed with the corresponding numbered quadrangle. The faults in each quadrangle map are marked according to confidence levels. 'A' faults are those known definitely to exist; 'B' faults very probably exist; 'C' faults probably exist; and 'D' faults may possibly exist. Faults that had been previously mapped and numbered by Verbeek and Clanton (1979 and 1980) retain their original numbering scheme in this presentation. They are depicted in a lighter line weight than faults identified or modified in the current study (Figure 53).

In the fault descriptions, aerial photographic evidence is presented in abbreviated form as follows:

IR 69-127 = False-color infra red imagery,
Mission #145, Roll #69, photo #127.

B&W 1974 I3 = Black and White imagery, flown
January 29, 1974, photo #I3.

Selected Fort Bend County photos from 1941, 1957 and 1972 have been used to delineate the western end of the Arcola Fault in that county.

The photographic sets most often cited are both sets of infra red images and the 1974 black and white photos. The very nature of the infra red images facilitates fault

TOPOGRAPHIC QUADRANGLE

LEGEND

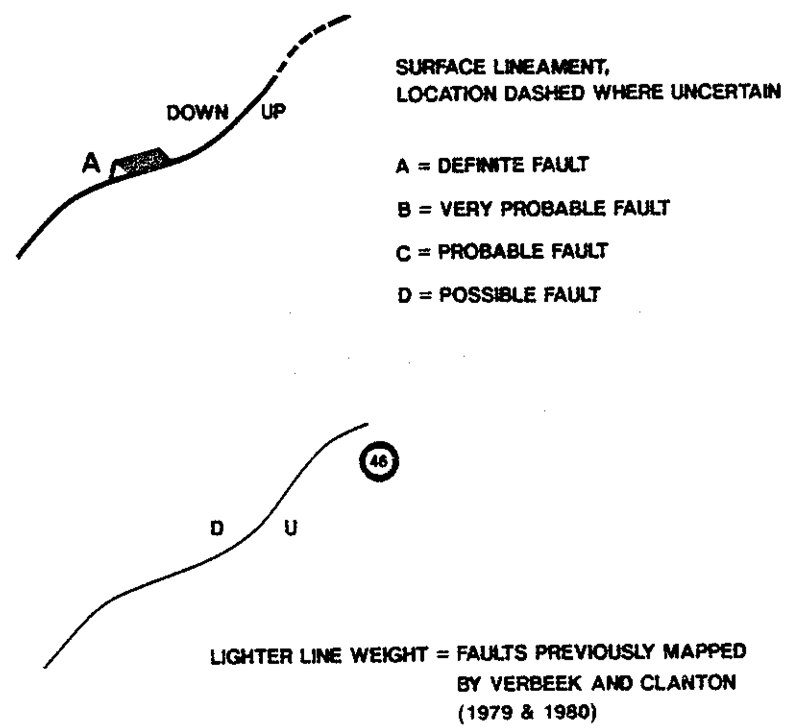

FIGURE 53: Legend for all following USGS 7½' topographic quadrangles, Plates #1-23.

lineament identification. Apparently the 1974 black and white photos were taken under very favorable soil moisture conditions for they show fault lineaments more clearly than any of the other black and white sets available.

Accuracy of Positioning

Great care has been taken to transfer all fault lineaments from aerial images to USGS 7 1/2 minute topographic quadrangles as accurately as possible. In most cases positioning of a linear feature can be done best with the use of observations from both aerial photos and field investigations. However, it must be stressed that with the possible exception of faults passing through urban areas, the locations shown on the maps cannot be taken as precise locations. Wherever possible, faults are plotted to an accuracy within 1 mm. At a map scale of 1:24000 this corresponds to a band 24 m wide on the ground. To compound this inaccuracy, there are other possible errors of which to be aware. The postion of a fault lineament may vary slightly in different generations of airphotos due to variations in soil moisture conditions. During wet conditions, an airphoto lineament may appear at the top of a fault scarp, during drier conditions it may appear lower or near the bottom of the fault scarp. In addition, an

airphoto lineament may be absent for a portion of a fault. In this case, interpolation and extrapolation are necessary to estimate the location of the fault. Moreover, there is often difficulty finding points by which to register the exact position of a fault lineament in open areas.

Lineaments were originally mapped at a scale of 1:24000 and reduced 50% for presentation in the thesis. Currently at a 1:48000 scale, the graphic scale on the maps, not the written ratio, should be used when computing distances. At this scale, fault lineaments are shown at a line width of 0.5 mm, so the line still represents a band 24 m wide on the ground.

In most cases, accuracy of positioning of a fault is within 25 m (82 feet). Where the position of the fault is interpolated or extrapolated, accuracy may decay to 100 m (328 feet). These maps should, therefore, be reviewed and used with full awareness of their limitations. Future land use planning should not rely on these maps alone since it would be difficult to determine if a fault intersects, or only lies near an individual site. Site-specific studies are advised and should be required if the effects of faulting will prove harmful or costly to the planned land use.

The best way to pinpoint the location of a fault is by drilling and logging closely spaced boreholes. Use of subsurface data in conjunction with surface data may place a fault to within a few meters accuracy.

A number of topographic quadrangles have been designated as containing 'No Faults'. Although surface faults have not been identified on these quadrangles, it does not mean they do not exist. This also applies to other 'unfaulted' areas of the county. The current inactivity of a fault may prevent its identification at the earth's surface at present, but a fault may again become active at any time.

FAULTS ON THE ALMEDA QUADRANGLE
(Plate 1)

DEFINITE FAULTS

Arcola Fault (SC)

The Arcola Fault strikes N 70 E (downthrown to the east-southeast) for over six miles from 600' south of Mustang Bayou at FCR 84, across Old Airline Road (FCR 48), Del Bello Road (FCR 58), and FCR 173, and into Fort Bend County.

The fault presents a striking lineament on IR 11-238, B&W 1974 G3 and F3, B&W 9-26-41, B&W 1-16-72, and B&W

2-27-57. It has an excellent subsurface expression as determined from well logs (see Chapter 3). Seismic sections indicate over 200 feet of vertical separation at depths of 5700 feet and the feature is recognizable to depths of 13,000 feet. It is the most pronounced down-to-coast fault in this area.

Arcola Branch Fault (SC)

This definite fault branches off the Arcola Fault 2000' east of the Fort Bend County line. The fault trace is 6000' in length and strikes N 55 E northeast (downthrown to the southeast) from 400' south of Post Road to 500' north of the western end of Hudspeth Dr.

It appears clearly on IR 11-238 and B&W 1974 G3 and shows a 5 cm scarp on Hudspeth Drive (unpaved) approximately 60 feet from its west end. No measurable vertical offset appears on Post Road (unpaved). A fault at this site can be inferred from structure and isopach maps (Figures 36, 39 and 40).

McKeever Road Fault (SW)

The McKeever Road Fault in adjacent Fort Bend County strikes N 60 E (downthrown to the southeast) and extends horizontally for 8000′. It is part of the Arcola-Iowa Colony fault system.

It shows as a fair lineament on IR 11-238, and does possess some subsurface expression (See Figures 36, 39 and 40).

PROBABLE FAULTS

Hudspeth Drive Fault (SC)

This fault is located 500 feet southeast of the Arcola Branch Fault. It strikes N 65 E (downthrown to the southeast), for 1500′ from 1000′ southwest of Hudspeth Dr., across the Hudspeth Dr./Central Ave. intersection, before it disappears into a wooded area 200′ north of Hudspeth Dr.

The fault is marked by a clear lineament on IR 11-238 and B&W 1974 G3. Approximately 4 cm of elevation change exists on Hudspeth Dr. 10′ west of Central Ave. Hudspeth Dr. (unpaved) shows evidence of recent gravel infilling and regrading at the fault crossing point.

Nuera Drive Fault (SC)

South of the Hudspeth Dr. fault, about 1.5 mile east of the Fort Bend County line the Nuera Dr. fault strikes N 58 E for

2600′ (downthrown to the northwest), from FCR 58 (Post Road), across Central Ave. and Neura Dr., and terminating at Old Airline Road

The fault presents a good lineament on B&W 1974 G3 and IR 11-238; an abnormal decrease in the gradient of Central Ave. (unpaved), equivalent to a vertical offset of approximately 15 cm, and an 8 cm offset along the unpaved road immediately to the south of Neura Dr. marks its location at those points.

FAULTS ON THE ALMEDA AND PEARLAND QUADRANGLES

(Plates 1 and 2)

DEFINITE FAULTS

Del Bello Lane Fault (SE/SW)

This fault is located 0.5 miles east of SH 288, some 5.0 miles south of the Harris County line. The feature is approximately 1.5 miles long striking N 65 W (downthrown to the northeast), from 0.5 miles east of SH 288, across Del Bello Lane (FCR 234) to Del Bello Road (FCR 90). It lies directly along strike of a lineament mapped by Dr. C. Norman 4000′ to the east on FM 1128; it is likely that these two features are actually one and the same making the overall length of the fault just over 2 miles.

The fault appears as a good lineament on B&W 1974 G3, B&W 1980 8-1-72, and IR 11-237. It produces a 26 cm vertical offset on Del Bello Lane (FCR 234; paved) and a small scarp crosses fields adjacent to, and toward Mr. Eugene Del Bello's house. The house appears to lie on the upthrown block and, according to Mr. Del Bello, has not been affected in any way since its construction 12 years ago. The fault has not disturbed Del Bello Road (FCR 90; paved).

The Del Bello Lane Fault and the Del Bello Road Fault (described next), may both be related to a deep fault showing 500′ of throw on the Frio Formation (McNaughton, 1953, p. 136). The deep fault emerges from the northwest edge of the Manvel Dome. A fault is also visible on a seismic profile with a projected surface location which coincides with the surface location of this fault.

The good lineament, scarp, and the subsurface evidence, make this feature a definite fault.

<u>Del Bello Road Fault (SE/SW)</u>

This definite fault is located on SH 288, 5.0 miles south of the Harris County line, to the north of the Del Bello Lane fault. The Del Bello Road Fault has a distinctly convex to

the north trace, and strikes roughly N 60 W (downthrown to the northeast), for 1.5 miles from SH 288, across FCR 82 and FCR 58, to terminate at Del Bello Road.

This fault is marked by a lineament clearly visible on B&W 1974 G3 and IR 11-237. Along the badly potholed and patched Del Bello Road (paved), 12 cm of cumulative vertical offset occurs on FCR 58, while no offset appears on FCR 82 or SH 288. This feature and the Del Bello Lane Fault probably join at a fairly shallow depth to become a single fault with 500′ of throw, (McNaughton, 1953, p. 136), on the upper Frio Formation. At shallow depths this fault is recognized on seismic profiles as a distinct feature lying to the north of the Del Bello Lane Fault. Its surface projection from seismic profiles places it at the surface location of the Del Bello Road Fault.

The very good lineation, and subsurface evidence indicate this feature should be classified as a definite fault.

<u>FAULTS ON THE PEARLAND QUADRANGLE</u>

<u>(Plate 2)</u>

<u>DEFINITE FAULTS</u>

<u>South Park Cemetery Fault (NC)</u>

This fault is located west of SH 35, 0.5 miles south of the Harris County line at Clear Creek. This new extension of Verbeek and Clanton's (1980) Fault #41 strikes N 45 E for approximately 0.75 miles, from Knapp Road, across South Park Cemetery, the A.T.&.S.F. Railroad, Brookside and Comal Roads, to intersect with the Verbeek and Clanton fault 400' south of Scott Road

it is marked by a good lineament on IR 69-151. Four topographic profiles in South Park Cemetary measured 5 to 8 cm scarps across the fault. Its surface trace is associated with pools of standing water in wet weather and some possible buckling of the rails along the A.T.&.S.F. Railroad. No obvious scarp occurs on Brookside Road, Comal Road, or Scott Street.

The good lineament and field evidence suggest this is a continuation of Verbeek & Clanton's (1980) fault #41.

John Lizer Road Fault (EC/SE)

Located 1.8 miles south of Pearland, this fault strikes N 5 W (downthrown to the east) for 0.9 miles from 0.2 miles north of John Lizer Road, south across SH 35 to terminate in fields 0.25 miles south of SH 35.

It appears as a good lineament on B&W 1980 1-6-100. Ponded drainage is appparent along roadside ditches on SH 35 along with a pavement break. An east-west line of exploratory boreholes drilled across the fault and logged in the summer of 1988 (Dr. C. Norman, personal communication), proved conclusively the existence of this fault.

Morris Street Fault (SC)

Four miles south of central Pearland this fault strikes N 80 E (downthrown to the south) for 1.5 miles, from 100' north of Edith Drive and Christie Lane. It bypasses the north end of Morris Street and terminates in fields approximately 1 mile to the west.

It appears as a poor lineament on B&W 1974 H3, and as stacked ricefield levees on B&W 1980 7-158. These levees have since been ploughed over for other crops and as a consequence, no scarp is currently visible. The fault appears on seismic profiles with the same sense of offset indicated by the rice levees. It appears to have significant offset at depth, and its projection to the earth's surface places it at the airphoto lineament.

The lineament, stacked levees and subsurface evidence merit its classification as a definite fault.

PROBABLE FAULT

Harkey Road Fault (EC/SE)

3.7 miles southwest of central Pearland is a probable fault that strikes N 60 E (downthrown to the northwest) for 2500′ from 300′ south of the intersection of Harkey Road (FCR 103) with McKeever Road (FCR 100), to a point approximately 450′ west of the American Canal.

This feature is classified as a probable fault because it appears as a good lineament on B&W 1974 H3, but does not have a convincing scarp in the fields south of McKeever Road.

POSSIBLE FAULTS

Tower Scarp (SE)

This possible fault was first identified by Dr. C. Norman from a small escarpment located on SH 35, 4.75 miles south of Pearland, some 1100 feet north of Cowart Creek. It strikes N 55 E, and its sense of offset appears to be down to the north. No definite lineament appears on aerial photographs. A low scarp occurs on the property west of SH 35, but the sense of throw is opposite to that noted along

SH 35. The scarp may correspond to a property boundary. Although this feature may be man-made, some impaired drainage (ponding) is evident in ditches alongside SH 35 where property boundaries should show no effect.

Lack of aerial photo evidence and ambiguous field evidence suggest this feature is a possible fault.

Pearland Sites Road Lineament (C/EC)

About 0.5 miles south of Pearland is a possible fault which strikes N 35 E (apparently downthrown to the southeast) for 5000′, from the A.T.&.S.F. railroad (750′ south of West Walnut Road), to a point 0.1 miles east of McLean Road and 0.3 miles south of Mary's Creek.

It is marked by a poor lineament on IR 69-151, IR 11-236, and B&W 1974 H1, and is inaccessible to field checking except along Pearland Sites Road, where an appropriately located disturbance occurs.

The poor, but persistent, lineament and sparse field evidence suggest a possible fault.

East Pearland Lineament (EC)

Located in east-central urban Pearland this apparent fault strikes N 60 E (apparently downthrown to the southeast) for

6500', from Linwood Oaks East, across the Linwood Oaks West and East Plum intersection, Old Alvin Road, Pearland High School grounds, East Broadway (FM 518), Galveston Road, Park Road, Grand Road, the intersection of Houston and East Rear, and SH 35 to terminate 0.2 miles west of the A.T.&.S.F. Railroad.

Despite a lack of field confirmation, the presence of a poor lineament, in spite of pervasive urbanization, suggests a possible fault designation is appropriate.

Hatfield Road Lineament (C)

This possible fault, located in northwest Pearland, strikes N 40 E (apparently downthrown to the southeast) for 2.2 miles, from about 0.2 miles west of SH 35, across the Hickory-Slough waterway, Mykawa Road, Shank Road, and Orange Street (FCR 114), and ending at O'Day Road (FCR 103) just north of West Broadway (FM 518).

This feature appears as a poor lineament on IR 69-151. Field expression includes ponded water in fields north of Shank Road during wet weather, but no unequivocal evidence of a fault is apparent. Consequently, this feature is designated a possible fault.

Woody Road Lineament (C)

This possible fault is located in west central Pearland, striking N 35 W (apparently downthrown to the northeast) for one mile from Anthony Road, across Goodrich Road, Woody Road, Pear Road, Lynn Road, Cunningham, and West Walnut at Halbert, to die out in open fields to the south.

It appears as a poor lineament on IR 69-151 and B&W 1974 H1. Lack of clear field evidence for this feature requires that it be designated as a possible fault.

Garden Road Lineament (C)

A possible fault is located in far north Brazoria County passing through the vicinity of Brookside Village. It strikes N 42 W (apparently downthrown to the southwest) for 0.45 miles, from east of Roy Road and across fields north of Sharon Drive, to end north of the Garden Road/Sharon Drive intersection.

It is expressied only as a poor lineament on B&W 1974 H1 and is classified as a possible fault.

Hickory Slough Lineament (C)

field expression includes a low scarp in fields accessed by oil field lease roads and a well developed scarp, 0.4 miles long with an associated vegetation change, passing through fields between FCR 129 and an oilfield lease road to the north.

The Cowart Creek Fault may be one of the features resulting from the 'horsetailing' of a fault with 300' of throw mapped on the Frio Formation (at approximate 7000 ft. depth) in the Hastings Oilfield (McNaughton, 1953, p. 122). The Cowart Creek Fault has the appropriate positioning, orientation and sense of throw to be related to this subsurface feature.

Based on the excellent lineament on aerial photographs, the excellent field confirmation, and associated subsurface infornation, this feature is classified as a definite fault.

North Hastings Fault (SW)

This fault is located 4.5 miles southeast of central Pearland along SH 35. Strike of the North Hastings averages at N 50 E (downthrown to the southeast) for approximately 5500'. Beginning from 1900' northeast of SH 35, the fault crosses three oilfield lease roads, SH 35, FCR 28, and four additional lease roads.

The North Hastings Fault appears as an exceptionally good lineament on IR 11-235 and B&W 1974 H3. An excellent scarp with approximately 20 cm of throw crosses SH 35 and may be followed across fields for some 1200' northeast of SH 35. The North Hastings appears to have the correct positioning, orientation and sense of throw to be the surface expression of a fault showing 500' of throw mapped on the Frio Formation (McNaughton, 1953, p. 122) within the Hastings Oilfield.

The exceptionally good aerial photo expression, good field evidence and subsurface confirmation make this a definite fault.

VERY PROBABLE FAULTS

Standolind Road Fault (SW)

This feature is located east of the Clover Field Airport 500' from the Galveston Co. line, where it strikes N 10 W (downthrown to the west) for 5800', from open ground north of FCR 125, across FCR 125, FCR 129 (Standolind Road), to die out soon after crossing Cowart Creek.

The Standolind Road Fault appears as a good lineament on IR 11-235 and B&W 1974 I3. The fault exhibits geomorphic control, apparantly causing Cowart Creek to take 2 right angle turns in course before crossing onto the upthrown block of the fault. Disturbed pavement occurs along FCR 125 (paved) with an appropriately located hump in the roadside ditch. A small scarp exists in pastures south of FCR 125, along with a small dip in the pavement along FCR 129 (Standolind Rd). The fault is probably related to a large fault mapped on the top of the Frio Formation in the Hastings Oilfield; this subsurface fault possesses the correct subsurface position, orientation, and sense of motion (McNaughton, 1953, p. 122).

On the basis of the good lineament, reasonable field evidence, and the subsurface coincidence of a major fault, this is considered a very probable fault.

<u>Clover Field Fault (SW)</u>

Located 4.5 miles southeast of Pearland within the Clover Field Airport complex, this feature strikes N 20 W (downthrown to the east) for 4700', across three airport runaways, Cowart Creek, FCR 130 (Brown Road), FCR 430 (Dace Road), and dies out in the Hastings Oilfield to the south.

The fault appears on IR 11-235 and B&W 1974 H3 as a very good lineament. Impaired drainage exists in the drainage ditches adjacent to the runways and FCR 430 and a small scarp occurs in fields south of FCR 430. The Clover

Field Fault may be a feature resulting from the 'horsetailing' of a fault with 300' of throw mapped in the Hastings Oilfield on the top of the Frio Formation; it has the correct position, orientation and sense of throw to be related to this subsurface fault (McNaughton, 1953, p. 122).

On the basis of the very good lineament, the subsurface evidence and the field confirmation, this feature should be considered a very probable fault.

<u>PROBABLE FAULTS</u>

<u>Kimble Road Fault (SW)</u>

This feature lies 4.5 miles southeast of Pearland, some 2000' south of the Clover Field Airport, striking N 9 W (downthrown to the east) for 1400', from south of Cowart Creek, across Kimble Road and FCR 430.

Identified by a faint lineament on IR 11-233, field expression includes a small scarp and rippled fence north of FCR 430, and a small scarp located in the backyard of a house adjacent to Kimble Road

The convincing field observations suggest a probable fault designation despite the poor lineament.

<u>Longwood Fault (WC)</u>

Located some 1500′ south of the Harris County line and 500′ west of the Galveston County line, this feature trends N 10 W for approximately 4000′ from Longwood Road, across McDonald Road and Paul Road, to terminate in open country within Galveston County.

Because the feature is visible as a good-contrast lineament on on IR 11-235, I feel it should be considered a probable fault despite the absence of field confirmation.

POSSIBLE FAULTS

Rustic Lane Fault (SW)

Located 4.2 mile southeast of central Pearland, this possible fault strikes N 35 E (apparently downthrown to the southeast) for 0.55 miles, from the Galveston County line (approximately 0.2 miles south of FM 518) to terminate about 800′ north of Rustic Lane (FCR 131).

The poor lineament visible on IR 11-235, and the lack of field confirmation (because of inaccessibility), suggest this feature should only be considered a possible fault.

South FCR 129 Fault (SW)

This possible fault is located approximately 7000′ south of Clover Field Airport, it strikes N 70 E for 1500′ apparently downthrown to the south-southeast, from a private road southeast of FCR 129, to the intersection of the private road with a Hastings Oilfield lease road.

Identified by a poor lineament on IR 11-235, this feature may be the surface expression of a much larger fault mapped in the subsurface by Amoco Production geologists; this feature is classified as a possible fault.

FAULTS ON THE JULIFF QUADRANGLE

(Plate 4)

DEFINITE FAULTS

Iowa Colony Fault (NC/NE)

This fault is located 800′ north of the community of Iowa Colony, close to the intersection of SH 288 and SH 6. The fault trace is over 5 miles long, and strikes roughly N 70 E (downthrown to the northwest), from west of the Fort Bend County line, across FCR 573, FCR 383 (Karsten Road), the West Fork Chocolate Bayou and the Briscoe Canal, FCR 190, FCR 48 (Morris Ave.) at the A.T.&.S.F. railroad, SH 6 (0.57 miles north of the SH 6-SH 288 intersection, SH 288 (0.8 miles northeast of the SH 6-SH 288 intersection), FCR 82 (Iowa Lane), and terminates in fields to the east of Iowa Lane. The Iowa Colony fault appears to influence the course of the West Fork Chocolate Bayou as it flows from the downthrown to the upthrown block.

This fault appears as an excellent lineament on B&W 1974 G3 and F4, IR 11-238, and IR 69-212. An excellent scarp appears on Morris Ave. (FCR 48; paved) and SH 6; the A.T.&.S.F. railway line showed signs of disturbance at the FCR 48 intersection, and railroad workers confirmed that the railroad bed at this site required frequent maintenance. Structure contour maps reveal excellent subsurface expression for this fault (See Chapter 3), and it is probable that it is the same fault as that mapped on the top of the Frio Formation entering the western edge of the Manvel Dome with about 300′ of throw (McNaughton, 1953). Excellent subsurface confirmation for this fault occurs on seismic profiles. The seismic data clearly shows the Iowa Colony to be a major up-to-the-coast fault antithetic to the primary down-to-the-coast Arcola Fault.

The good, long lineament, good field evidence, and excellent subsurface evidence indicate a definite fault classification.

Stevens Road Fault (NE)

Located within the southern portion of the community of Iowa Colony the surface expression of this fault extends 2 miles trending N 50 E (downthrown to the northwest), from FCR 57 (Juliff-Manvel Road), across FCR 48 (Old Airline Road), FCR 78, FCR 79 (West Colony Loop Road), FCR 80 (East Colony Loop Road), the A.T.&.S.F. railroad, Briscoe Canal, and SH 6, to terminate in the rice fields north of SH 6.

The fault appears as a good lineament between FCR 57 (Juliff Manvel Road) and FCR 80 (East Colony Loop Road) on IR 11-238 and IR 69-212; it is present as a faint lineament on B&W 74 F5. It occurs as a weaker lineament between FCR 80 (E. Colony Loop Road) and SH 6, and as stacked rice field levees in fields north of SH 6. Field expression includes: a scarp with 11 cm of cumulative throw on FCR 81 (Stevens Road; paved) 800′ west of the FCR 80-FCR 81 intersection; no throw on FCR 79; 6 cm of cumulative throw on FCR 78 some 2200′ west of the FCR 79-FCR 78 intersection; and a slight disturbance on heavily travelled SH 6 about 0.8 miles east of its intersection with SH 288. In addition, the fault has possible influence over a small ephemeral tributary to Chocolate Bayou and exhibits good subsurface expression as determined from well logs (See Chapter 3) and seismic profiles.

On the basis of the prominent air photo lineament, consistent field evidence and subsurface confirmation, this feature is classified as a definite fault.

<u>Old Airline Road Fault (NC/NE)</u>

This feature is located within the community of Iowa Colony approximately 0.5 miles south of the Iowa Colony Fault. It strikes roughly N 55 E (downthrown to the southeast) for 2.2 miles, roughly parallel to the Iowa Colony Fault. Beginning from the intersection of West Chocolate Bayou with FCR 81, the fault crosses Old Airline Road (FCR 48) approximately 2000′ north of FCR 81, and dies out at the intersection of SH 288 and FCR 190.

Although present as a weak lineament on IR 11-238, a 5 cm scarp occurs along Old Airline Road (paved), 0.2 miles north of Shaw Road (FCR 418), and a larger 8 cm scarp is present along FCR 81 (paved) at the southwestern terminus of the fault. A fault occurs on seismic profiles with the same sense of throw and projected surface location as the Old Airline Fault. A measured throw of 245 feet occurs at depths of 9000 feet.

Based on consistent field evidence, the presence of a lineament in this highly faulted area, and the subsurface expression, this feature is ranked as a definite fault.

<u>VERY PROBABLE FAULT</u>

<u>West Fork Chocolate Bayou Faults (EC)</u>

These faults are located in northern Brazoria County, five miles east of the Fort Bend County line. The northernmost feature strikes N 56 W, downthrown to the southwest for approximately three miles and parallels the West Fork Chocolate Bayou for 1.23 miles at which point a branching feature becomes visible. The branch fault is throw to the southwest with roughly the same direction of strike but with an opposite sense of motion.

These features appear on IR 69-213 and B&W 1974 F5 as fairly good lineaments. There is also subsurface evidence for the larger feature on seismic profiles which indicate a fault with the same sense of motion and projected surface location. Measured throws are very small, perhaps 30 feet at depths of 1200 feet.

The fairly good lineaments, coupled with the subsurface evidence suggest very probable faults.

PROBABLE FAULT

Hayes Creek Fault (SC)

This probable fault is located in north-central Brazoria County, 3.5 miles northeast of central Rosharon bordering the northern edge of the Sandy Point Oilfield. It is approximately 9000′ in length, strikes N 45 W (downthrown to the southwest), from the southern Iowa Colony city limits, east of FCR 48 to cross SH 288 (north of FCR 572), and continues southeast to a small canal west of FCR 65 (Iowa School Road).

The southeast portion of this feature appears on B&W 1974 F6 as stacked ricefield levees; the remainder as a poor lineament on the same photograph. 19 cm of cumulative throw occurs on the SH 288 southbound feeder road, marked ponding is also present on the grassy island area between the feeder road and the main highway.

On the basis of the poor lineament, stacked levees, and good field evidence, this feature is ranked as a probable fault.

POSSIBLE FAULTS

Thurmond Lake Lineament (SW)

Located approximately 2 miles north of central Rosharon on FM 521 (approximately 0.5 miles south of the FM 521/FCR 42 intersection), this apparant fault is 6500′ long and strikes N 15 E (downthrown to the east), from the northwest extremity of Thurmond Lake, across FM 521, to terminate in fields north of FM 521.

A poor lineament appears on IR 11-297, IR 69-212, B&W 1974 F6 and B&W 1965 12-320. Offset measuring 5 cm occurs on FM 521 (paved) along with a small crack in the pavement. The southern extremity of the lineament appears to act as a natural dam along the northwestern corner of Thurmond Lake.

Although the lineament is short, it occurs on several generations of aerial photographs, along with some topographic and field evidence making this a possible fault.

Mowery Lake Lineament (SC)

This feature is located 2 miles north of central Rosharon, where it borders the southern edge of the Sandy Point Oilfield. 6000′ in length, it strikes N 45 W (apparently downthrown to the northeast), from Mowery Lake across open fields to intersect FCR 48 north of FCR 52.

Although recognized as a very faint lineament on IR 11-297, IR 69-212, and B&W 1980 11-308, the feature does not appear on B&W 1974 F6. Cumulative throw of 13 cm exists outside the main gates of the Schlumberger Co. Buildings along FCR 48.

On the basis of the fairly consistent, but faint lineament, and the sparse field evidence, I consider this feature to be only a possible fault.

__Iowa Colony School Road Lineament (SE)__

Located in northern Brazoria County within the Iowa Colony City limits, this apparent fault strikes N 50 W (with downthrow to the northeast) for 2500′, crossing Iowa School Road (FCR 65, unpaved) north of FCR 63 (Kelly Leigh Road).

The feature appears as a fairly good lineament on B&W 1974 F6 and IR 69-212, but no field evidence is apparent for this feature allowing only a possible fault designation.

__Iowa Colony Lineaments (SE)__

In the eastern-most section of Iowa Colony, two faint lineaments, with a combined length of 1.7 miles, strike N 65 W, roughly parallel to the West Fork Chocolate Bayou. The lineament to the south of the bayou appears to indicate

downthrow to the southwest, while the northern lineament has an indeterminable throw direction.

Both lineaments are fair to poor on IR 69-212 and B&W 1974 F6. These features are considered possible faults.

__FAULTS ON THE MANVEL QUADRANGLE__

__(Plate 5)__

__DEFINITE FAULTS__

__Oilfield Road Fault (NC)__

Located 5.5 miles south of central Pearland on the west side of the Hastings Oil Field, this fault strikes due east (downthrown to the north) for 1 mile, from FCR 98 (Oilfield Road) to the Brazos River Authority Canal.

It appears as a good lineament on B&W 1980 7-158 and 7-156, and as stacked rice field levees at its westernmost extremity. A scarp with 11 cm of throw occurs at the appropriate point on Oilfield Road (unpaved; the only road crossing); an apparent vegetation change also occurs in adjacent fields at this site. The Oilfield Road Fault is present on seismic profiles which show a fault whose projected surface trace coincides with the location of this feature.

The good lineament, stacked levees, consistent field evidence, and good subsurface evidence, confirm this feature to be a definite fault.

Heights Road Fault (NC/NE)

This fault is located south of central Pearland some 1.5 miles west of the Hastings Oil Field. It strikes roughly N 75 E (downthrown to the north), for 2.7 miles, from FCR 393 (Lipicland Lane), across Pearland Sites Road (FCR 99), Heights Road (FCR 541), and the Brazos River Authority Canal System, to die out in rice fields beyond.

This feature appears as a good tonal change (except at its westernmost extremity) on B&W 1974 H3, and as stacked rice field levees on IR 11-236 and B&W 1980 1-6-102. Impaired drainage (ponding), and a vegetation change (dry/brown versus moist/green plants), is in evidence in the roadside ditches on Heights Road (FCR 541; unpaved), along with a 12cm scarp which can be traced into the backyard of an adjacent house; a scarp with 12 cm of cumulative throw exists on FCR 537 (paved); a scarp with 25 cm of cumulative throw on Pearland Sites Road (paved) is accompanied by a bulge of similar magnitude south of the FCR 98-FCR 99 intersection; a weak scarp can be followed across the field to the east of Lipicland Lane.

The fairly good lineament, along with the stacked rice field levees, and excellent field evidence suggest this feature is a definite fault.

Manvel School Fault (NW)

Located about 4000′ north of central Manvel on FM 1128, this fault strikes N 60 E (downthrown to the southeast), across FM 1128 and Lewis Lane (FCR 543), to die out in fields 600′ to the west. The feature is 2700′ in length, it is apparant as a very poor lineament on IR 11-237 and B&W 1980 8-174, no clear field evidence is present for this feature. Based on the above evidence alone, this feature would be classified as a possible fault. However, a fault is present on seismic profiles with a projected surface trace which coincides with the location of this surface feature.

The seismic evidence along with presence of a lineament in this pervasively faulted area suggest this feature should be classified as a definite fault. The poor expression of the lineament and lack of field evidence suggest this fault is not currently active.

Mississippi Road Fault (NW/WC)

This fault is located within the city of Manvel on SH 6 0.7 miles east of the FM 1128/SH6 intersection. The fault strikes N 10 E (downthrown to the east) for some 4000′ beginning a short distance north of SH 6 and extending just to the south of FCR 190.

Recognized on IR 11-237 and IR 69-214 only as a poor lineament, the fault shows an excellent, gently rolling scarp with over 17 cm of throw in the field immediately north of SH 6 and east of the "La Casita" restaurant; a good scarp with at least 5 cm of throw occurs on the well maintained SH 6. Additional confirmation of this feature appears on seismic lines which show this fault to be a major down-to-the-coast growth fault with nearly 700 feet of throw at a depth of 3500 feet.

A poor aerial photo lineament is overshadowed by the well developed field evidence and subsurface confirmation making this feature a definite fault.

Mustang Bayou Fault (C)

This apparent fault, first recognized by Dr. C. Norman, is located in northeast Brazoria County, 5 miles north of Alvin on SH 6. The short surface feature (less than 2000′ long) strikes N 31 E (downthrown to the northwest), across SH 6 two miles southeast of the SH 6/FM 1128 intersection.

Present as a very poor lineament on B&W 1974 H11, a small 3 cm scarp and pavement break are present on SH 6. Workers in the refinery immediately to the south of SH 6 reported some building disturbance, but levelling along FCR 190 (paved) shows no conclusive throw. Confirmation for this feature occurs on seismic profiles which show the up-to-the-coast Mustang Bayou Fault to be an antithetic feature to the larger down-to-the-coast Mississippi Road Fault. The Mustang Bayou Fault has measured throw of 300 feet at 3500 feet.

The fairly good field evidence, presence of a faint lineament, and the subsurface confirmation make this a definite fault.

Alvin Fault (SE)

Located in southwest urban Alvin, this fault strikes N 25 E (downthrown to the southeast) for 4300′, from Kost Street, across the eastern end of Fulton Street, Alta Vista and Coffee Street; it continues across open fields to catch the southern end of Callaway St, crosses South Street, and terminates in the grounds of Alvin Junior High School.

The feature appears as a poor lineament (probably because of urbanization) on IR 11-300 and B&W 1980 1-6-106. Structural damage includes: a crack in the cement driveway of #1200 Kost Street; a crack in the pavement in front of #1713 Fulton and #1821 Goode; a ridge in the road at #1803 Alta Vista; and an appropriately located crack in the cement pavement at #1808/1809 Coffee Street Along strike in the schoolyard of Alvin Junior High, the driveway blacktop is heavily patched and a 4.5 cm scarp is in evidence.

The visible lineament despite heavy urbanization, coupled with the consistent field evidence, designate a definite fault.

Davis Bend Road Fault (SC)

Located approximately 3 miles southwest of Alvin, this fault is 7500′ long striking N 20 E (downthrown to the east), across FCR 392 (Davis Bend Road; paved) northeast of FCR 998; across FCR 184 south of the FCR 392/FCR 184 intersection, and dies out in fields southwest of FCR 184.

Although it appears as a good lineament on IR 69-214, this feature is poor, or absent, on other generations of aerial photographs. No obvious throw occurs on FCR 184, however, diminishing of the measured average gradient does occur at the correct position on FCR 392, corresponding to over 8 cm of possible cumulative throw. In addition, a fault with the same sense of throw and coinciding projected

surface location occurs on seismic profiles. Offset of 210 feet is present at 4200 foot depths.

The subsurface evidence coupled with the inconsistently developed lineament and the sparse field evidence suggest a definite fault that is not currently active.

POSSIBLE FAULTS

Del Bello Road Lineament (NW)

This feature is located on the western edge of the Manvel Oil Field, in northern Brazoria County, and trends due east (downthrown to the south) for 2500′, from west of Del Bello Road, across Del Bello Road and FM 1128, to terminate in fields to the east.

This poor lineament was visible on IR 11-237, B&W 1974 G3, and B&W 1980 8-172. Field expression includes a small, but discernible scarp in fields just to the east of FM 1128.

The poor, but persistent lineament, and the sparse field confirmation suggest this feature to be a probable fault.

Scott Spur Lineament (NW)

The Scott Spur Lineament lies south of the Manvel Oil Field, 8000′ north of central Manvel. This possible fault strikes N 60 E (apparently downthrown to the northwest) for 2000′, across Scott Spur and adjacent fields.

A poor lineament, first noted by Dr C. Norman, appears on IR 11-237, and B&W 1974 G3. Limited access to this feature does not present strong field evidence.

On the basis of the poor, but persistent lineament, this feature is deemed a possible fault.

<u>American Canal Lineament (NC)</u>

Located in open country 0.2 miles north of the Oilfield Road Fault in northern Brazoria County, this lineament strikes N 82 E (downthrown to the north) for 0.5 miles.

Recognized from stacked rice field levees on B&W 1980 7-158, access was not gained to these actively cultivated fields. The lack of field evidence and appearance of the lineament on only one generation of airphoto designates a possible fault.

<u>Chigger Creek Lineament (NC)</u>

This apparent fault is located in rice fields 6 miles south of central Pearland some 1200′ north of the western terminus

of Chigger Creek. The concave surface trace trends roughly due east (apparently downthrown to the north), for 4700′ from south of Oil Field Road (FCR 98), to northeast of FCR 397.

The feature is recognized from the close spacing of rice field levees on IR 11-236. Field confirmation is not obtainable as the fault is located entirely on actively cultivated land.

The fairly good aerial photographic evidence suggests that this feature is a possible fault.

<u>Alvin Lineament (SE)</u>

This possible fault is located in southwest Alvin, approximately 900′ east of, and apparantly antithetic to the Alvin Fault in northern Brazoria County. The lineament is 2000′ long striking N 30 E (apparently downthrown to the northwest), from south of Hampton Street, across Alta Vista and Casa Court (east of Kost Street), Kost Street, and appears to die out as it reaches South Street

The feature appears as a poor lineament on B&W 1980 1-6-106 and is classified as a possible fault.

<u>FCR 183 Lineament (SC)</u>

This possible fault is located southwest of Alvin in Northern Brazoria County. It strikes N 65 W (downthrown to the southwest) for 2500′ from northwest of FCR 392 (paved) to terminate just southeast of FCR 183. This feature appears as a poor lineament on IR 11-300 and is considered a possible fault.

FCR 436 Lineament (SC/SE)

This feature is located 2.5 miles southwest of Alvin. It is approximately 7000′ in length and strikes N 75 W (downthrown to the south), from FM 1462, across FCR 436 and FCR 435.

This apparent fault is seen as a poor lineament on IR 11-300 and B&W 1980 7-152. No convincing scarp is visible on FCR 436 (unpaved)

The poor lineament and lack of field confirmation suggest a possible fault designation.

Briscoe Canal Lineament (SE)

This apparent fault is located 2 miles south of Alvin, in northern Brazoria County; it is 1.5 miles in length, and strikes N 45 W (apparently downthrown to the southwest) from FCR 172, across SH 35 north of the Brazos River Authority Briscoe Canal, terminating at FM 2403.

IR 11-300 and B&W 1974 H5 showed this feature as a fair lineament. A pavement break but no throw was in evidence at the single road crossing along SH 35. Any throw that may exist at this point has been masked by construction of a new canal bridge on SH 35.

The fair lineament and the lack of field confirmation suggest this feature to be a possible fault.

FAULTS ON THE MANVEL AND ALGOA QUADRANGLES
(Plates 5 and 6)

DEFINITE FAULTS

South Hastings Fault (NE/NW)

This fault crosses SH 35 and Hastings Oilfield approximately 5 miles south of Pearland. This feature strikes N 42 E (downthrown to the northwest) for about 2.2 miles beginning at FCR 731-S and running across FCR 552 (unpaved), SH 35 (paved), six oilfield lease roads (unpaved), Chigger Creek (which jogs south as it crosses onto the upthrown side of the fault), another unnamed oilfield lease road (unpaved), and Heights-Hastings Rd. (FCR 281; paved), to terminate just southwest of FCR 294 (paved).

The South Hastings Fault appears as a very good lineament on B&W 1974 H3 and IR 11-235, weakening somewhat between Chigger Creek and FCR 294. Fifteen profiles through the Hastings Oilfield revealed a diffuse but consistent scarp with throw ranging between 5-15 cm; 20-27 cm of throw exists along a prominant scarp on oilfield grounds immediately west of SH 35; ponded drainage and a dip in the roadside ditch embankment exists along SH 35; 9 cm of cummulative throw occurs at the southern extremity of the fault on FCR 294, ponding is also apparent in the roadside ditch; and a small scarp occurs in the backyard of a house located at the corner of FCR 294 and FCR 281. A vegetation change from fresh green to dry straw yellow is associated with this scarp.

Exhibiting correct positioning, orientation and sense of throw, the South Hastings Fault may be the surface expression of a fault mapped on the Frio Formation (McNaughton, 1953, p. 122). The combination of an excellent aerial photo lineament, consistent field confirmation and subsurface evidence make this a definite fault.

POSSIBLE FAULTS

FM 2403 Lineament (SE/SW)

This feature is located in northern Brazoria County, 1.7 miles south of the Alvin City limits on FM 2403; it strikes roughly N 80 W for 9000′ (with apparent downthrow to the south), from fields west of SH 35, across FM 2403 (paved), FCR 424 (unpaved), FCR 424B (unpaved), FCR 424A (unpaved), and FCR 833 (paved).

The apparent fault appears as a weak lineament on B&W 1974 H5. The lineament is coincident with a pavement patch on SH 35 and a change in the average gradient, or average land slope, corresponding to 4 cm of throw.

On the basis of the poor aerial photograph lineament and the sparse field confirmation, I consider this feature to be a possible fault.

FAULTS ON THE ALGOA QUADRANGLE
(Plate 6)

DEFINITE FAULT

Moore Road Fault (NW)

The Moore Road Fault is located on the border of Brazoria and Galveston Counties 1 mile north of Alvin. The fault strikes N 50 W for 1.5 miles from 3800′ southeast of the Galveston County line, crossing Friendswood Road (FM 528), Mandale Road and Moore Road (FCR 133) and terminating 1400′ northwest of where it crosses Chigger Creek.

The Moore Road Fault presents a very good lineament on B&W 1974 I3, IR 69-217, and IR 11-235. It is marked by a substantial scarp (greater than 35 cm) and a pavement break on FM 528, and a very good scarp on the lawn of a house on the east side of the road. A cumulative scarp height of 38 cm exists on Moore Road (unpaved); 15 to 20 cm on Mandale Road (unpaved); and the scarp appears to effect the course of Chigger Creek causing it to make a right angle turn as it crosses from the downthrown to the upthrown block. Surface projection of a substantial feature identified on a seismic profile clearly coincides with the surface location of the Moore Road Fault. The profile shows the up-to-the-coast Moore Road Fault to be antithetic to a much larger down-to-the-coast fault located approximately 2 miles to the northeast in Galveston County.

The excellent airphoto lineament, excellent field expression and seismic expression of the fault leave no doubt as to its existence.

PROBABLE FAULTS

Hastings Oil Field Fault (NW)

This probable fault, located 6.2 miles southeast of central Pearland, was first identified by Dr. Carl Norman, University of Houston. With 17 cm of cummulative throw and evident pavement breaks, this fault extends for a short distance, less than 1000′, striking N 60 W (downthrown to the northeast). The excellent field expression is not reflected on aerial photographs.

The excellent scarp and pavement break suggest a good feature, however, the lack of aerial photographic evidence is a factor that reduces the certainty of this feature to probable.

POSSIBLE FAULTS

Hastings Oil Field Lineament (NW)

This possible fault was first noted by Dr. Norman on the basis of a scarp on SH 35 (paved). Located south of FCR 281 (Heights-Hastings Road) 6.4 miles southeast of Pearland, field expression is very subtle. A small scarp striking N 70 E (downthrown to the northwest) may be present associated with possible building damage. This feature is not visible on airphotos. The lack of a positive airphoto lineament plus uncertain field evidence makes this a possible fault.

FAULTS ON THE GUY QUADRANGLE
(Plate 7)

DEFINITE FAULT

Damon Quarry Fault (EC)

In an article by Baker (1978, p. 15), a very short fault is described within Damon Quarry. The quarry is located on the northwest flank of the Damon Mound salt dome. The fault strikes N 70 E for 400', downthrown to the north. It bounds a block of *Heterostegina* limestone of the Oligocene Anahuac Formation which has been downfaulted into the caprock limestone of the Damon Mound salt dome.

This fault is not visible on aerial photographs and probably would not be visible at the earth's surface if not for quarry operations.

VERY PROBABLE FAULT

FCR 522 Fault (C)

This feature is located approximately four miles west of central Damon and strikes N 12 W (downthrown to the west), for 7300', from 3000' north of the Fort Bend County line,

across FCR 522 to terminate in fields and woods some 4300' to the south.

Along FCR 522 (unpaved) 7.5 cm of correctly oriented throw corresponds to the fairly good lineaments on IR 69-257 and B&W 1974 A8.

FAULTS ON THE DAMON QUADRANGLE
(Plate 8)

DEFINITE FAULTS

North Damon Fault (WC)

This fault is located 1.5 miles north of the town of Damon. It strikes due north, downthrown to the west for 7000' from 1200' north of the SH 36/FCR 11 intersection to open ground in Fort Bend County.

The North Damon Fault appears as an indistinct lineament on IR 11-292 and has been recognized in the subsurface on seismic profiles.

VERY PROBABLE FAULTS

South Damon Fault (SW)

This fault is located 2.2 miles southwest of central Damon. It strikes N 5 W (downthrown to the west) for 5000′, from 1000′ south of the FCR 643/FCR 4 intersection, trending roughly parallel to FCR 4.

Field evidence is inconclusive, but a lineament exists on IR 69-255, and a large north-south trending fault recognized on seismic profiles has the correct throw direction and subsurface position to be related to this surface fault.

POSSIBLE FAULTS

Beacon Lineament (SW)

This possible fault is located in westernmost Brazoria County, some 1.8 miles southeast of central Damon; the nearest distinguishable feature being a beacon marked on the topographic sheets. The feature strikes N 20 E (apparently downthrown to the east) for 2800′ across FCR 18, to die out in fields to the south.

This feature appears as a poor lineament on B&W 1974 G8 and is considered a possible fault.

Windmill Lineament (SC)

This possible fault is located in western Brazoria County, some 3.1 miles southeast of central Damon in fields dotted by numerous working windmills. Stike is roughly N 10 W (apparently downthrown to the west) for 4300′, from just south of FCR 18 into the fields beyond.

Recognized form a very poor lineament on IR 69-255, this feature is considered a possible fault.

FAULT ON THE ROSHARON QUADRANGLE
(Plate 9)

DEFINITE FAULTS

Chenango Pond Fault (SW/SC)

Located in central Brazoria County, about 7.5 miles north of central Angleton, this fault strikes N 70 E for 2.5 miles (downthrown to the southeast) from Chenango Pond Road, across Old Houston Road (FM 521), old SH 288, new SH 288, to terminate east of FCR 48.

A very good lineament appears on IR 69-250, IR 69-251, B&W 1974 F8, and B&W 1980 11-302. No throw is thus far evident on the recently resurfaced FM 521, however a 20 cm scarp occurs on old SH 288 accompanied by small pavement breaks. No throw is currently present on new SH 288 (recently constructed), but a scarp with 14 cm of cumulative throw does occur on FCR 48 along with some pavement breaks. This fault is recognized on seismic profiles as a substantial down-to-the-coast feature with greater than 500 feet of throw at depths of 5700 feet.

The very good lineament, excellent field expression and subsurface confirmation indicate a definite fault.

FAULTS ON THE LIVERPOOL QUADRANGLE
(Plate 10)

DEFINITE FAULTS

Rowan Oil Field Fault (NE)

This slightly convex to the south feature is located 4.5 miles south-southwest of Alvin striking N 80 W (downthrown to the south) for 4800′ from Parker Road (FCR 172), just west of Rowan Oil Field.

Although it appears as a very poor lineament on IR 11-300 and B&W 1974 H6, and lacks field evidence, the feature may be related to a large subsurface fault displaying a similar orientation and polarity (McNaughton, 1953, p. 101), which forms the northern boundary of the

Chocolate Bayou Oil Field in the subsurface. Additional subsurface evidence for this fault exists on seismic lines. A fault showing 158 feet of throw at 7100 feet has a projected surface trace which coincides with the location of the Rowan Oil Field Fault.

The convincing subsurface evidence indicates a definite fault designation for this feature, however, the poor lineament and lack of field evidence suggest it is not currently active.

VERY PROBABLE FAULTS

Danbury-Liverpool Road Faults (SC)

These two faults are located in central Brazoria County, approximately 3.5 miles northeast of Danbury on FCR 171 (Danbury - Liverpool Road). The northernmost feature strikes roughly due east (downthrown to the south) for over two miles, extending from Austin Bayou, across the northern portion of Danbury Dome, the Missouri-Pacific Railroad and Danbury-Liverpool Road (FCR 171), terminating in rice fields to the east. The shorter feature strikes N 72 E branching from the northern fault from its eastern end, and extending 700′ east of the Danbury-Liverpool Road.

Both features appear on IR 69-249 and B&W 1974 G9 as a combination of poor lineaments and stacked rice field levees at their eastern extremities. Little field evidence, beyond a sag on FCR 171 (paved), is present and the Missouri Pacific Railroad line appears to be unaffected. However, substantiating evidence does exist on seismic profiles. At their eastern extremity where these two surface lineaments converge, a large amount of throw is visible on a seismic section which clearly indicates a fault downthrown to the north with nearly 400 feet of throw at 7100 feet.

On the basis of the long, but poor lineament, the closely spaced rice field levees, and the poor field expression, these features would normally have been considered to be possible faults. In this case it is reasonalble to conclude that the combination of poor surface expression with very good subsurface throw indicates a definite fault which is undergoing very little if any current movement.

POSSIBLE FAULTS

North Danbury Lineament (SW)

Located two miles north of central Danbury on SH 35, this apparent fault strikes due east (downthrown to the south)

for approximately 1.7 miles from the the vicinity of the Danbury Dome Oil Field, across SH 35, to die out in fields approximately 200′ east of FCR 46.

This feature is expressed as a combination of a poor lineament and stacked rice field levees on IR 69-249, but field checking failed to find evidence of it on SH 35 (the only accessible point on the fault trace). This feature is considered to be a possible fault.

Snug Harbour Lineament (SE)

Located in the Snug Harbour community, some six miles northeast of central Danbury. The sinous surface trace strikes roughly N 5 W (with apparent downthrow to the east) for approximately two miles. It runs south of Halls Road (FCR 198), across rice fields, Chocolate Bayou, FCR 210, FCR 779 (Hailey Road), FCR 730 (Snug Harbour Dr.), FCR 730C (Fathom Road), FCR 203 (Liverpool-Hoskins Road), and terminates in fields to the south.

Seen as a fair lineament to the south of Chocolate Bayou and as stacked ricefield levees to the north on IR 69-247 and B&W 1974 H8, the apparent fault is not in evidence on the ground, except for a small scarp on FCR 210 (paved), and Hailey Road (paved).

The poor to fair lineament and the inconclusive field evidence suggest that this is a possible fault.

FAULTS ON THE WEST COLUMBIA QUADRANGLE
(Plate 11)

POSSIBLE FAULTS

Mound Creek Lineaments (WC,C,SW,SE)

Five lineaments are located in the vicinity of Mound Creek four miles northwest of the town of West Columbia. They average less than a mile in length with two striking due south, downthrown to the west, two striking N 45 W, downthrown to the southwest and one striking N 80 E, downthrown to the south. These lineaments appear as poor features on IR 69-255, IR 69-256, and IR 11-330.

The persistence of the lineaments on several generations of airphotos suggest they are possible faults.

FCR 21 Lineament (NC)

This possible fault is located in west Brazoria County on FCR 21, 5.5 miles southeast of central Damon. It strikes N

50 E (apparently downthrown to the southeast), for 1700′, in open ground to the east of FCR 21.

Appearing as a very poor lineament on IR 69-255 this feature is considered a possible fault.

FAULTS ON THE ANGLETON QUADRANGLE
(Plate 12)

DEFINITE FAULTS

Chenango Oil Field Fault (NW)

Located just to the north of the Chenango Oil Field in central Brazoria County, approximately 4.5 miles northwest of central Angleton on FM 521, this fault strikes N 50 E (downthrown to the southeast) for 2.3 miles. It crosses fields southwest of FCR 32, FCR 32, FM 521 and oil field roads east of FM 521, to die out in open ground to the northeast.

This feature is seen as a very good lineament on IR 69-251; a weak lineament on IR 11-327, and a portion is visible on B&W 1974 F9 and B&W 1980 11-300. 19 cm of throw is seen on FM 521 (Old Houston Road; paved); 10 cm of relief on an oil field road; no throw is evident on SH 32. There can be little doubt that this is the same fault as that mapped with 800′ of throw, and with an identical trend, on top of the Frio Formation, just to the southwest in Angleton Oil Field (McNaughton, 1953, p. 75).

The good lineament, consistent field evidence, and subsurface evidence suggest that this feature is a definite fault.

FAULTS ON THE HOSKINS MOUND QUADRANGLE
(Plate 13)

DEFINITE FAULTS

Horse Grove Point Fault (SW,C,EC,NE)

This fault is located on the northeast flank of Hoskins Mound. It strikes N 45 E (downthrown to the northwest) for 6 miles, from 4500′ northeast of the Hoskins Mound summit across Chocolate Bay and Horse Grove Point to terminate some 6000′ northeast (inland) of the Humble Cut.

This feature appears as an excellent lineament, between Hoskins Mound and Horse Grove Point and continues as a poor lineament northeast of Horse Grove Point between Chocolate Bayou and its terminus on IR 11-322 and B&W 1974 I10. The fault also shows geomorphic expression as it appears to control stream patterns along its length and may even

provide the cause for sediment accumulation at Horse Grove Point where it extends into Chocolate Bay.

Three separate seismic profiles show this fault to have substantial throw at depth with displacements extending well into Oligocene age layers. Measurements made from seismic profiles indicate throws of 311 feet at 5300 foot depths, and 636 feet of throw at 7550 foot depths. The surface projection of the fault seen on seismic profiles coincides exactly with the location of this surface trace. On the basis of the excellent lineament, the apparent geomorphic expression and the subsurface confirmation, this feature is classified as a definite fault.

South Ingleside Barrier Fault (SC,SE)

Located in far eastern Brazoria County 2.5 miles east of Hoskins Mound, this fault strikes N 66 E (downthrown to the northwest) for over 3 miles. The feature extends from the waters of West Galveston Bay, and continues roughly parallel to the ocean facing edge of the ancient Ingleside Barrier Island Complex. The fault appears to control the location of a shallow but aerally large lake situated between the upthrown block of the fault and the high relief relict barrier island.

This feature is recognized from the suspiciously straight lake front edge on IR 11-322 and B&W 1974 I11. Reinforcement of the fault identification is gained from the earliest aerial photograph available, B&W 1938 BRQ2-13, which reveals a wetland area, not a lake, at this location (Figure, photo). In addition, this older photograph shows the expression of the fault continuing well into the waters of West Galveston Bay. This bayward extension is not evident in later generation photographs due to construction of the Intercoastal Waterway.

The excellent geomorphic expression of this feature earn it a definite fault designation. It is not unreasonable to conjecture that this fault may continue southward and join the Alligator Lake Lineament which occurs along strike to the south.

3 Hoskins Mound Faults (SW,C)

These three faults are located 6000′ northeast of Hoskins Mound north of the Horse Grove Fault. All three trend roughly N 25 E (downthrown to the northwest) for an average of 6000′ across open marshland. They are recognized from good to fair lineaments on IR 11-322 and B&W 1974 I9. These airphotos show greater marsh development on the downthrown blocks of these faults.

Seismic evidence exists for all three of the Hoskins Mound faults. The southernmost fault has the shortest surface expression but is visible in the subsurface as a substantial feature with displacements visible at 13,000 foot depths. Measured throws are 138 feet at 2750 foot depths; 211 feet at 5475 foot depths; and 472 feet at 7250 foot depths.

The middle Hoskins Mound Fault has the best surface expression of the three and is probably the most active at present. On seismic profiles the fault appears as a relatively young feature with small shallow throws and no displacements apparant deeper than 4800 feet. Measured throws are 64 feet at 1700 foot depths and 133 feet at 2500 foot depths.

The northwesternmost Hoskins Mound Fault has the weakest surface expression and shows very small throws on seismic profiles. The good lineaments, geomorphic expression and seismic evidence confirm the designation of all three of these features as definite faults.

North Ingleside Barrier Fault (SC)

The North Ingleside Barrier Fault is located 2.5 miles east of Hoskins Mound. Strike is N 45 E (downthrown to the southeast) for 3800′ along the northern edge of the ancient

Ingleside Barrier Island complex. The fault appears as a fairly good lineament on IR 11-322. A fault with the same sense of throw and coinciding surface projected location is visible on seismic profiles with measured throw of 66 feet at 2050 foot depths and 140 feet at 3175 foot depths. The good lineament and seismic confirmation designate a definite fault.

PROBABLE FAULTS

Oyster Lake Fault (SC)

Located in easternmost Brazoria County, this probable fault strikes roughly N 10 W (downthrown to the west) for 5500′ from marshy ground 2200′ north of the Intracoastal Waterway, to the northern shore of Oyster Lake. This feature appears as a good lineament on B&W 1974 I11 and is considered to be a probable fault.

FAULTS ON THE HOSKINS MOUND AND SEA ISLE QUADRANGLES (Plates 13 and 14)

DEFINITE FAULTS

Persimmon Bayou Fault (NE/NW)

This fault crosses Persimmon Bayou 4000 feet north of its intersection with New Bayou. It strikes roughly due east (downthrown to the south) for 2.1 miles. A poor to very poor lineament appears on IR 69-244, IR 11-321, and B&W 1974 J9. This lineament corresponds in sense of motion and projected surface location with a fault visible on seismic profiles with measured offsets of 340 feet at 5000 foot depths.

VERY PROBABLE FAULTS

Halls Bayou Fault

Extending 4.4 miles from New Bayou on the west, to Halls Bayou to the east, this fault may influence the course of a small Hall Bayou tributary. The tributary runs along the fault scarp on the downthrown block for approximately 400 feet before continuing southward. This fault was recognized from lineaments appearing on IR 69-244, IR 11-321, and B&W 1974 J9.

PROBABLE FAULTS

New Bayou Fault

This fault extends 2.3 miles due east of New Bayou, downthrown to the south. Lineaments appear on IR 11-231 and B&W 1974 J9. At its western end the fault appears to influence the course of New Bayou creating a right angle bend in the course of the stream.

FAULTS ON THE ASHWOOD QUADRANGLE

(Plate 15)

POSSIBLE FAULT

Dance Bayou Lineament (NE)

The Dance Bayou Lineament lies in southwest Brazoria County about 2.5 miles northwest of the town of Old Ocean; it strikes N 10 E (apparently downthrown to the east), for 5000′ from just north of Dance Bayou to FCR 3 near its intersection with FM 524.

This feature shows as a fairly good lineament on IR 11-332 running parallel to Dance Bayou for some 2700′, thereby implying drainage control (or alternatively implying this is a drainage feature too!). No clear field evidence is seen for this possible fault.

FAULTS ON THE SWEENY QUADRANGLE

(Plate 16)

PROBABLE FAULT

Sweeny Fault (C)

This probable fault is located on the outskirts of the town of Sweeny. It trends roughly due east (downthrown to the south), for 2800′, from west of Brookman St., to cross Brookman St., Ross St., Second St. (FM 1459), McKinney St., and Ave A, before terminating in open ground to the east.

A poor lineament, probably due to urbanization, appears on IR 69-304. A fault with the same sense of throw and projected surface location is recognized on seismic profiles. This feature is considered a probable fault.

POSSIBLE FAULTS

Northwest Sweeny Lineaments (WC)

Two lineaments are located to the northwest of Sweeny, Texas within the Old Ocean Oil Field. The southern lineament is located 2.3 miles northwest of central Sweeny and strikes N 81 E, downthrown to the south for 3000′. It is bounded by an ephemeral stream to the west and an oil field road to the east. The northern lineament is located 2.8 miles northwest of Sweeny striking N 72 E, downthrown to the north for 6000′. Identified on IR 69-304 and B&W 1974 I13, both these lineaments have weak expression on aerial photographs, however, they may both have an influence on the course of an ephemeral stream and are considered possible faults.

FAULTS ON THE BRAZORIA QUADRANGLE
(Plate 17)

POSSIBLE FAULT

Zion Temple Cemetery Lineament (SW)

This feature is a possible fault located in southern Brazoria County approximately 2.5 miles southwest of the town of Brazoria. The lineament strikes roughly N 30 E (apparently downthrown to the northwest), for 3200′, from 2000′ southwest of the San Bernard River to FM 529, some 1000′ west of Zion Temple Cemetery.

This possible fault is based upon a poor lineament on IR 11-383.

FAULTS ON THE OYSTER CREEK QUADRANGLE
(Plate 18)

DEFINITE FAULTS

Essex Bayou Fault (SE)

This probable fault is located at Essex Bayou some 5.5 miles northeast of central Freeport. The fault strikes N 81 E (downthrown to the north) for 2.4 miles from the edge of the Slop Bowl, across Essex Bayou terminating at Oyster Creek.

The fault is evident as a good lineament on IR 11-388, B&W 1974 H14 and B&W 1980 1-7-134. This fault also appears to influence the course of Essex Bayou as it flows onto the unthrown block. This feature is recognized on seismic profiles with throws greater than 200 feet at depths of 5950 feet. The good lineament, evident stream control and subsurface confirmation indicate a definite fault.

Slop Bowl Fault (SE)

This definite fault is located in the Slop Bowl 7 miles northeast of central Freeport. The fault strikes N 80 E (downthrown to the north) for 1.1 miles from the Slop Bowl Lakes across marshy ground to terminate at the north end of the East Branch of Essex Bayou.

This fault appears as a good lineament on IR 11-388, B&W 1974 H14 and B&W 1980 1-7-134. This fault may have some influence on the course of Esses Bayou. A fault with the same sense of throw and projected surface location is recognized on seismic profiles. Offsets greater than 200 feet are present at depths of 5700 feet.

<u>POSSIBLE FAULT</u>

<u>Nicks Lake Lineament (SE)</u>

This possible fault is located near Nicks Lake 7 miles northeast of central Freeport. It strikes N 50 E (downthrown to the southeast) for 1.5 miles from Nicks Lake, across the northern margin of the Slop Bowl possibly intersecting with the Slop Bowl Fault.

Visible as a poor lineament on IR 11-388 and IR 69-313, this fault appears to dam the northern margins of several of the small Slop Bowl Lakes. This fault was inaccessible for field checking. On the basis of the lineament and good geomorphic expression, this feature is considered a possible fault.

FAULTS ON THE OYSTER CREEK AND CHRISTMAS POINT QUADRANGLES

(Plates 18 and 19)

<u>DEFINITE FAULT</u>

<u>Salt Lake Fault (SE,EC/WC)</u>

The southernmost end of this fault extends to within 6.7 miles of central Freeport. It is over 5.7 miles in length and strikes N 35 E from 1 mile south of Salt Lake, across Salt Bayou, crosses onto the Christmas Point Quadrangle (27) and continues across Big Slough, and Cox Lake to die out into Lost Lake.

This prominent airphoto feature is visible on IR 11-388, IR 69-313, B&W 1974 I12 & I13, B&W 1980 11-6, and 1938 4-9-13. Good geomorphic expression is visible where the lineament forms a conspicious boundary separating swampland containing linear ponds along the fault scarp from relatively well drained ground. This is most noticeable south of Salt Lake and between Salt Lake and Big Slough. The channel of Big Slough visibly widens as it crosses from the upthrown to the downthrown block of this fault. The southwestern end of this fault is recognized on seismic profiles with 200 feet of measured throw at depths of 3600 feet.

The very good lineament seen on several generations of aerial photos plus the convincing geomorphic expression indicate a definite fault.

FAULTS ON THE CHRISTMAS POINT QUADRANGLE (Plate 19)

DEFINITE FAULTS

Alligator Lake Fault (NW)

This fault is located 1.2 miles southeast of central Hoskins Mound in southeast Brazoria County. It strikes roughly N 15 W (downthrown to the southwest), across marshlands for approximately one mile from the outer limits of the Hoskins Mound enclosure to the north shore of Alligator Lake.

The Alligator Lake Fault produces a well defined lineament on IR 11-322 and B&W 1974 I12. Seismic profiles indicate a fault with approximate throws of 400 feet at 3500 feet; 500 feet at 5050 feet; and 700 feet at 6650 feet. The association with a saltdome, the good lineament and subsurface evidence support a definite fault classification.

Mud Island Faults (NE)

These roughly parallel faults have an average N 80 E strike across Mud Island, each approximately 1.2 miles in length.

The lineaments are very distinct on IR 69-315 and B&W 1974 I12 and appear to form a graben-like feature about 1000-1500′ across.

PROBABLE FAULTS

Big Slough Fault (WC)

This probable fault is located one mile southeast of the Salt Lake Fault. It strikes N 43 E (downthrown to the northwest) for 7000′, from the eastern edge of Salt Lake, across Big Slough, to end 1500′ north of the Big Slough terminus.

The fault is visible as a fair lineament on IR 11-388, IR 69-313 and B&W 1974 H13. The fault appears to form the boundary between marshland on the downthrown block and drier land on the upthrown block and it may have an effect on the meander pattern of Big Slough.

The fair lineament and good geomorphic expression of this feature indicate a probable fault.

Drum Bay Fault (SW,WC,C)

This fault is located in southeast Brazoria County where it parallels the Intercoastal Waterway some 9 miles northeast of Freeport. The feature is approximately 6.2 miles in length striking N 19 E (downthrown to the southeast) from Drum Bay to Bastrop Bay.

This feature is visible as a fair to very poor lineament on IR 69-315, IR 11-329, B&W 1974 I12 and B&W 1938 11-6-8. Significant ponding occurs along its northern portion and the lineament appears to separate dry from swampy ground along the Drum Bay shoreline. This feature appears as a weak but persistent lineament on several generations of aerial photographs and exhibits good geomorphic expression, so is designated a probable fault.

POSSIBLE FAULTS

Alligator Lake Lineament (NC)

This possible fault is located to the north of Alligator Lake. It strikes N 25 E (downthrown to the northwest) for 4500' across marshlands and is visible as a fair lineament on IR 11-322 and B&W 1974 I12. It is not unreasonable to assume this feature is the southern extension of the South

Ingleside Barrier Fault described on the Hoskins Mound quadrangle (20). On the basis of a fair lineament and apparent continuation along strike into a more certain feature, this is considered a possible fault.

Lost Lake Lineament (NW)

This possible fault is located 3.7 miles east of of the town of Demi John in southeast Brazoria County. The lineament strikes N 30 W (downthrown to the southwest) from northwest of Lost Lake for 1 mile across open marshlands.

Visible as a poor lineament on IR 69-313, this feature is considered a possible fault.

Bastrop Bayou Lineament (NW)

This feature is located 2.3 miles east of Demi John. It is 0.5 miles in length and strikes N 49 E (downthrown to the northwest) across marshlands north of Bastrop Bayou. It is visible as a good lineament on B&W 1974 I12 and so is considered a possible fault.

FAULTS ON THE CEDAR LANE NE AND JONES CREEK QUADRANGLES

(Plates 20 and 21)

POSSIBLE FAULTS

Redfish Bayou Lineaments (EC/WC)

The Redfish Bayou Lineaments are found in southernmost Brazoria County, located in swamplands between the San Bernard River and Jones Creek, north of Redfish Bayou.

Three poor lineaments appear on IR 69-327 and B&W 1974 E16. The longest lineament strikes roughly due east (apparantly downthrown to the south) for 6.25 miles, from the vicinity of Jones Creek to the San Bernard River; it appears to exhibit some control over small stream courses and swamp distribution along its length. The intermediate lineament strikes N 70 E, downthrown to the south, is considerably shorter (1.9 miles) and also appears to affect drainage. The third feature is 2.0 miles in length, strikes N 27 E (apparently downthrown to the southeast) and has little geomorphic expression.

The consistent appearance of these features on several generations of air photos and their geomorphic expression suggest a possible fault classification.

FAULTS ON THE FREEPORT QUADRANGLE

(PLATE 22)

DEFINITE FAULTS

Freeport Fault and 2 Subsidiary Faults (NW,WC,SW)

Located in and around the city of Freeport, the 7 mile long Freeport fault has an average N 22 E strike, downthrown to the east, from 0.4 miles north of SH 332, across SH 332 (paved), and East Union Bayou which makes a bend at this crossing, through the Dow Chemical Plant grounds and Dow Barge Canal into the city of Freeport. Within urban Freeport the fault crosses Division St., and then bordered by Division and Fisher Sts., strikes south-southwest to the Old Brazos River. The fault trace is picked up again in the Freeport Golf Club lawn and continues south to the Jane Long School playing field exiting urban Freeport by crossing two canals and SH 288. South of urban Freeport the fault forms the western border of a swampland area until the surface trace is lost upon entering the Bryan Mound compound. A continuation of this fault appears along strike with the same sense of motion south of Bryan Mound crossing the Intercoastal Waterway and terminating north of Bryan Beach State Park.

Aerial photo evidence for the northern portion of the Freeport Fault is very strong. A good lineament appears on IR 69-324, IR 11-387 and B&W 1974 G15. (Going back to the earliest aerial photographs available, this fault is not visible on B&W 1938 6-36.) As is often the case in urbanized areas, a clear air photo lineament is not visible within the city of Freeport. South of urban Freeport, a good lineament appears on IR 69-324, IR 11-387 and B&W 1974 G15. The lineament marks a division between upthrown dryland and downthrown swampland. South of Bryan Mound a short, fairly good lineament appears along strike on IR 69-324.

A detailed record of the field expression of this fault includes at the north end of the fault trace, a pavement break and small scarp on SH 332 0.88 miles northwest of the FM 523/SH 332 intersection, and some slight disturbance to a man-made levee surrounding a petroleum storage tank on the Dow Chemical grounds. Within urban Freeport there is evidence of road repairs at the Division St./Gulf Blvd. intersection. Employees of a hardware store on the south side of Gulf Blvd. report frequent pavement breaks in the store parking lot adjacent to Division St. on the west side of the building. Continuing south, a diffuse scarp exists in an empty lot between Ave. C and Ave. D. On S. Ave. A west of Fisher St., Tanya's Mexican Bakery straddles a a 22

cm scarp (measured aong S. Ave. A) and shows extensive damage. On North Front St. where the fault crosses east of Fisher St. before entering the Old Brazos River channel, a 3 cm throw occurs.

The artificial levee on the south bank of the Old Brazos River apparantly is not affected, however, a prominant, east facing scarp does appear on the south side of the levee in the Golf Club lawn and continues across Second St. (SH 36), west of Locust.

To the south on W. Broad St. the Freeport Fault forms a 44 cm scarp. Residents of 1210 W. Broad St., Mr. and Mrs. Stinton, report that their house has been levelled three times over the last 50 years. Mrs. Stinton's father, the original owner of the house, was forced to cover the downthrown side of the fault with tar paper to prevent upwelling salt water from killing the vegetation. Across the street at 1211 W. Broad St. Billy Seay reports that her house had been levelled just before she moved in 15 years ago. Within the first 5 years of occupation new damage appeared and Ms. Seay has subsequently had plumbing problems, apparently unrelated to winter weather conditions. It is apparent, even to the naked eye, that this structure again requires levelling. Very prominent scarps, of the same order of magnitude as that seen on W. Broad St., are present on W. 4th through W. 8th Sts.

Located between Mesquite and Locust Sts. at 1210 W. 5th St. stands a house built by Mr. Fred David in 1941. Mr. David reports that within the first 3 years of occupation the ground had shifted 7 to 8 inches. Initially a continuous effort was made to to compensate for the throw as it occurred. In 1961 an addition was built and unfortunately, this newer structure is also now in need of relevelling.

South of W. 8th St., the strike of the fault shifts slightly to the southwest disturbing an old holding tank. A new tank has since been constructed, apparantly to to replace the old one. Other field evidence includes: substantial scarps on Mesquite, W. 9th St., W. 10th St., and W. 11th St.; and a very good scarp across the Jane Long School playing field and disappears into a stand of trees north of the canal along SH 288. There is no apparent throw on the recently modernized SH 288, but the fault scarp can be followed by eye south of SH 288 as a color contrast created by a vegetation change from swampland species to drier ground varieties. An attempt was made to follow the fault into the Bryan Mound compound but access was not gained to this Department of Energy Property.

Two minor faults appear approximately 500′ and 1500′ east of the northern terminus of the Freeport Fault on SH 332. These features are apparently subsidiary faults,

striking due north for about 3000′ each and are downthrown toward the Freeport Fault to the west. These features appear as good lineaments on IR 11-387 and IR 69-324 and appropriately located road disturbances do occur on SH 332.

On the basis of the very good aerial photograph expression, and the excellent field evidence, this feature is designated a definite fault.

<u>VERY PROBABLE FAULTS</u>

<u>Velasco Fault (NW,WC)</u>

This fault, associated with the much larger Freeport Fault, is located within northern urban Freeport. Strike is N 37 E for 4800 ft., downthrown to the southeast. Extending from 1500′ north of Gulf Blvd. (where it joins the Freeport Fault), this feature crosses Gulf Blvd., N. Ave. D, N. Ave. C, N. Ave. B, N. Ave. A and N. Front St., then crosses the Old Brazos River Channel and open ground to the south, terminating at Second St. (SH 36).

The feature appears as a very poor lineament on IR 69-324, IR 11-387 and B&W 1974 G15, this is probably due to its urban location, since the lineament is clearer, although still poor, where it crosses open ground between the Old Brazos River Channel and Second St.

Small scarps of less than 10 cm, exist on Gulf Blvd., Ave. D and Ave C. A 7.5 cm scarp is present on N. Ave. B, and standing water was present on the downthrown block when this measurement was taken. Small scarps exist on N. Ave. A and along N. Front St. (unpaved), north of the Old Brazos River channel levee. A pavement break and 9 cm scarp are present along Second St., west of Mulberry St.

On the basis of the very consistent field evidence, and persistent lineament despite urbanization, this feature is designated a very probable fault.

PROBABLE FAULTS

Horseshoe Lake Fault (NC)

Located about 2.5 miles north of central Freeport, south of Oyster Creek on SH 332, this fault is over 3000′ in length and strikes N 8 W, downthrown to the west. The fault trends from an abandoned meander loop of Oyster Creek (Horseshoe Lake) north of SH 332, across SH 332 (1.5 miles southeast of the SH 332-FM 523 intersection), to terminate in a small lake north of East Union Bayou.

This feature appears as a fairly good lineament on B&W 1974 H5 and B&W 1980 1-7-132. A good scarp with more than

10 cm of throw exists on SH 332 outside the entrance to a Shell Refinery Plant.

On the basis of the fair lineament and the good scarp, this feature is designated a probable fault.

East Union Bayou Fault (NC)

Located northwest of Surfside, this fault is 5500′ in length, strikes N 4 E (downthrown to the east), from north of East Union Bayou, across SH 332 (0.5 miles south of the SH 332-FM 690 intersection), to terminate south of the canal portion of East Union Bayou.

The fault appears as a poor lineament on IR 69-324 and IR 11-387. A scarp with 8 cm of cumulative throw is present along SH 332, and the fault appears to exhibit some control over the meander pattern of East Union Bayou in the immediate vicinity.

Although this feature appears as a poor lineament, it is located for much of its length close to the bayou channel; the apparent stream control and reasonable field evidence, suggest a probable fault.

Surfside Fault (EC)

Located in northeast Surfside, this probable fault strikes N 41 W (downthrown to the southwest) for 0.5 miles, from the Intercoastal Waterway, across Gaffney St., Pampano St., Tarpon St., and Bluewater Hwy.

The feature appears as a poor lineament on IR 11-387 and B&W 1974 H15. Cumulative throw of 7.5 cm exists on Bluewater Hwy. (paved), and 15 cm of cumulative throw (ranging over a 60 m distance) exists on Pampano St. (unpaved).

In spite of the poor lineament, the field evidence supports a probable fault classification.

POSSIBLE FAULT

East Union Bayou Lineament (NC)

This feature is located just northwest of Surfside 1800′ east of the East Union Bayou Fault. It is approximately 2200′ long and strikes N 3 E, downthrown to the west.

This apparent fault appears as a poor lineament on IR 11-387, IR 69-324 and B&W 1974 H15, in swamplands without access roads. Topographic maps and air photos show possible control over the meander pattern of the East Union Bayou and small ephemeral streams associated with this bayou.

The consistent but poor lineament, coupled with the possible stream control suggest a possible fault.

FAULTS ON THE CEDAR LANE NE AND CEDAR LAKES WEST QUADRANGLES

(Plates 20 and 23)

POSSIBLE FAULTS

Cow Trap Lake Lineaments (SC/NC)

These two possible faults are located in southernmost Brazoria County, just northwest of Cow Trap Lake, some 2 miles west of the San Bernard River. They strike roughly N 55 E (apparently downthrown to the southeast) for 3.7 miles and 1.1 miles, respectively, across inaccessible swamplands. Seen as fair to poor lineaments on IR 69-328 and B&W 1938 12-8, they are not visible on B&W 1974 E17. Some evidence that these features control local drainage patterns appears on the quadrangle map and airphotos, lending possible fault designations.

FAULTS LOCATED WITHIN BRAZORIA COUNTY, TEXAS

(Plate 24)

Plate 24 is a composite map of all surface faults mapped in Brazoria County, Texas.

APPENDIX C

SEISMIC PROFILES

In this section two seismic lines are presented as representative examples of the 395 miles of seismic data used in the study. Seismic data was acquired over areas where possible surface faults were identified from aerial photographs and field investigations. Faults have been interpreted to the near-surface limits of the seismic data and then projected to the surface.

Figure 54 shows the approximate location of example seismic profiles Line #1 and Line #2. Figure 55, is example Line #1. As is often the case, it is scaled to within 500 feet (0.2 seconds) of the surface, but most of the data were not recorded any shallower than 1500 feet (0.5 seconds). Figure 56, Line #2, is displayed in the same manner. Typically, the density of faulting is not so high that a fault visible at depths of 1000 feet cannot be reliably correlated with its equivalent at the earth's surface.

On Line #1, the surface projection of the up-to-coast fault at the southeastern end of the line coincides with the surface location of the northeastern end of the Horse Grove Point Fault, the only up-to-coast fault in the area. The Horse Grove Point Fault is measured to have over 300 feet of

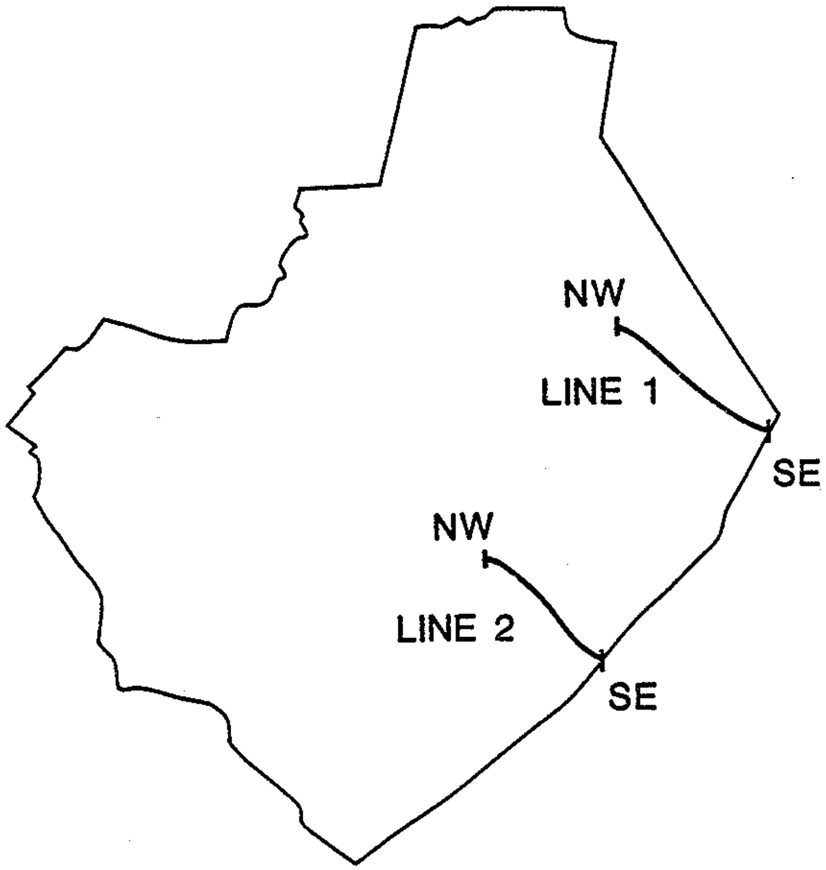

FIGURE 54: Approximate location of example seismic profiles, Line #1 and Line #2.

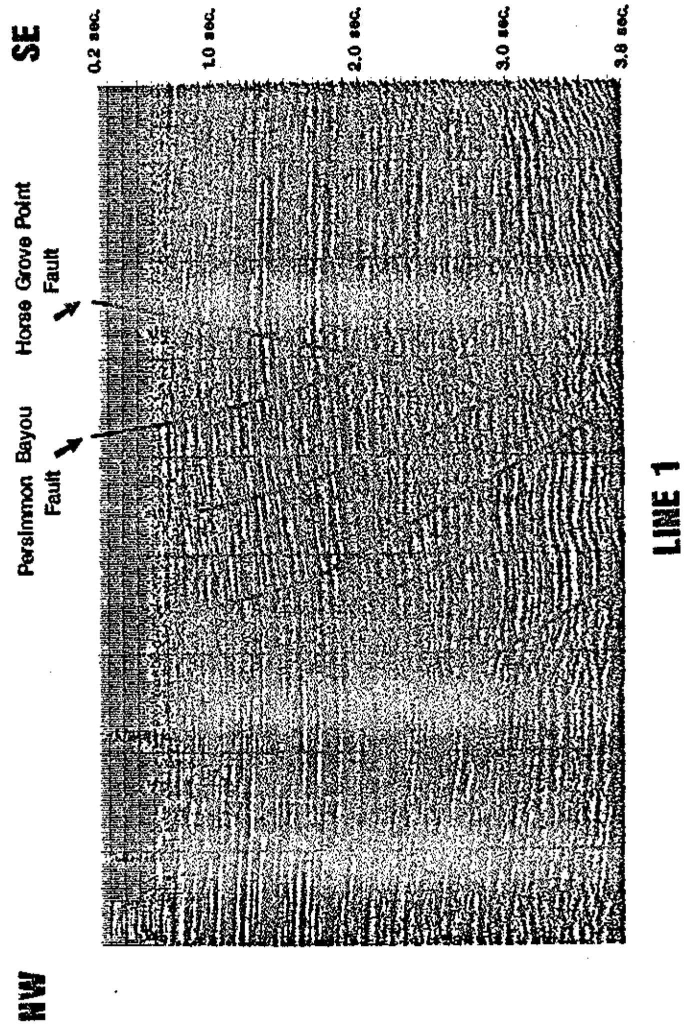

FIGURE 55: Example seismic profile, Line #1. This profile depicts Persimmon Bayou Fault and Horse Grove Point Fault plus several buried faults which show no expression at the surface.

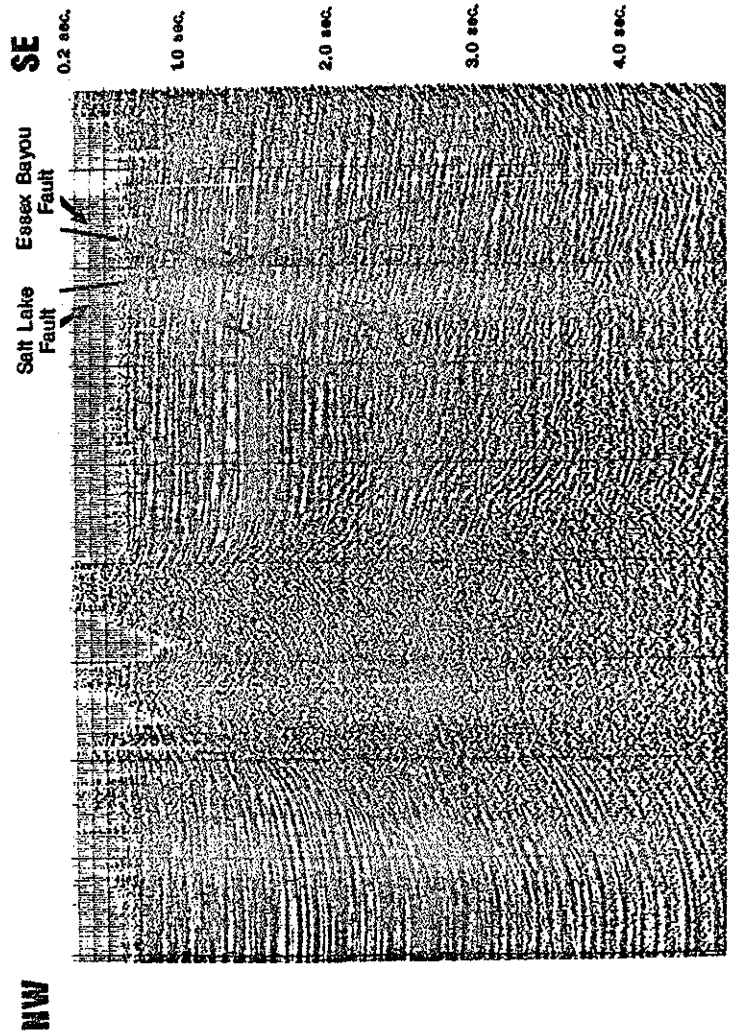

LINE 2

FIGURE 56: Example seismic profile, Line #2. This profile depicts the Salt Lake Fault and the Essex Bayou Fault plus two buried faults near Stratton Ridge salt dome.

throw at depths of 5300 feet, and over 600 feet of throw at depths of 7500 feet. The surface projection of the down-to-coast fault immediately to the northwest coincides with the surface location of the Persimmon Bayou Fault. This fault has measured throw of over 300 feet at depths of 5000 feet. Both of these faults are mapped on the Hoskins Mound and Sea Isle quadrangles, Plates 13 and 14. The next two down-to-coast faults to the northwest do not possess any surface expression and, therefore, have not been mapped as surface faults.

Line #2 crosses the Oyster Creek and Freeport quadrangles, Plates 18 and 22, respectively. A large salt dome, Stratton Ridge, is a prominent feature visible near the northwest end of the line where coherent reflections are absent. To the southeast, two faults are interpreted to extend to the surface. The surface projection of the down-to-coast fault coincides with the surface location of the Salt Lake Fault. This fault has measured throw of 200 feet at depths of 3600 feet. The surface projection of the up-to-coast fault immediately to the southeast coincides with the surface location of the Essex Bayou Fault, which has measured throw of over 200 feet at depths of 5700 feet.

Measurements of throw with depth were made for many faults. The average time-depth curve in Figure 57 was used to convert time measurements to depth measurements. The

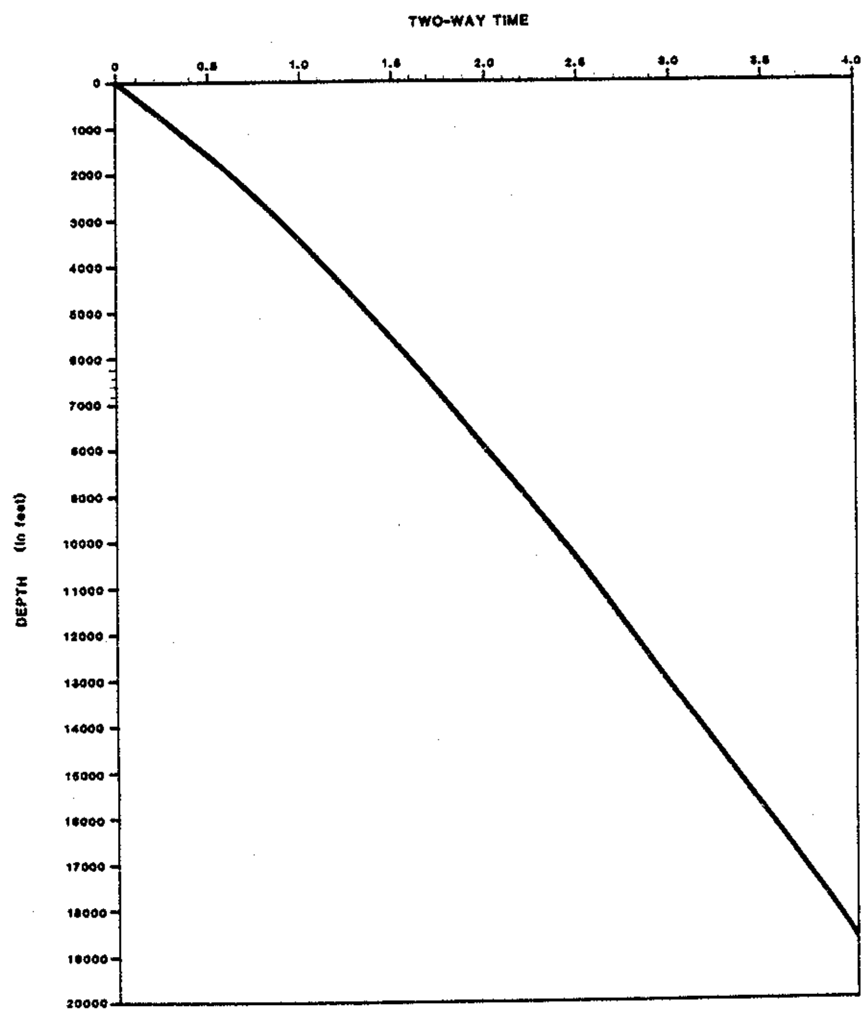

FIGURE 57: Average time - depth curve obtained by plotting values from 20 Brazoria County velocity surveys and applying a best-fit curve to the data.

time-depth curve was obtained by plotting values from 20 Brazoria County velocity surveys and applying a best fit curve to the data.

APPENDIX D

WELL LOG LISTING

In this section the well logs used to conduct the Arcola area subsurface investigation are catalogued. The wells are listed by the following identifying attributes:

Operator Name (API Number)
Lease Name, Well No.
TD = Total Depth
KB = Kelly Bushing
Compl. = Month/Year of completion
(County, if not in Brazoria County)

Depths in the well, including the total depth, is measured from the kelly bushing, a part of the drilling rig located at a specified height above ground level. The kelly bushing height above ground level plus the elevation of the ground above sea level are subtracted from the depth read off a well log to convert the reading to a true depth below mean sea level.

The well logs used in the Arcola subsurface investigation include the following:

#1: Cities Service Oil Co. (42-157-02786)
Octavia Hinton #1
TD = 8250'
KB = 82'
Compl. 9/53
(Fort Bend Co.)

#2: Dick Schwab & Gem Oil Co. (42-157-02787)
Arcola Sugar Mills #1
TD = 6540'
KB = 73'
Compl. 7/8/37
(Fort Bend Co.)

#3: Sam G. Harrison (42-157-02795)
Citizens State Bank Unit #2, Well #1
TD = 6920'
KB = 72'
Compl. 4/1/56
(Fort Bend Co.)

#4: A. Herzstein
H.H. White #1
TD = 8345'
KB = 73'
Compl. 7/27/58
(Fort Bend Co.)

#5: A. Herzstein, et al. (42-157-02793)
(was Beck Oil Co.)
Hall Etter #1
TD = 8042'
KB = 72'
Compl. 9/20/55
(Fort Bend Co.)

#6: Harry Leyendecker & Beck Oil Co. (42-157-02792)
Hall Etter-City Investment Co. #1
TD = 8100'
KB = 69'
Compl. 4/9/56
(Fort Bend Co.)

#7: Navidad Oil & Gas
& Davidson Geochemical (42-157-02791)
Hall Etter #1
TD = 10,000'
KB = 73'
Compl. 9/20/62
(Fort Bend Co.)

#8: Harry Leyendecker Trustee (42-157-02790)
Hall Etter-City Investment Co. #2
TD = 8100′
KB = 76′
Compl. 12/3/56
(Fort Bend Co.)

#9: Davidson Geochemical Co.
& Cooperative Refinery (42-157-12789)
Hall Etter #1
TD = 8207′
KB = 69′
Compl. 6/8/61
(Fort Bend Co.)

#10:Dyco Petroleum Corp. (42-039-30712)
J.E. Price #1
TD = 8216′
KB = 74′
Compl. 8/6/76

#11:Floyd L. Karsten (42-039-01345)
R.W. Sharp, et al. #4
TD = 7618′
KB = 71′
Compl. 8/16/51

#12:Floyd L. Karsten (42-039-01343)
Sharp #2
TD = 8206′
KB = 71′
Compl. 3/2/51

#13:Floyd L. Karsten (42-039-01346)
Sharp #5
TD = 7852′
KB = 70′
Compl. 1/11/52

#14:Floyd L. Karsten (42-039-01342)
Richard W. Sharp #1
TD = 8752′
KB = 70′
Compl. 9/25/50

#15:Rowan Drilling Co. (42-039-01349)
Vivian Vilvan #1
TD = 6515′
KB = 69′
Compl. 7/31

#16:Floyd L. Karsten (42-039-01350)
V. Vilvan #1
TD = 8256′
KB = 69′
Compl. 5/15/51

#17:Quintex Petroleum (42-039-31531)
Price #2
TD = 8215′
KB = 73′
Compl. 6/3/80

#18:Floyd L. Karsten (42-039-01338)
John B. Sharp #1
TD = 8260′
KB = 68′
Compl. 9/10/51

#19:Floyd L. Karsten (42-039-01348)
Hansen #2
TD = 7710′
KB = 68′
Compl. 2/25/52

#20:Floyd L. Karsten (42-039-01340)
J.E. Price #1
TD = 8703′
KB = 71′
Compl. 10/12/51

#20A:Quintex Petroleum (42-039-31537)
Sharp Corp. #1
TD = 8216′
KB = 74′
Compl. 6/1/80

#21:Quintex Petroleum (42-039-31827)
W.L. Goldston Unit #1
TD = 8266′
KB = 73′
Compl. 5/2/83

#22:Floyd L. Karsten (42-039-01337)
Nellie B. Hazard Unit #1
TD = 8288′
KB = 67′
Compl. 4/16/52

#23:Intercoastal
Joe Rowland #1
TD = 8266′
KB = 74′
Compl. 11/12/79

#24:Houston Natrual Gas Prod. Co. (42-039-01332)
Law #1 et al Unit
TD = 8220′
KB = 58′
Compl. 3/23/60

#25:J. Ray McDermott & Co., Inc. (42-039-01331)
Joe Berwick #1
TD = 8245′
KB = 71′
Compl. 8/12/53

#26:Housch & Thompson (42-039-01333)
L.C. Allen #1
TD = 7021′
KB = 69′
Compl. 4/18/39

#27:H.E. Williams (42-039-01335)
Burrow-Winans Unit #1
TD = 8200′
KB = 69′
Compl. 6/18/54

#28:Dynamic of Texas (42-039-31973)
Schenck #1
TD = 8676′
KB = 74′
Compl. 4/19/84

#29:Jack W. Frazier (42-039-01334)
M.E. Milks #1
TD = 8214′
KB = 63′
Compl. 11/4/53

#30:Grover J. Geiselman & Benz Oil Co. (42-039-05028)
Anderson #1
TD = 8113′
KB = 68′
Compl. 11/3/67

#31:Mellon Energy Co. (42-039-31196)
Sharp Corp #1
TD = 6010′
KB = 65′
Compl. 2/6/78

#32:The Westland Oil Co. (42-157-00039)
Julia Teague #1
TD = 6292′
KB = 75′
Compl. 1/9/44
(Fort Bend Co.)

#33:Sparta Oil Co. (42-157-02796)
R.I. Furnace #1
TD = 7002′
KB = 76′
Compl. 7/17/48
(Fort Bend Co.)

#34:Sparta Oil Co. (42-157-02797)
Myrtle Ramsey #1
TD = 8671′
KB = 73′
Compl. 5/23/48
(Fort Bend Co.)

#35:Brazos Oil & Gas Co. (42-039-00007)
F.M. Pearce #1
TD = 7778′
KB = 75′
Compl. 4/26/62

#36:Claud B. Hamill (42-039-00006)
John B. Sharp et al. #1
TD = 7858′
KB = 80′
Compl. 2/11/52

#37:McCormick Operating Co. (42-039-31873)
Arcola Properties, Ltd. #1
TD = 8326'
KB = 79'
Compl. 1/6/83

#38:Amerada Petroleum Corp. (42-039=01329)
Jennie Stancliff #1
TD = 7735'
KB = 76'
Compl. 5/29/51

#39:R.O. Mangum et al. (42-039-00008)
Leslie Glaze #1
TD = 7818'
KB = 73'
Compl. 6/25/51

#40:Southern Minerals Corp. (42-039-00009)
Adams #1
TD = 7815'
KB = 78'
Compl. 12/10/53

#41:Jack W. Frazier (42-039-00005)
J.C. Thompson et al. #1
TD = 6054'
KB = 69'
Compl. 4/29/45

#42:Salt Dome Oil Corp. (42-039-00012)
A.E. Martin #1
TD = 8032'
KB = 71'
Compl. 3/3/44

#43:Salt Dome Oil Corp. et al. (42-039-01328)
F.P. Law #1
TD = 8015'
KB = 68'
Compl. 1/9/45

#44:Salt Dome Oil Corp. (42-039-00011)
T.G. Tripp #1
TD = 6342'
KB = 75'
Compl. 8/18/45

#45:Windsor Oil Co. (42-039-06411)

Croix #1
TD = 6144'
KB = 74'
Compl. 12/12/45

#46:Texaco (42-039-30543)
M.B. Shannon Unit #1
TD = 8700'
KB = 77'
Compl. 12/5/74

#47:Tauber Oil Co. (42-039-04779)
Ella Corbett Heirs #1
TD = 6017'
KB = 67'
Compl. 12/1/63

APPENDIX E

COMPACTION MODEL EQUATIONS

The following is the derivation of the equations used to construct the pure sandstone and pure shale curves. These curves are used in conjunction with knowledge of the subsurface stratigraphy to construct the predicted listric shape of growth faults.

The pure shale curve used in this study has been modified from the equation printed in the Xaio and Suppe (1986) progress report. It was found that the pure shale curve did not work as printed. When the derivation of equation 11 was worked through it was apparent that the original equation was in error. The error has been corrected in this study.

An additional modification was made to the pure shale curve. In the Xaio and Suppe study, the regression coefficient, 'c', was obtained from the best-fit curve tracing percent shale porosity with depth for south Louisiana data. In this study, shale porosity data specific to Brazoria County (Gregory, 1980) was used to obtain a best-fit curve. Thus coefficient 'c', the regression coefficient, and coefficient 'd', the initial porosity value of 81.6%, are specific to Brazoria County. The values used

by Xaio and Suppe for initial sandstone porosity and sandstone porosities at depth are consistent with those reported for Brazoria County.

<u>Derivation</u> <u>of</u> <u>the</u> <u>Sandstone</u> <u>Curve</u>

1) The dip of a normal fault will decrease with depth, due to compaction, in response to increasing overburden pressure:

$$\frac{\tan\theta}{\tan\theta_o} = \frac{1 - \phi_o}{1 - \phi}$$

where ϕ_o and ϕ are the initial and present porosity, and θ_o and θ are the initial and present fault dip.

2) As the rock porosity ϕ will approach zero with depth:

$$\tan\theta = (1 - \phi_o)\tan\theta_o$$

as a limit.

3) Assume a linear porosity versus depth relationship:

$$\phi = aY + b$$

where b is the initial porosity (in this case 0.334), a is a regression coefficient (in this case equal to -0.000003441), and Y is depth.

4) Substituting equation 3 into equation 1:

$$\frac{\tan\theta}{\tan\theta_o} = \frac{1 - \phi_o}{1 - (aY + b)}$$

5) Let $k = (1 - \phi_o)\tan\theta_o$ and $\tan\theta = dY/dX$:

$$\frac{dY}{dX} = \frac{k}{1 - aY - b}$$

therefore:

$$\frac{dX}{dY} = \frac{1}{k}(1 - aY - b)$$

6) Integrating equation 5:

$$X = 1/k \int(1 - aY - b)$$

$$X = \frac{1}{k}\left(Y - \frac{aY^2}{2} - bY\right)$$

gives the predicted fault shape equation in pure sand:

$$X = \frac{Y}{k}\left(1 - b - \frac{aY}{2}\right)$$

Derivation of the Shale Curve

7) Assume an exponential porosity versus depth relationship:

$$\phi = d - c\log_{10}Y$$

where d is the initial porosity (in this case 0.816), c is a regression coefficient (in this case equal to -0.15513), and Y is depth.

8) Substituting equation 7 into equation 1:

$$\frac{\tan\theta}{\tan\theta_o} = \frac{1 - \phi_o}{1-(c\log_{10}Y+d)}$$

$$\tan\theta = \frac{(1 - \phi_o)(\tan\theta_o)}{1-c\log_{10}Y-d}$$

9) Substituting k for $\tan\theta_o(1 - \phi_o)$:

$$\tan\theta = \frac{k}{1-c\log_{10}Y-d}$$

10) In the limit $\tan\theta = dY / dX$, therefore:

$$\frac{dY}{dX} = \frac{1}{k(1-c\log_{10}Y-d)}$$

and

$$\frac{dX}{dY} = \frac{1}{k}(1-c\log_{10}Y-d)$$

11) Substituting $c\log_{10}Y = \frac{c}{\ln 10}\ln Y$ and integrating:

$$X = \frac{1}{k}\left(\int 1 - \int d - \frac{c}{\ln 10}\int \ln Y\right)$$

$$X = \frac{1}{k}\left(Y - dY - \frac{c}{\ln 10}(Y\ln Y - Y)\right)$$

$$X = \frac{1}{k}\left(Y - dY - \frac{c}{\ln 10}Y\ln Y + \frac{c}{\ln 10}Y\right)$$

gives the predicted fault shape equation in pure shale:

$$X = \frac{Y}{k}\left(1 - d - \frac{c}{\ln 10}\ln Y + \frac{c}{\ln 10}\right)$$

(modified from Xaio and Suppe, 1986)